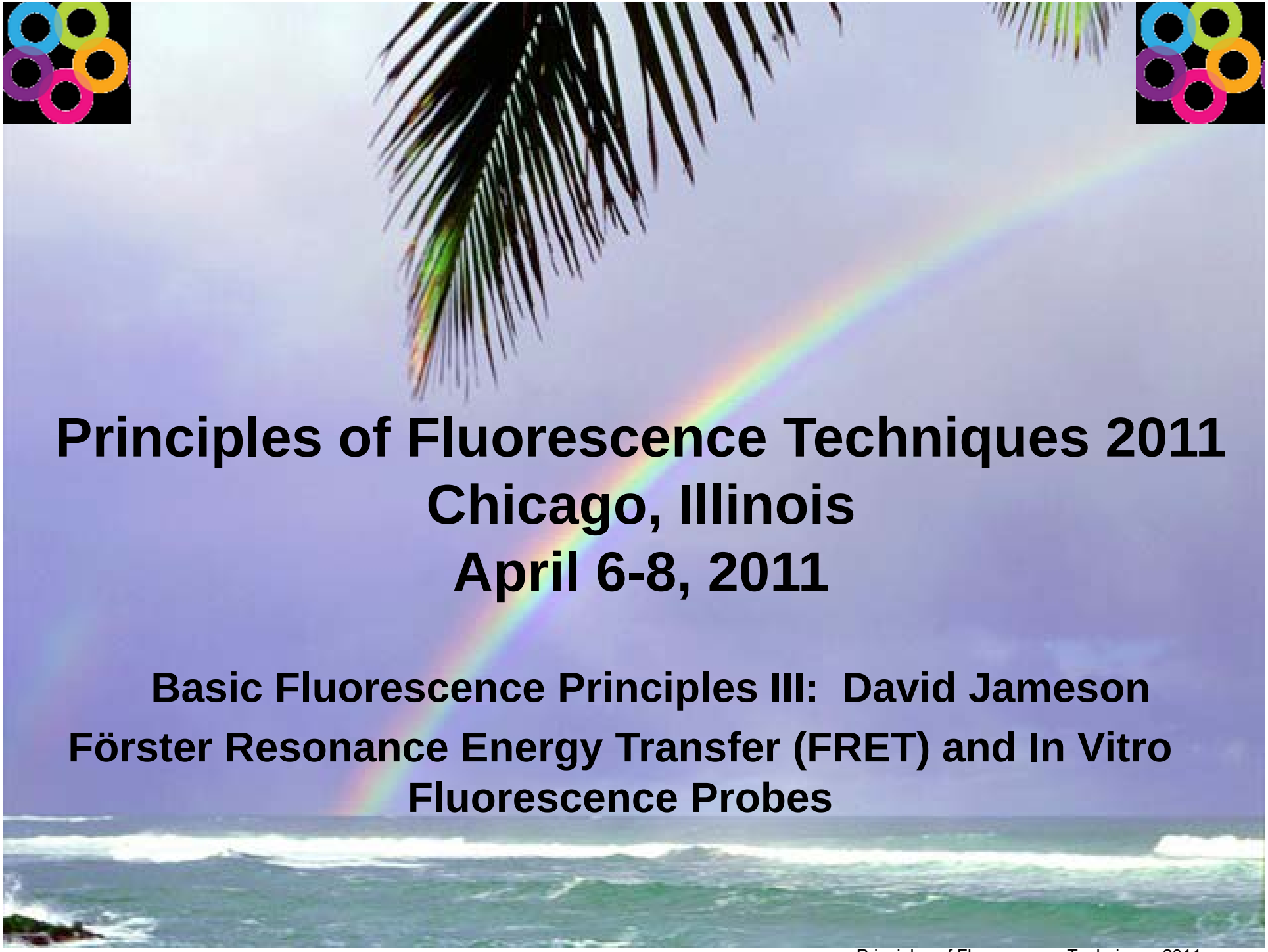

Principles of Fluorescence Techniques 2011
Chicago, Illinois
April 6-8, 2011

Basic Fluorescence Principles III: David Jameson

Förster Resonance Energy Transfer (FRET) and In Vitro Fluorescence Probes

Förster Resonance Energy Transfer
FRET

I should note before we start that the Merriam-Webster online dictionary defines “FRET” as:

“to cause to suffer emotional strain”

Some of these slides were prepared by Pierre Moens

This sentence appears in a 2006 book!

Let's correct this mistake!

More than 50 years ago, the German scientist Förster discovered that close proximity of two chromophores changes their spectral properties in predictable ways (Förster, 1948a).

Milestones in the Theory of Resonance Energy Transfer

1922 G. Cario and J. Franck demonstrate that excitation of a mixture of mercury and thallium atomic vapors with 254nm (the mercury resonance line) also displayed thallium (sensitized) emission at 535nm.

1924 E. Gaviola and P. Pringsham observed that an increase in the concentration of fluorescein in viscous solvent was accompanied by a progressive depolarization of the emission.

1925 J. Perrin proposed the mechanism of resonance energy transfer

1928 H. Kallmann and F. London developed the quantum theory of resonance energy transfer between various atoms in the gas phase. The dipole-dipole interaction and the parameter R_0 are used for the first time

1932 F. Perrin published a quantum mechanical theory of energy transfer between molecules of the same specie in solution. Qualitative discussion of the effect of the spectral overlap between the emission spectrum of the donor and the absorption spectrum of the acceptor

1946-1949 T. Förster develop the first complete quantitative theory of molecular resonance energy transfer

What is FRET ?

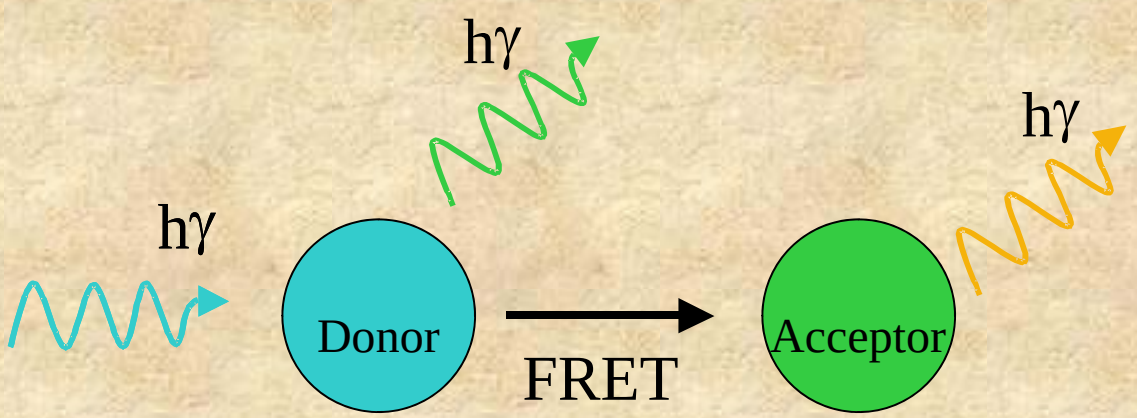

When the donor molecule absorbs a photon, and there is an acceptor molecule close to the donor molecule, radiationless energy transfer can occur from the donor to the acceptor.

FRET results in a decrease of the fluorescence intensity and lifetime of the donor probe, It enhance the fluorescence of the acceptor probe when the acceptor is fluorescent.

PM

Tuning fork analogy for resonance energy transfer

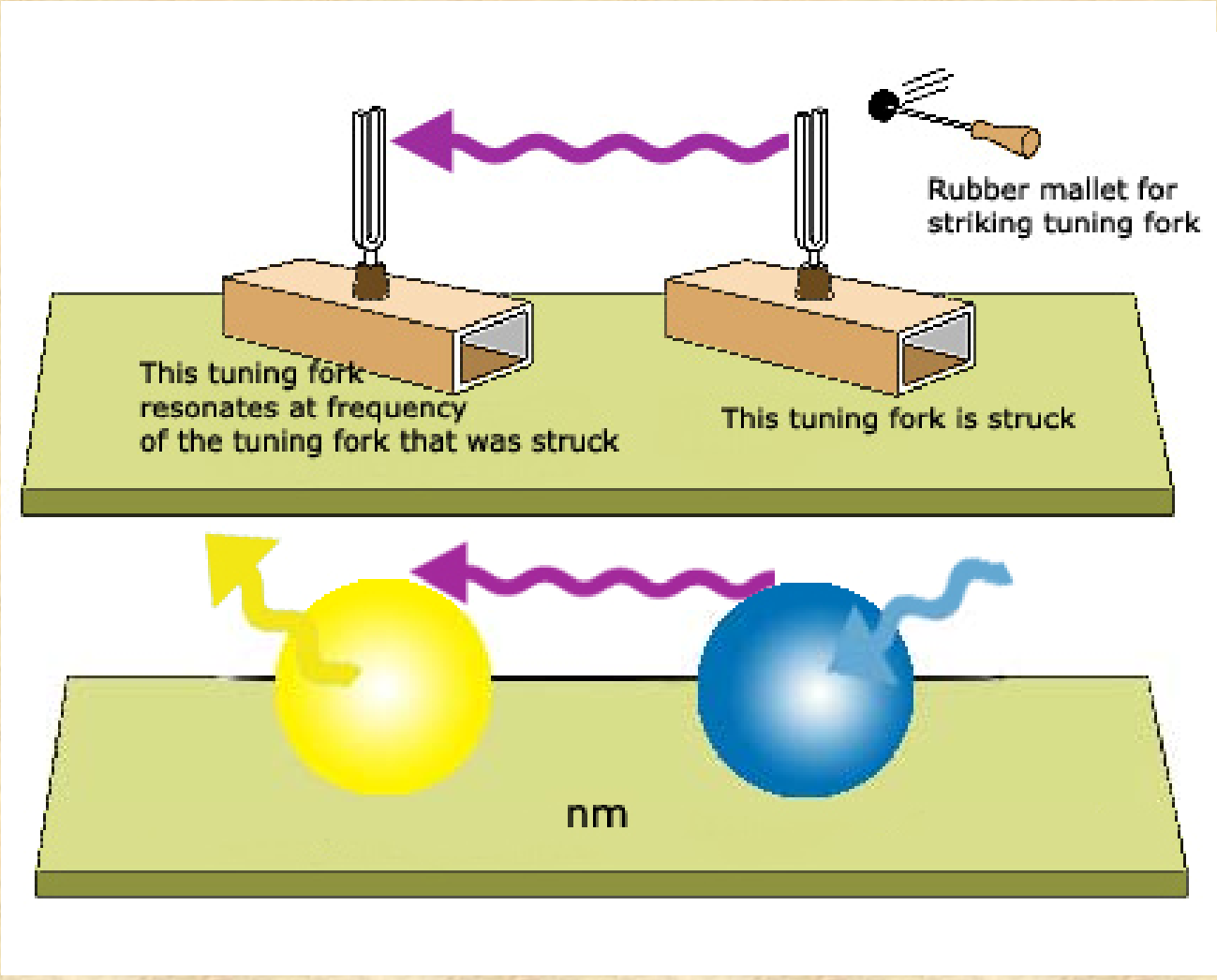

TV

Simplified FRET Energy Diagram

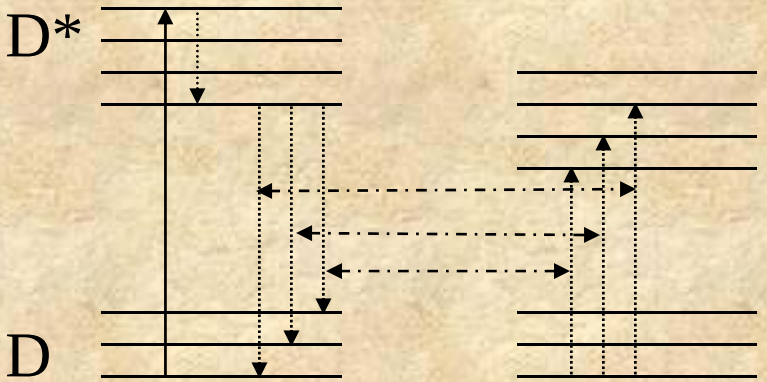

Coupled transitions

Suppose that the energy difference for one of these possible deactivation processes in the donor molecule matches that for a possible absorption transition in a nearby acceptor molecule. Then, with sufficient energetic coupling between these molecules (overlap of the emission spectrum of the donor and absorption spectrum of the acceptor), both processes may occur simultaneously, resulting in a transfer of excitation from the donor to the acceptor molecule

The interaction energy is of a dipole-dipole nature and depends on the distance between the molecules as well as the relative orientation of the dipoles

PM

Dipole-dipole interaction

The rate of transfer (k_T) of excitation energy is given by:

$$k_T = (1/\tau_d)(R_0/r)^6$$

Where τ_d is the fluorescence lifetime of the donor in the absence of acceptor, r the distance between the centers of the donor and acceptor molecules and R_0 the Förster critical distance at which 50% of the excitation energy is transferred to the acceptor and can be approximated from experiments independent of energy transfer.

Förster critical distance

$$R_0 = 0.2108\,(n^{-4} Q_d \kappa^2 J)^{1/6} \text{ Å}$$

n is the refractive index of the medium in the wavelength range where spectral overlap is significant (usually between 1.2-1.4 for biological samples)

Q_d is the fluorescence quantum yield of the donor in absence of acceptor (i.e. number of quanta emitted / number of quanta absorbed)

κ^2 (pronounced “kappa squared”) is the orientation factor for the dipole-dipole interaction

J is the normalized spectral overlap integral [$\varepsilon(\lambda)$ is in $M^{-1}\,cm^{-1}$, λ is in nm and J units are $M^{-1}\,cm^{-1}\,(nm)^4$]

The overlap integral *J* is defined by:

$$J = \int_0^\infty I_D(\lambda)\varepsilon_A(\lambda)\lambda^4 d\lambda$$

Where λ is the wavelength of the light, $\varepsilon_A(\lambda)$ is the molar absorption coefficient at that wavelength and $I_D(\lambda)$ is the fluorescence spectrum of the donor normalized on the wavelength scale:

$$I_D(\lambda) = \frac{F_{D\lambda}(\lambda)}{\int_0^\infty F_{D\lambda}(\lambda)d\lambda}$$

Where $F_{D\,\lambda}(\lambda)$ is the donor fluorescence per unit wavelength interval

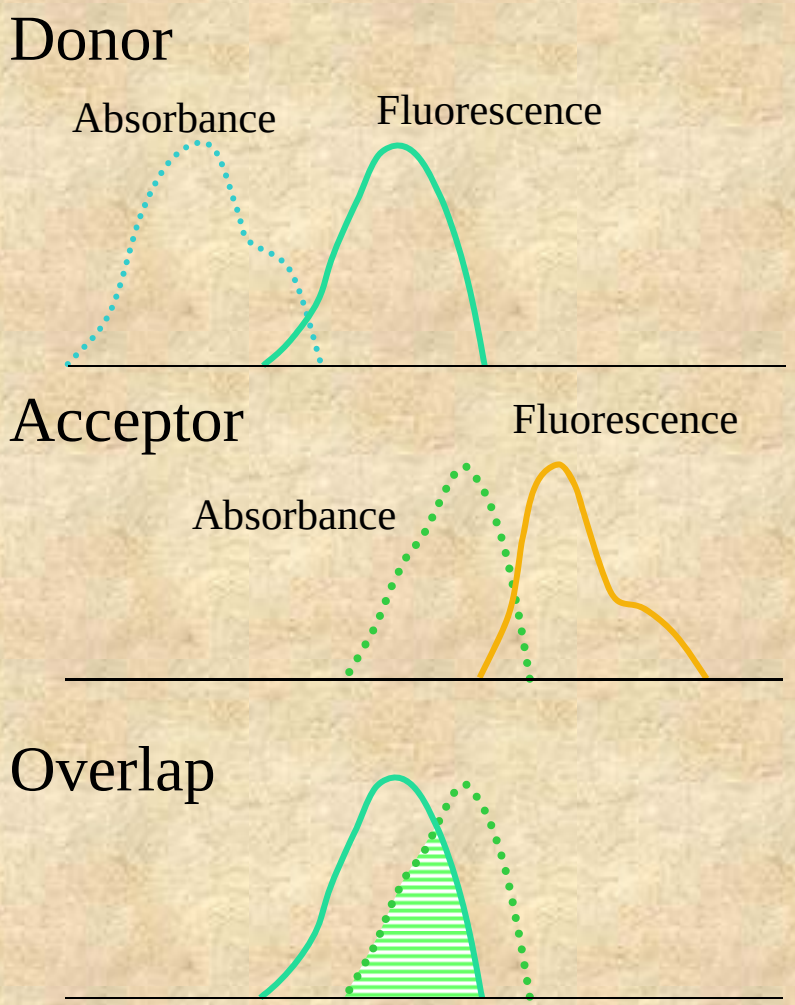

Determination of the efficiency of energy transfer (*E*)

Steady state method: *Decrease in donor fluorescence.* the fluorescence intensity of the donor is determined in absence and presence of the acceptor.

$$E = 1 - \frac{F_{da}}{F_d}$$

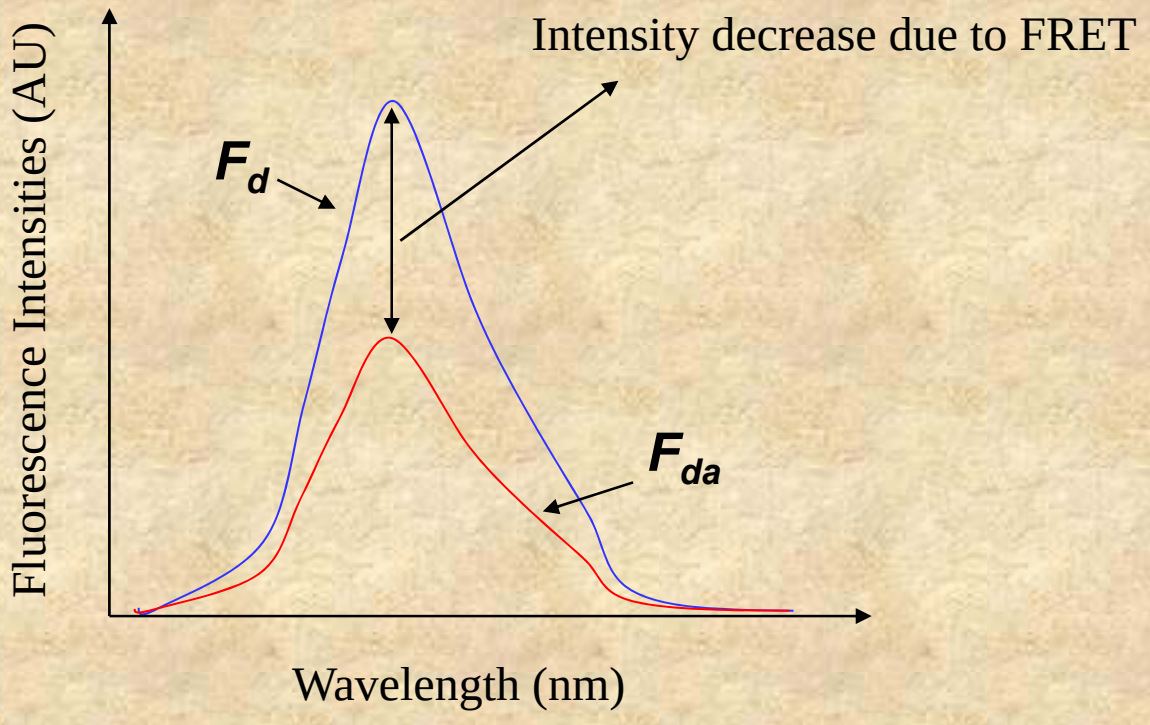

Determination of the efficiency of energy transfer (*E*)

Time-resolved method: Decrease in the lifetime of the donor

If the fluorescence decay of the donor is a single exponential then:

$$E = 1 - \frac{\tau_D}{\tau_D^0}$$

Where τ_D and τ_D^0 are the lifetime of the donor in the presence and absence of acceptor, respectively

Determination of the efficiency of energy transfer (*E*)

If the donor fluorescence decay in absence of acceptor is not a single exponential (probably resulting from heterogeneity of the probe's microenvironment) , then it may be modeled as a sum of exponential and the transfer efficiency can be calculated using the average decay times of the donor in absence and presence of acceptor:

$$E = 1 - \frac{\langle \tau_D \rangle}{\langle \tau_D^0 \rangle}$$

Where $<\tau>$ is the amplitude-average decay time and is defined as:

$$\langle \tau \rangle = \frac{\sum_i \alpha_i \tau_i}{\sum_i \alpha_i}$$

The distance dependence of the energy transfer efficiency (*E*)

$$r = \left(\frac{1}{E} - 1 \right)^{1/6} R_0$$

Where *r* is the distance separating the donor and acceptor fluorophores, R_0 is the Förster distance.

Many equivalent forms of this equation is found in the literature, such as:

$$E = R_0^6 / (R_0^6 + r^6) \text{ or } E = 1 / \left[1 + (r/R_0)^6 \right]$$

The distance dependence of the energy transfer efficiency (*E*)

The efficiency of transfer varies with the inverse sixth power of the distance.

R_0 in this example was set to 40 Å. When the *E* is 50%, $R=R_0$

Distances can usually be measured between 0.5 R_0 and ~1.5R_0. Beyond these limits, we can often only say that the distance is smaller than 0.5 R_0 or greater than 1.5R_0. If accurate distance measurement is required then a probe pair with a different R_0 is necessary.

How was FRET theory tested experimentally?

Energy Transfer. A System with Relatively Fixed Donor–Acceptor Separation

JACS 87:995(1965)

S. A. Latt, H. T. Cheung, and E. R. Blout

Contribution from the Department of Biological Chemistry, Harvard Medical School, Boston, Massachusetts. *Received August 24, 1964*

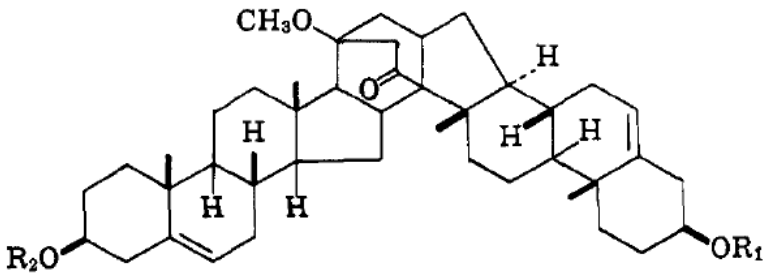

XIb, R_1 = *p*-methoxyphenylacetyl; R_2 = 1-naphthoyl
XIIb, R_1 = 1-naphthoyl; R_2 = anthracene-9-carbonyl

Table III

Compound	$\overline{K^2}$	R_{calcd}, Å.	R_{measd} (from Dreiding models), Å.
XI	$^2/_3$	21.3 ± 1.6	21.8 ± 2.0 (linear av.)
			19.2 ± 2.0 ($[\overline{1/R^6}]^{-6}$)
XII	$^2/_3$	16.7 ± 1.4	21.5 ± 2.0 (linear av.)
			19.4 ± 2.0 ($[\overline{1/R^6}]^{-6}$)

The most likely explanation for this discrepancy between the predicted and observed transfer in compound XII is that the value of the average orientation factor is greater than the estimate of $^2/_3$ which was used to calculate the predicted separation.

*DEPENDENCE OF THE KINETICS OF SINGLET-SINGLET ENERGY TRANSFER ON SPECTRAL OVERLAP**

BY RICHARD P. HAUGLAND,† JUAN YGUERABIDE,‡ AND LUBERT STRYER‡

DEPARTMENT OF CHEMISTRY, STANFORD UNIVERSITY, AND
DEPARTMENT OF BIOCHEMISTRY, STANFORD UNIVERSITY SCHOOL OF MEDICINE

Communicated by Harden M. McConnell, February 19, 1969 PNAS

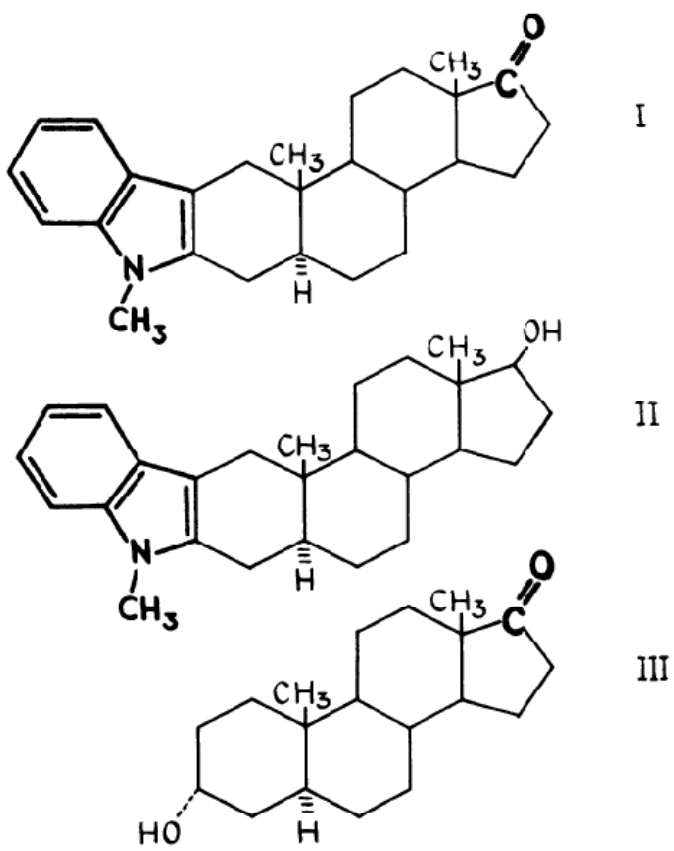

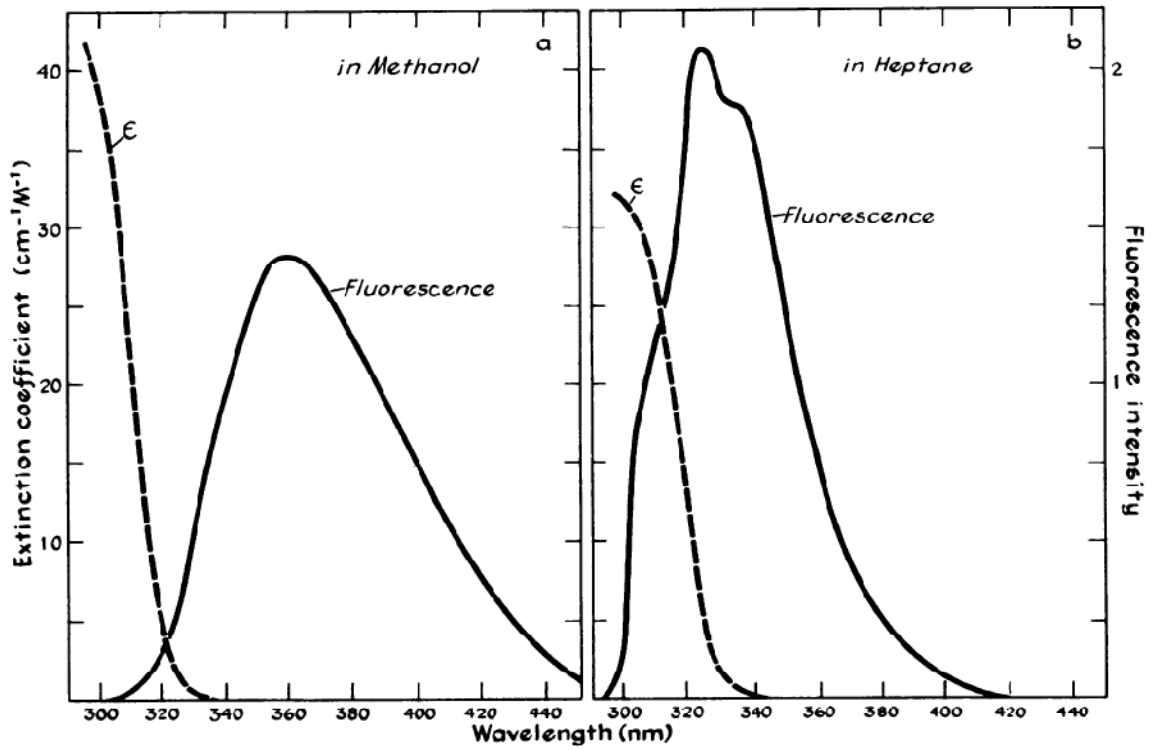

FIG. 2.—Overlap of the emission spectrum of the N-methylindole energy donor (II) and the absorption spectrum of the ketone energy acceptor (III) in (*a*) methanol and (*b*) heptane. III is nonfluorescent.

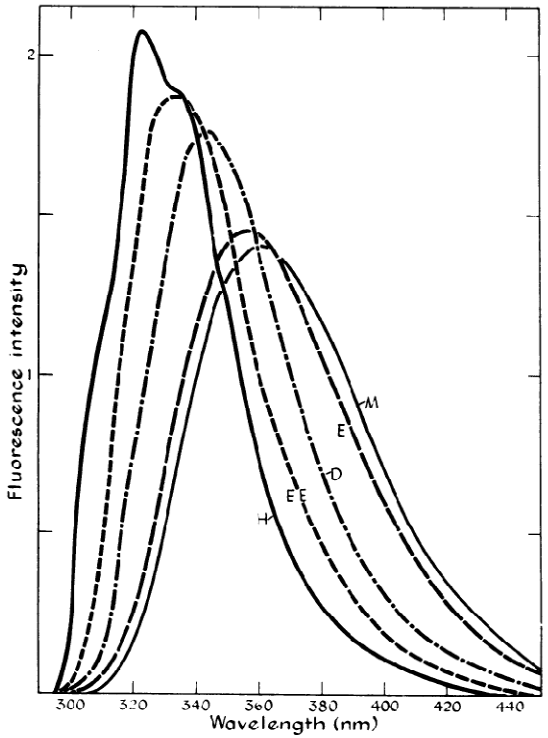

FIG. 3.—Fluorescence emission spectra of II in n-heptane (*H*), ethyl ether (*EE*), p-dioxane (*D*), ethanol (*E*), and methanol (*M*). The spectrum of II in ethyl acetate is virtually identical to that obtained in dioxane. The intensities have been normalized so that the areas under the curves are equal. The excitation wavelength was 290 nm.

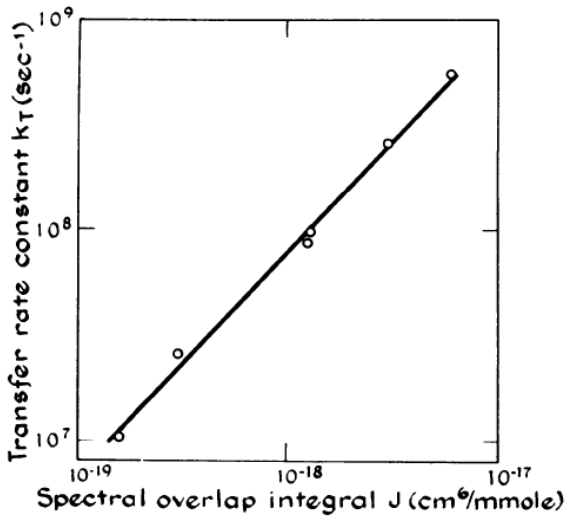

TABLE I. *Fluorescence properties of I and II in a series of solvents.*

Solvent	τ_I (nsec)	τ_{II} (nsec)	Fluorescence Quantum Yield Q_I	Q_{II}	Transfer Efficiency E_K	E_{SS}
Methanol	5.3	5.6	0.397	0.420	0.053	0.055
Ethanol	5.6	6.5	0.440	0.510	0.14	0.138
Dioxane	3.6	5.4	0.360	0.535	0.33	0.328
Ethyl acetate	3.3	4.7	0.286	0.418	0.30	0.315
Ethyl ether	2.1	4.5	0.247	0.515	0.53	0.52
Heptane	1.1	2.8	0.136	0.346	0.606	0.608

TABLE 2. *Transfer kinetics and spectral overlap integral of I in a series of solvents.*

Solvent	Transfer rate, k_T(sec^{-1}) $\times 10^{-7}$	Spectral overlap integral, J(cm^6 mmole^{-1}) $\times 10^{19}$	k_F (sec^{-1}) $\times 10^{-7}$	n_D	k_T/J $\times 10^{-26}$	$k_T/(Jk_F)$ $\times 10^{-18}$
Methanol	1.0	1.5	7.50	1.331	0.67	0.89
Ethanol	2.5	3.0	7.85	1.362	0.83	1.06
Dioxane	9.6	13.0	9.9	1.423	0.74	0.75
Ethyl acetate	11.3	12.8	8.9	1.372	0.88	0.99
Ethyl ether	25.5	30.0	11.5	1.349	0.83	0.72
Heptane	55.2	60.3	12.4	1.387	0.92	0.74

r^{-6} distance dependence?

$$k_T = (1/\tau_d)(R_0/r)^6$$

*ENERGY TRANSFER: A SPECTROSCOPIC RULER**

By Lubert Stryer and Richard P. Haugland†

Department of Biochemistry, Stanford University School of Medicine, Palo Alto, and the Department of Chemistry, Stanford University

Communicated by Arthur Kornberg, May 29, 1967 PNAS

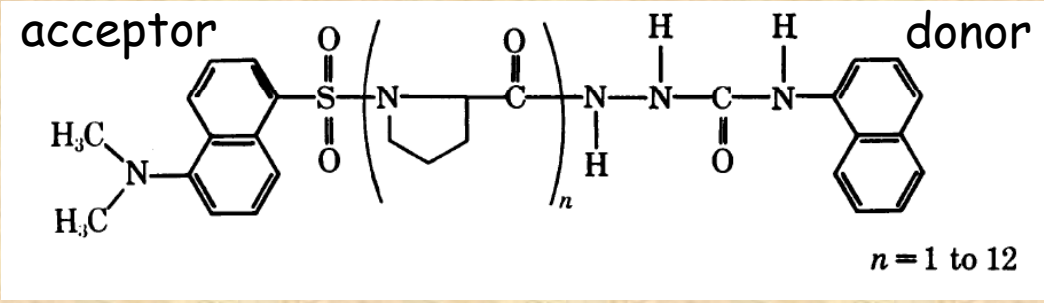

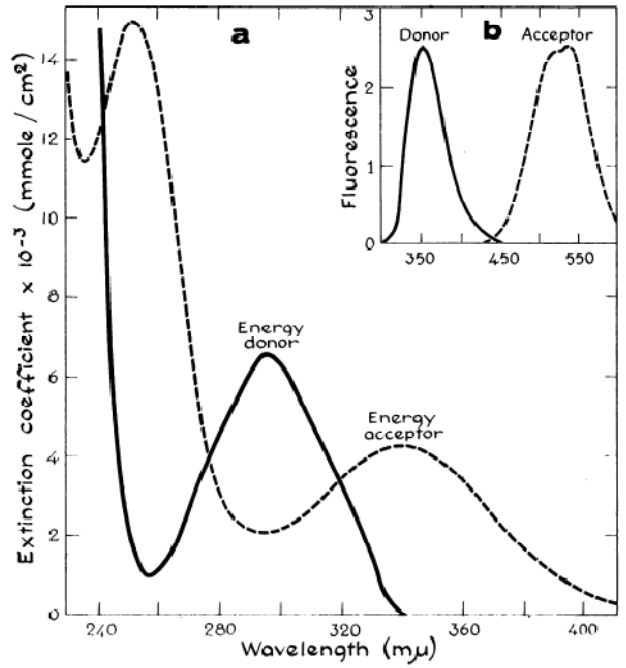

Principles of Fluorescence Techniques 2011

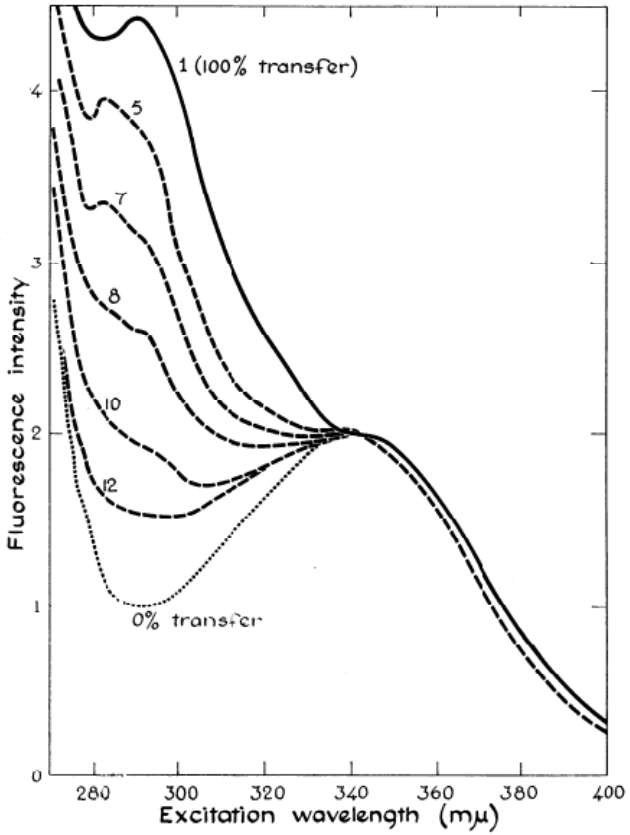

FIG. 3.—Excitation spectrum of dansyl-L-prolyl-hydrazide (·····, 0% transfer), dansyl-L-prolyl-α-naphthyl (———, 100% transfer), and dansyl-(L-prolyl)$_n$-α-naphthyl (- - - -, n = 5, 7, 8, 10, 12) in ethanol.

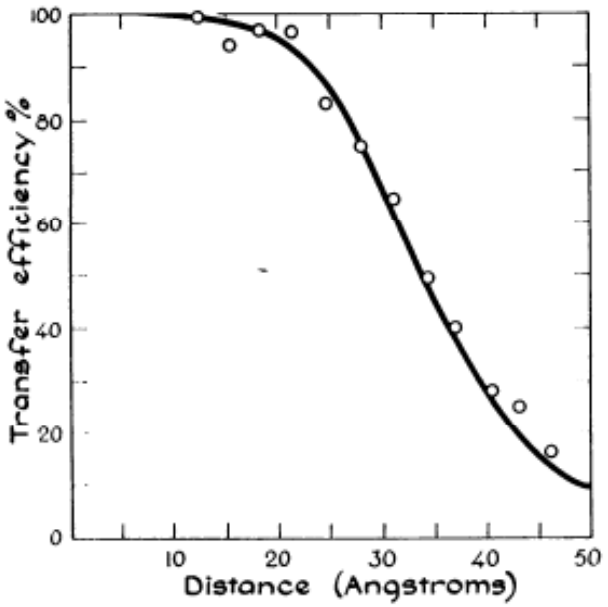

FIG. 4.—Efficiency of energy transfer as a function of distance in dansyl-(L-prolyl)$_n$-α-naphthyl, n = 1 to 12. The α-naphthyl and dansyl groups were separated by defined distances ranging from 12 to 46 Å. The energy transfer is 50% efficient at 34.6 Å. The solid line corresponds to an r^{-6} distance dependence.

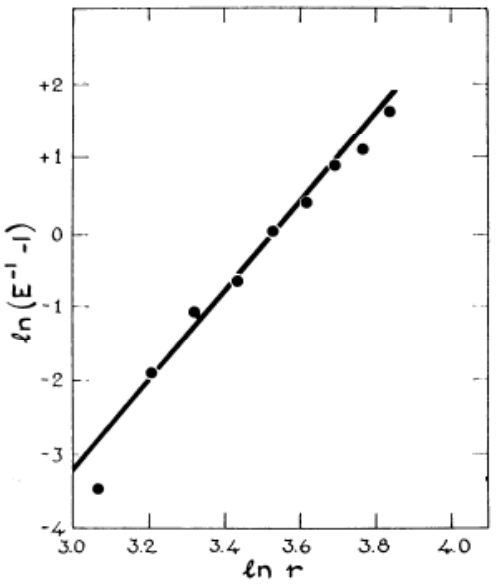

FIG. 5.—The dependence of the efficiency of energy transfer on distance is given by the slope in this plot of ln (E^{-1} − 1) versus ln r. The slope is 5.9, in excellent agreement with the r^{-6} dependence predicted by Förster.

For these parameters, R_0 is calculated to be 27.2 Å, *while the observed value is* 34.6 Å (Figs. 4 and 5). A rigorous comparison of the observed and calculated R_0 distances should be deferred until the value of K^2 is better defined. It would also be desirable to have independent confirmation of the estimated distances between the energy donor and acceptor groups.

More to the story???

Effect of flexibility and *cis* residues in single-molecule FRET studies of polyproline

Robert B. Best*†, Kusai A. Merchant*, Irina V. Gopich*, Benjamin Schuler*‡, Ad Bax*, and William A. Eaton*§

18964–18969 | PNAS | November 27, 2007 | vol. 104 | no. 48

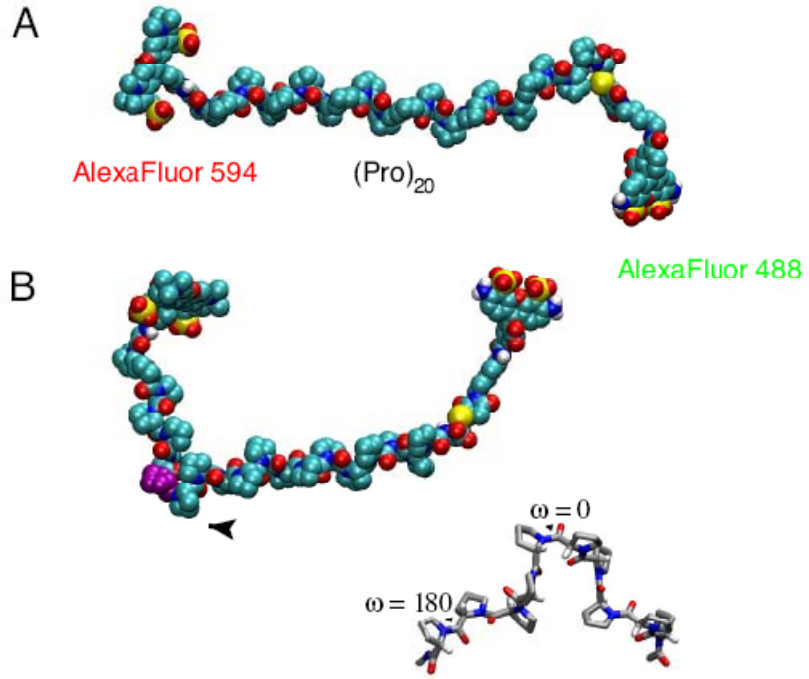

Fig. 1. Polyproline structures. Space-filling representation of polyproline-20 labeled with Alexa Fluor 488 (FRET donor) at the C-terminal cysteine and Alexa Fluor 594 (FRET acceptor) at the N-terminal glycine in the *all-trans* conformation (*A*) and with residue 8 (purple) in the *cis* conformation (*B*). (*B Inset*) A polyproline fragment with one *cis* peptide bond (shown as "$\omega = 0$"). One of the remaining *trans* peptide bonds is also indicated ("$\omega = 180$").

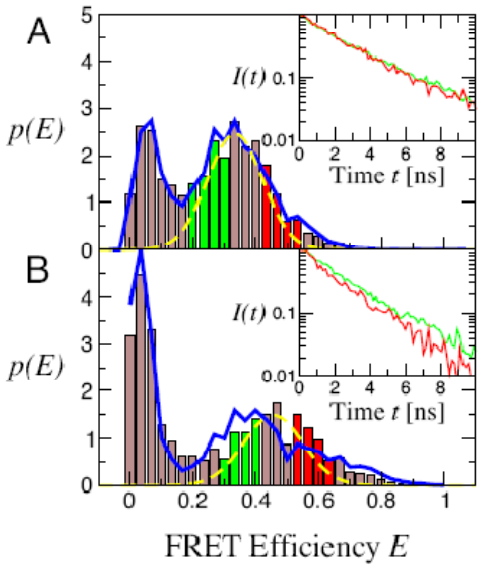

Fig. 3. Distributions of FRET efficiency for polyproline-20. The efficiency of each molecule $E = n_A/(n_A + n_D)$ was calculated from the (γ-corrected) n_A acceptor and n_D donor photons detected as it passes through the observation volume, in TFE (*A*) and water (*B*) (solid bars). Broken yellow lines indicate the shot-noise-limited width of the distribution (24, 19). Solid blue line in *A* gives a maximum likelihood fit of the data a multistate model. Solid blue line in *B* gives the expected efficiency distribution for a heterogeneous mixture of species containing *cis* proline, taking the relative populations from NMR and the efficiencies from simulation. (*Insets*) The donor fluorescence decays for donor photons from the subpopulations with corresponding colors in the efficiency histograms.

Distributions

Proc. Nat. Acad. Sci. USA
Vol. 68, No. 9, pp. 2099–2101, September 1971

Determination of Distance Distribution Functions by Singlet-Singlet Energy Transfer

(flexibility/Förster theory/fluorescence/molecular structure)

CHARLES R. CANTOR AND PHILIP PECHUKAS

Proc. Nat. Acad. Sci. USA
Vol. 69, No. 8, pp. 2273–2277, August 1972

Evaluation of the Distribution of Distances Between Energy Donors and Acceptors by Fluorescence Decay

(energy transfer/fluorescence/decay/conformation/polymers)

A. GRINVALD, E. HAAS, AND I. Z. STEINBERG

$$E(R_0) = \int_0^\infty dR\, f(R)\, \frac{R_0^6}{R_0^6 + R^6}$$

Distributions

Proc. Nat. Acad. Sci. USA
Vol. 72, No. 5, pp. 1807–1811, May 1975

Distribution of End-to-End Distances of Oligopeptides in Solution as Estimated by Energy Transfer

(fluorescence decay/conformation)

ELISHA HAAS, MEIR WILCHEK, EPHRAIM KATCHALSKI-KATZIR, AND IZCHAK Z. STEINBERG

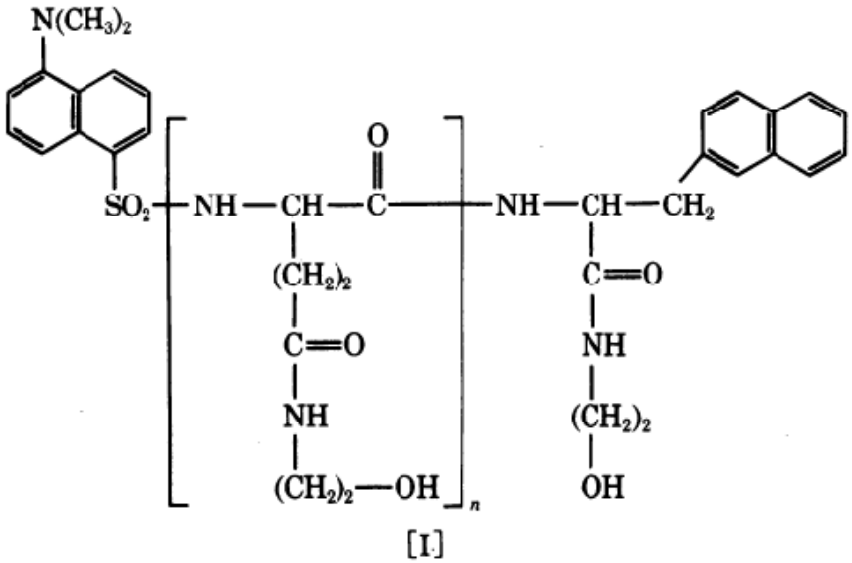

[I]

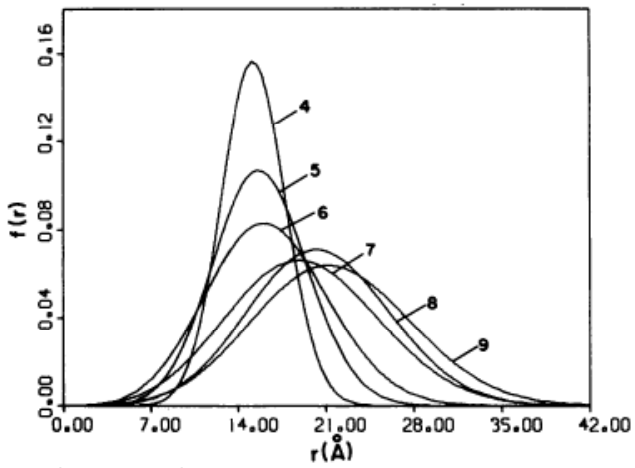

FIG. 4. The distribution function of the distances between donor and acceptor for the series of oligopeptides I, $n = 4, 5, 6, 7, 8$, and 9. The numbers in the figure refer to the values of n.

Distributions

Biochemistry **1988**, *27*, 9149–9160

Distance Distributions in Proteins Recovered by Using Frequency-Domain Fluorometry. Applications to Troponin I and Its Complex with Troponin C†

Joseph R. Lakowicz,*,‡ Ignacy Gryczynski,‡,§ Herbert C. Cheung,∥ Chien-Kao Wang,∥ Michael L. Johnson,⊥ and Nanda Joshi‡

 Biochemistry **1991**, *30*, 5238–5247

Distance Distributions and Anisotropy Decays of Troponin C and Its Complex with Troponin I†

Herbert C. Cheung,*,‡ Chien-Kao Wang,‡,§ Ignacy Gryczynski,∥ Wieslaw Wiczk,∥ Gabor Laczko,∥ Michael L. Johnson,⊥ and Joseph R. Lakowicz∥

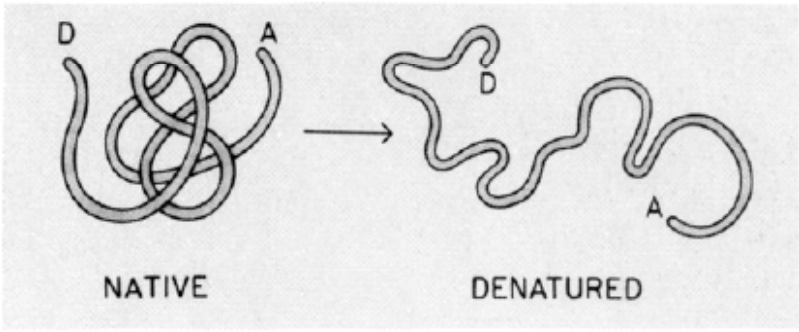

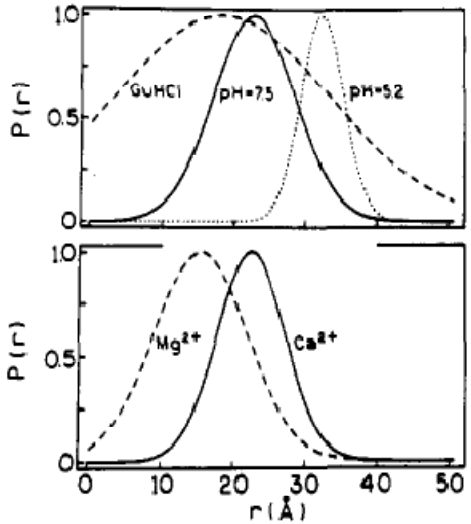

FIGURE 4: Distance distributions for TnC–DNZ–IAE in the absence of cations (top) and in the presence of Mg^{2+} and Ca^{2+} (pH 7.5, bottom). The pH for guanidine hydrochloride (GuHCl) was 7.5.

An impressive example of the use of FRET methodologies to study protein systems is given by the work of Lillo et al. ("Design and characterization of a multisite fluorescence energy-transfer system for protein folding studies: a steady-state and time-resolved study of yeast phosphoglycerate kinase" Biochemistry. 1997 Sep 16;36(37):11261-72 and "Real-time measurement of multiple intramolecular distances during protein folding reactions: a multisite stopped-flow fluorescence energy-transfer study of yeast phosphoglycerate kinase" Biochemistry. 1997 Sep 16;36(37):11273-81)

Site-directed mutagenesis was used to introduce pairs of cysteine residues in the protein at the positions shown

The pairs studied were:

135 – 290; 75 – 290

290 – 412; 412 – 202

135 – 412; 412 - 75

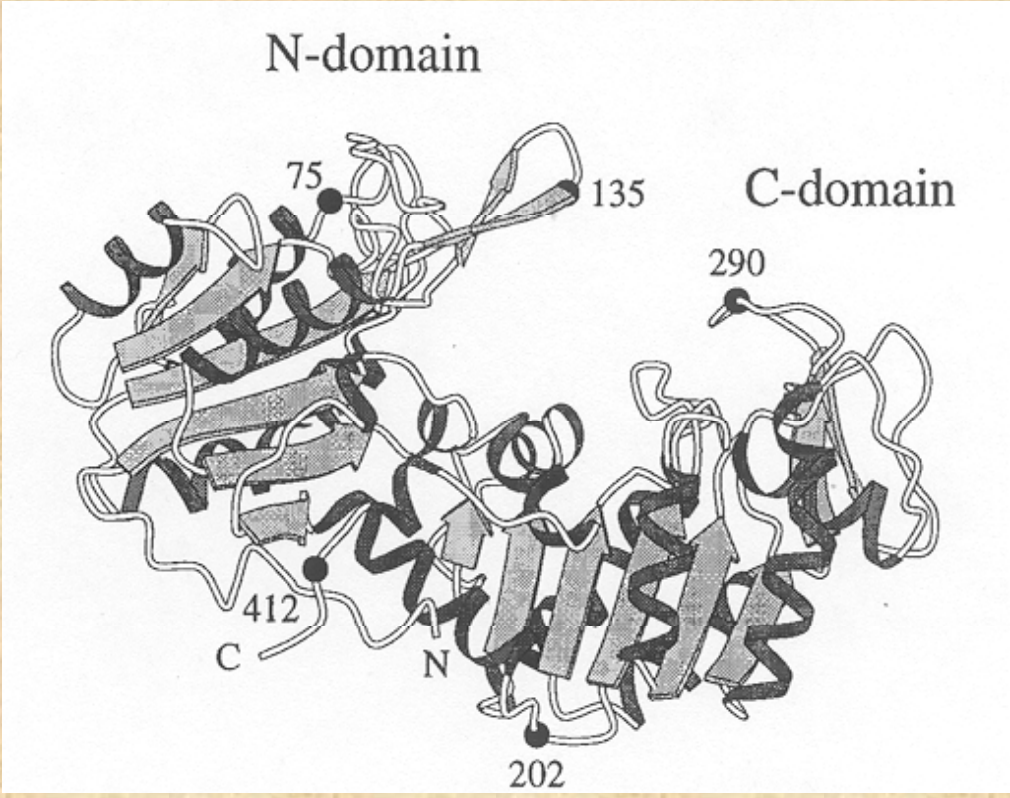

The donor was IAEDANS and the acceptor was IAF (iodoacetamindo-fluorescein). The various labeled protein products were separated by chromatography!

Table 1: Summary of the Labeled Proteins Examined for the Photophysical Characterization of Each Energy-Transfer Pair Cys*i* → Cys*j*

sample	name	Cys*i* → Cys*j*	no. of cysteines	fluorophore
donor only (D-PGK)	*i*-single cysteine	D- - -	1 (*i*)	AEDANS (*i*)
	j-single cysteine	- - -D	1 (*j*)	AEDANS (*j*)
	i-two cysteines	D- - -Cys	2 (*i*, *j*)	AEDANS (*i*)
	j-two cysteines	Cys- - -D	2 (*i*, *j*)	AEDANS (*j*)
	(*i*, *j*)-two cysteine average	D- - -Cys + Cys- - -D	2 (*i*, *j*)	AEDANS (*i*) + AEDANS (*j*)
	(*i*, *j*)-two cysteine "double donor"	D- - -D	2 (*i*, *j*)	AEDANS (*i*, *j*)
acceptor only	*i*-single cysteine	A- - -	1 (*i*)	AF (*i*)
	j-single cysteine	- - -A	1 (*j*)	AF (*j*)
donor-acceptor (D-PGK-A)	*i*, *j* specific label	D → A	2 (*i*, *j*)	AEDANS (*i*) and AF (*j*)
	j, *i* specific label	A ← D	2 (*i*, *j*)	AEDANS (*j*) and AF (*i*)
	i, *j* average label	D → A + A ← D	2 (*i*, *j*)	AEDANS (*i*) and AF (*j*) and + AEDANS (*j*) and AF (*i*)

Lifetime measurements were carried out on all samples

Table 5: Comparison of the Measured FRET Distances with That Predicted from the Crystal Structure[e]

energy-transfer pair	measured steady-state distance (Å)	measured time-resolved discrete distance		measured time-resolved distance distribution			crystal structure $C_\alpha \rightarrow C_\alpha$ (Å)[a]	estimated dye-to-dye distances (Å)[b]
		R (Å)	χ^2	R_c (Å) [±2]	σ (Å)	χ^2		
135 ↔ 290	43	43.3	2.7	39.4	7.3	1.3	39	39
		40.3[c]	1.6	38.8[c]	6.1	1.2		
135 ↔ 412	40	40.4	2.7	39.5	3.8	1.3	40	46
412 → 135	40	39.5	2.1	38.0	3.9	1.2		
		38.7	1.4	38.1[c]	3.4	1.3		
290 ↔ 412	69	63.6	1.4	64.8	13.5	1.3	48	56
		56.6[c]	1.8	58.6[c]	13.2	1.4		
75 ↔ 290	50	51.7	4.3	46.6	13.5	1.2	40	46
202 ↔ 412	39	41.7	1.5	37.8	6.6	1.1	26	34
412 → 75	47	48.2	3.1	44.8	13.5	1.4	32	46
all[d]	–	60–70	1.1	60–80	15–30	1.1	–	–

[a] Watson et al. (1982). [b] Donor-to-acceptor distance from MD simulations based on Watson et al. (1982) crystal structure. [c] Acceptor-side FRET measurements. [d] Unfolded samples (MOPS buffer at pH 7.5 and 25 °C and 2 M GuHCl). [e] MOPS buffer at pH 7.5 and 25 °C. D ↔ A: average labeled samples (donor distributed between the two Cys sites). D → A: specific labeled samples. Unless otherwise indicated, distance determinations are from donor-side experiments. The errors on the recovered distances are dominated by "nonfitting" sources and are estimated to be ±3 Å (see the text).

The intramolecular distances for the six energy transfer pairs are recovered for the each intermediate formed during the GuHCL induced unfolding of PGK

The authors proposed a specific structural transition associated with the unfolding of PGK from the native state (left) to the first unfolded state (right).

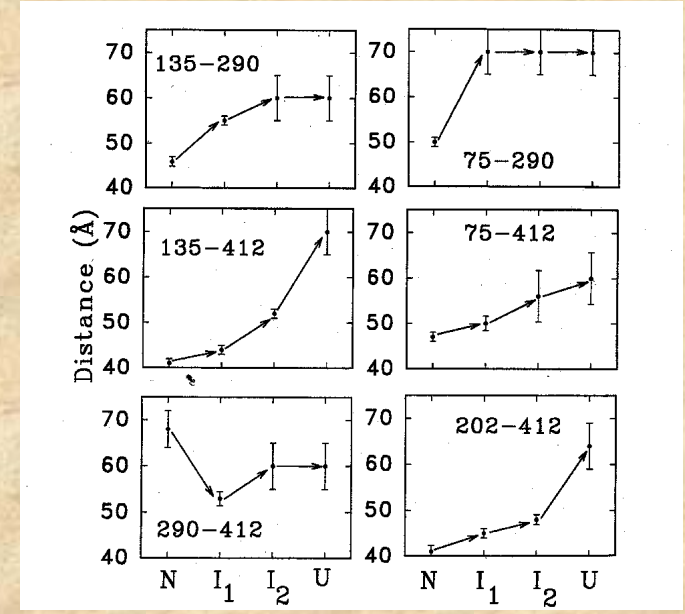

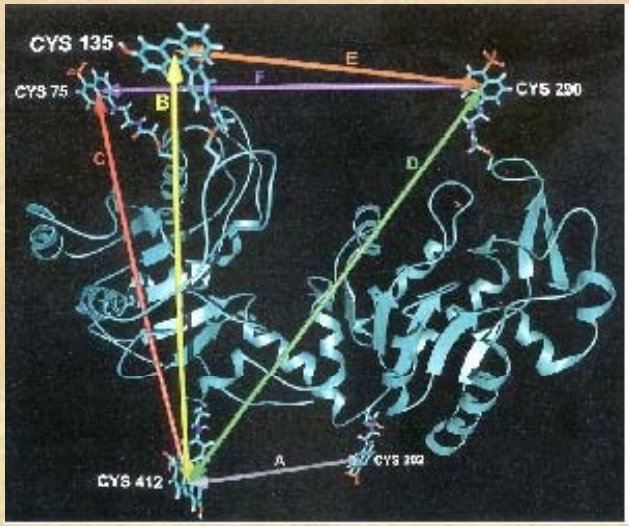

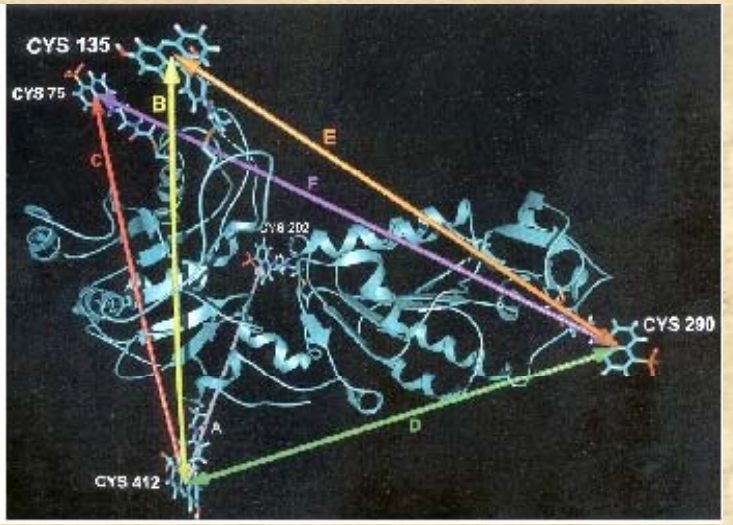

The C terminal domain (on the right of the monomer) is twisted by approximately 90º relative to the N-terminal domain resulting in an increase in the distances A,E and F and a shortening of the distance D.

The orientation factor κ^2

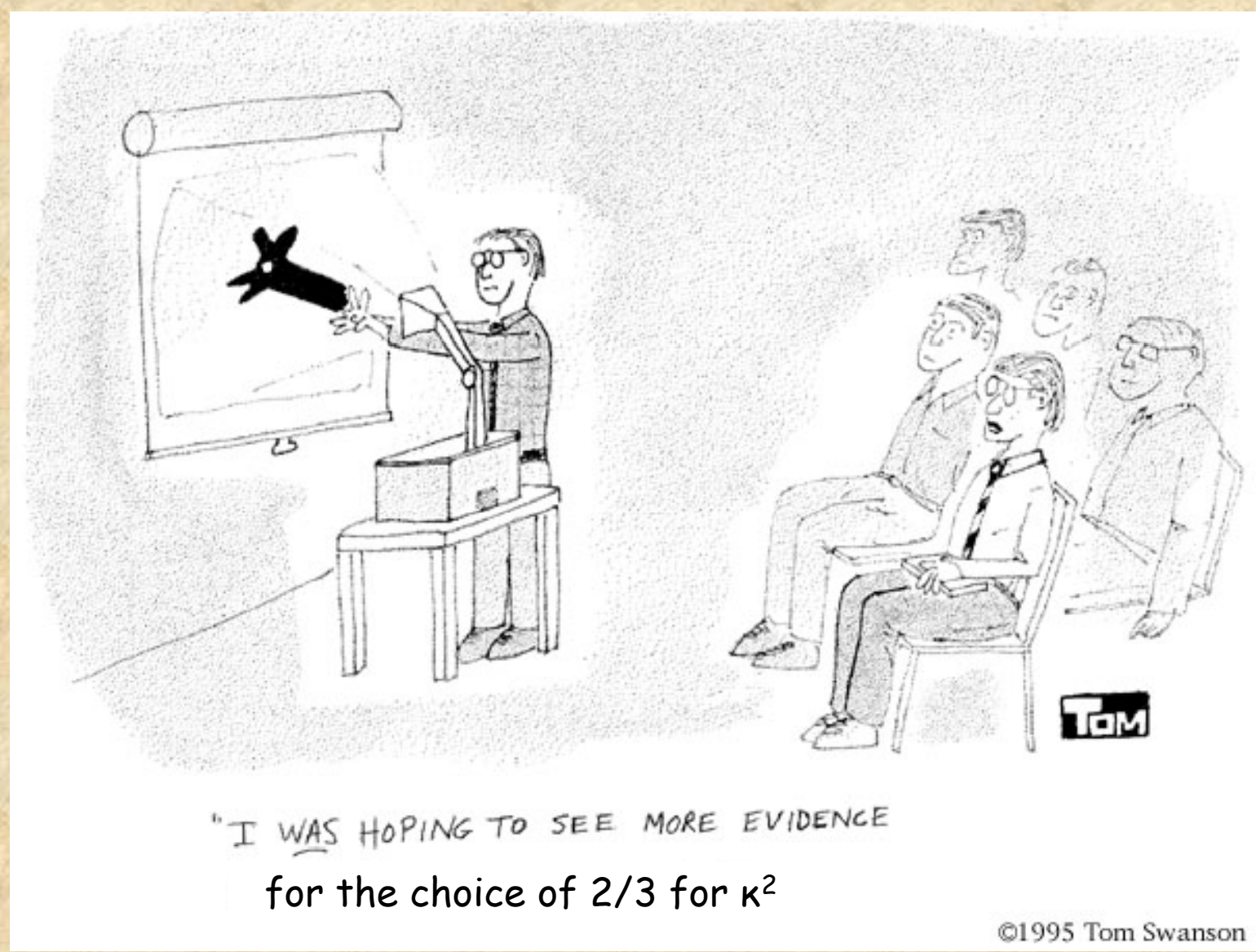

for the choice of 2/3 for κ^2

The orientation factor κ^2

$$\kappa^2 = (\cos\theta_T - 3\cos\theta_D \cos\theta_A)^2$$

Where θ_T is the angle between the D and A moments, given by

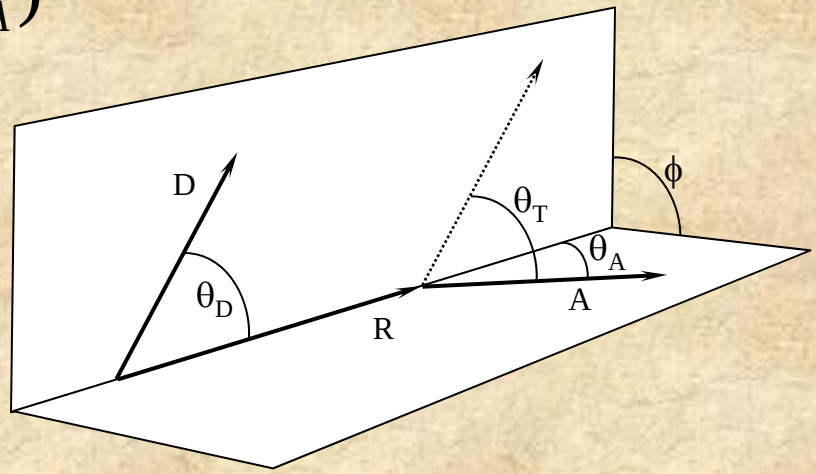

$$\cos\theta_T = \sin\theta_D \sin\theta_A \cos\phi + \cos\theta_D \cos\theta_A$$

In which θ_D, θ_A are the angles between the separation vector R, and the D and A moment, respectively, and ϕ is the azimuth between the planes (D,R) and (A,R)

The orientation factor κ^2

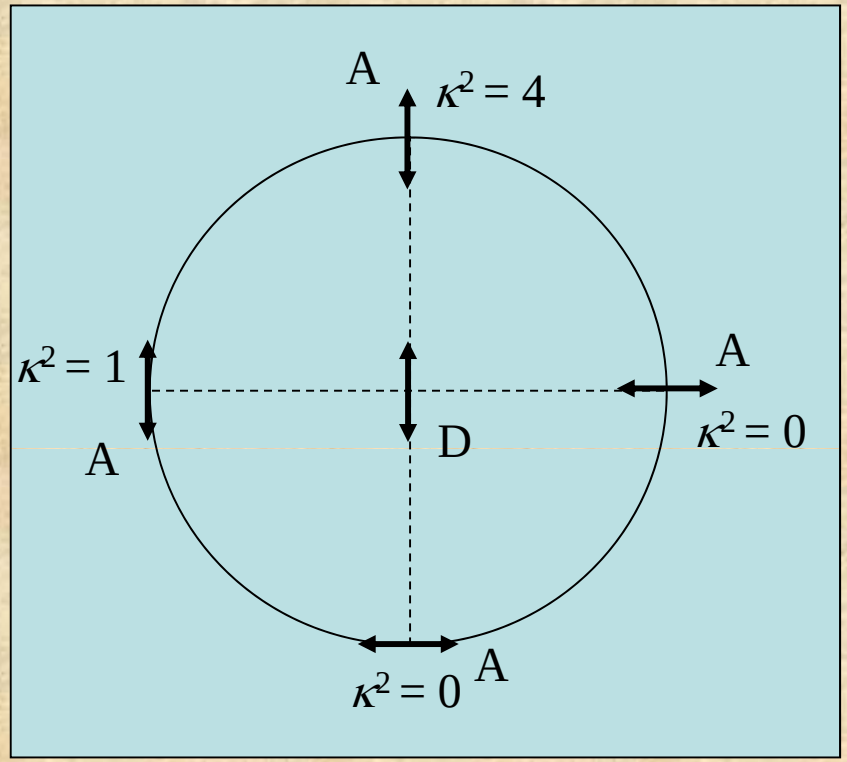

The limits for κ^2 are 0 to 4, The value of 4 is only obtained when both transitions moments are in line with the vector R. The value of 0 can be achieved in many different ways.

If the molecules undergo fast isotropic motions (dynamic averaging) then $\kappa^2 = 2/3$

From Eisinger and Dale in:"Excited States of Biological Molecules" Edited by John Birks (1976)

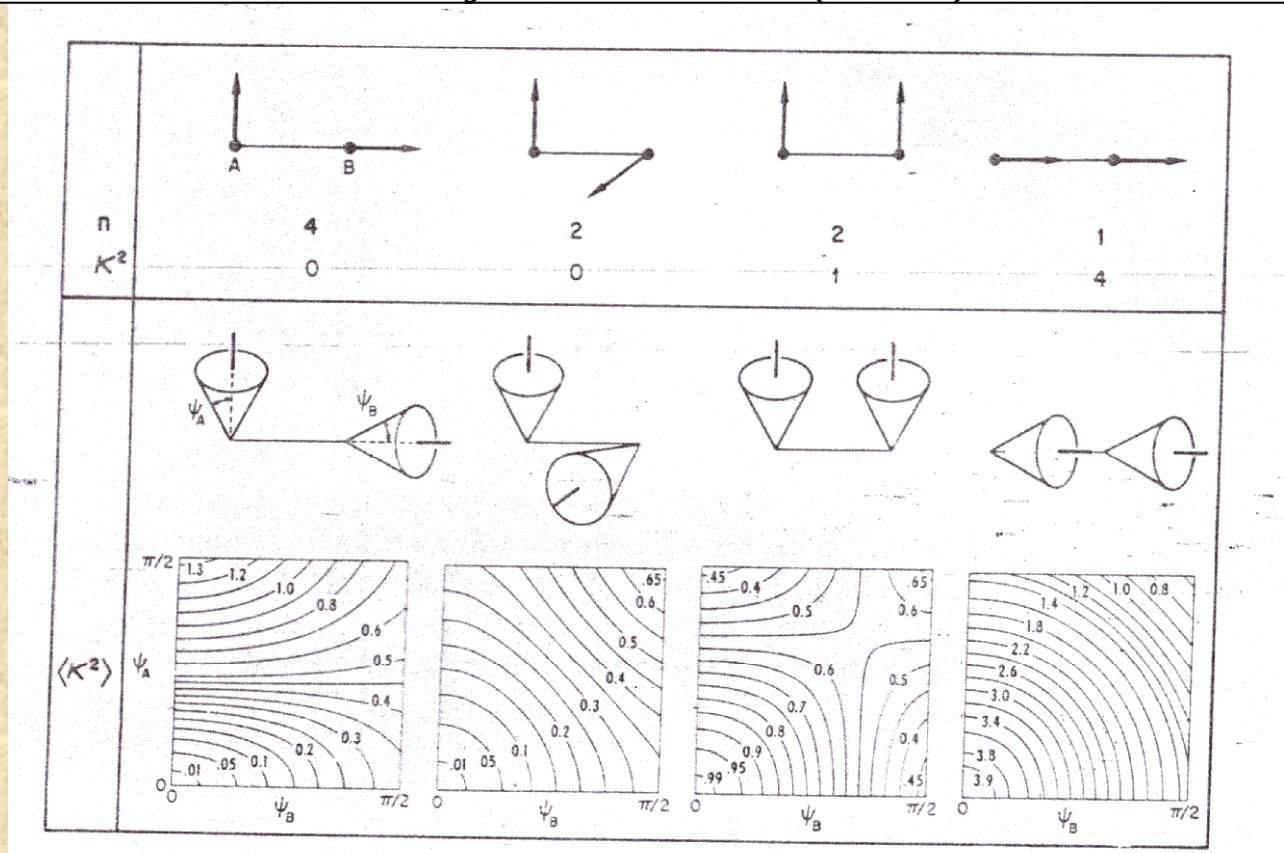

Figure 1 The upper part of the diagram illustrates the nine possible relative orientations of two transition dipoles each of which is fixed and can lie along either the x, y or z axis of a Cartesian triad. The corresponding κ^2 values are shown along with their statistical weights (n) and they are seen to lead to an average for κ^2 of 2/3, the same as for isotropically random orientations of the transition dipole moments. The lower part of the figure illustrates how these $\langle\kappa^2\rangle$ values change as the transition dipole directions are permitted orientational freedom within cones of half-angles ψ_A and ψ_B. Note that $\langle\kappa^2\rangle$ departs quite slowly from its fixed minimum and maximum values (0 and 4) as the two cones open up and that when each cone half-angle is $\pi/2$, corresponding to an isotropic distribution of the transition dipole directions, $\langle\kappa^2\rangle$ is equal to 2/3 for each of the cases considered

What if the system is static but randomly oriented?

For example for a system in a highly viscous solvent or in general if the fluorescence lifetimes are very short relative to any rotational motion.

Then $\kappa^2 = 0.476$

THE JOURNAL OF CHEMICAL PHYSICS VOLUME 48, NUMBER 6 15 MARCH 1968

Nonradiative Energy Transfer in Systems in which Rotatory Brownian Motion is Frozen

IZCHAK Z. STEINBERG

The Weizmann Institute of Science, Rehovoth, Israel

(Received 28 August 1967)

The effect of the complete restriction of rotatory Brownian motion of donor and acceptor molecules on the extent of nonradiative energy transfer in systems containing many donors and acceptors has been investigated. It is assumed that the molecules under discussion are randomly distributed and randomly oriented in space at the moment of excitation. The number of donor molecules which retain their excitation energy at time t after excitation is found to decrease exponentially with the sum of two terms: one proportional to t and the other proportional to $t^{1/2}$. This time dependence is similar in form to that found by Förster for systems in which donor and acceptor molecules undergo rapid rotatory diffusion. While the coefficient of $-t$ in the exponent is the same in both cases, the coefficient of $-t^{1/2}$ is smaller for systems in which molecular rotation is frozen than for systems in which rotatory Brownian motion is rapid.

But don't ask me to prove it!

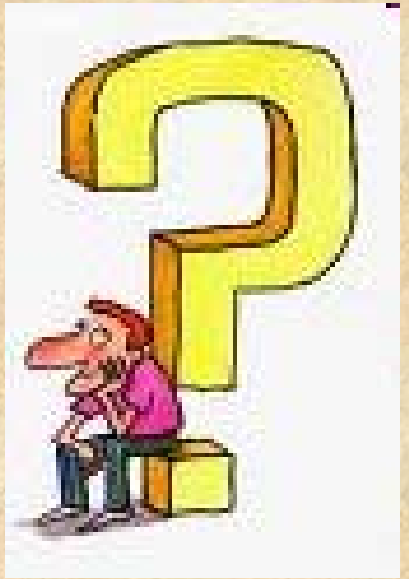

So how do we determine κ^2?

Except in very rare cases, κ^2 can not be uniquely determined in solution.

What value of κ^2 should be used ?

We can **assume** fast isotropic motions of the probes and value of $\kappa^2 = 2/3$, and verify experimentally that it is indeed the case.

We can **calculate** the lower and upper limit of κ^2 using polarization spectroscopy (Dale, Eisinger and Blumberg 1979).

Assuming $\kappa^2 = 2/3$

We can test this assumption experimentally:

***By swapping probes*:** The micro-environment of the probes will be different. Therefore, if the micro-environment affect the probes mobility and, κ^2 is not equal to 2/3, once swapped, the value of κ^2 will changed and hence the distance measured by FRET.

By using different probes: If the distance measured using different probe pairs are similar (taking into account the size of the probes) then the assumption that κ^2 is equal to 2/3 is probably valid.

Lower and upper limit of κ^2

We can **<u>calculate</u>** the lower and upper limit of κ^2 using polarization (Dale, Eisinger and Blumberg 1979).

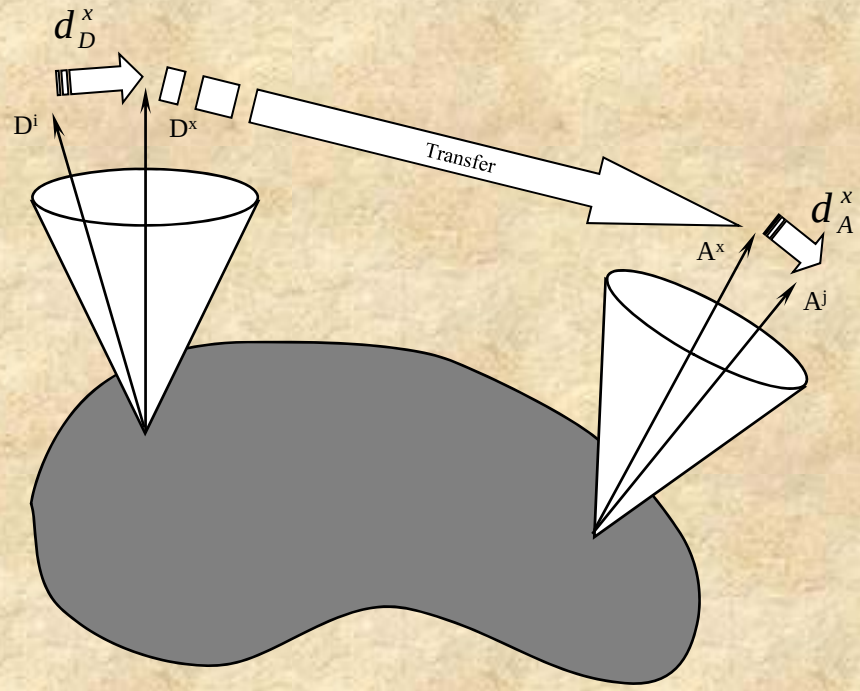

Lets consider that the each probe are rotating within a cone of axes D^x and A^x for the donor and acceptor, respectively, then 3 depolarization steps occurs after the absorption of the excitation energy by the donor: An axial depolarization of the donor, a depolarization due to transfer and an axial depolarization of the acceptor

In the Dale-Eisinger-Blumberg approach, one measures the ratio of the observed polarizations of donors and acceptors to their limiting polarizations and then uses the calculated contour plots to put limits on κ^2

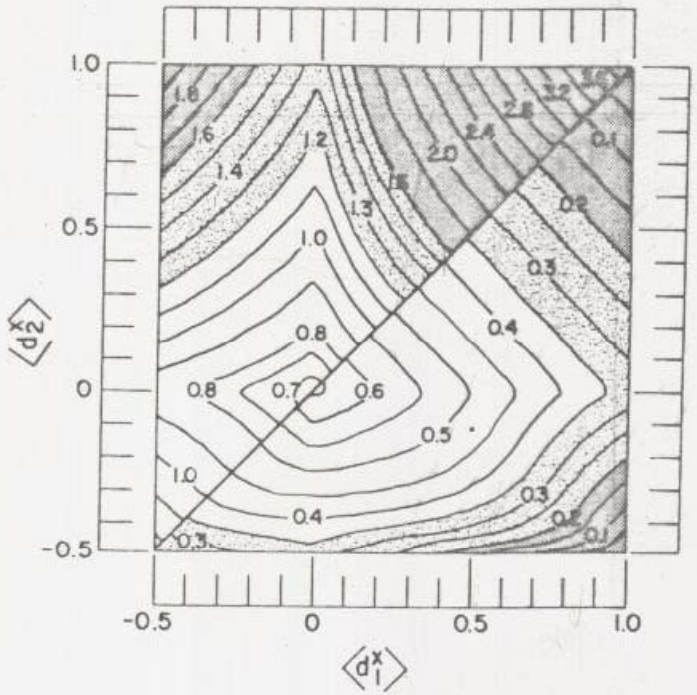

FIGURE 9 Contour plot similar to those shown in Figs. 4–8, but applicable in situations in which $\langle d_T \rangle$, and hence d_T^x, is unknown. It is obtained by maximizing and minimizing Eq. 21 and can be seen to lead to larger ranges between $\langle \kappa^2 \rangle_{min}$ and $\langle \kappa^2 \rangle_{max}$ than the plots of Figs. 4–8. In the heavily stippled regions the error in R resulting from the use of $\langle \kappa^2 \rangle = \frac{2}{3}$ instead of the indicated $\langle \kappa^2 \rangle_{min}$ and $\langle \kappa^2 \rangle_{max}$ is greater than 20%. It is between 10% and 20% in the lightly stippled regions and less than 10% in the unstippled ones.

This approach was used in:
Arbildua et al.,
Fluorescence resonance energy transfer and molecular modeling studies on 4',6-diamidino-2-phenylindole (DAPI) complexes with tubulin.
Protein Sci. (2006) 15(3):410-9.

FRET occurs between DAPI and TNP-GTP bound to tubulin – a heterodimer protein

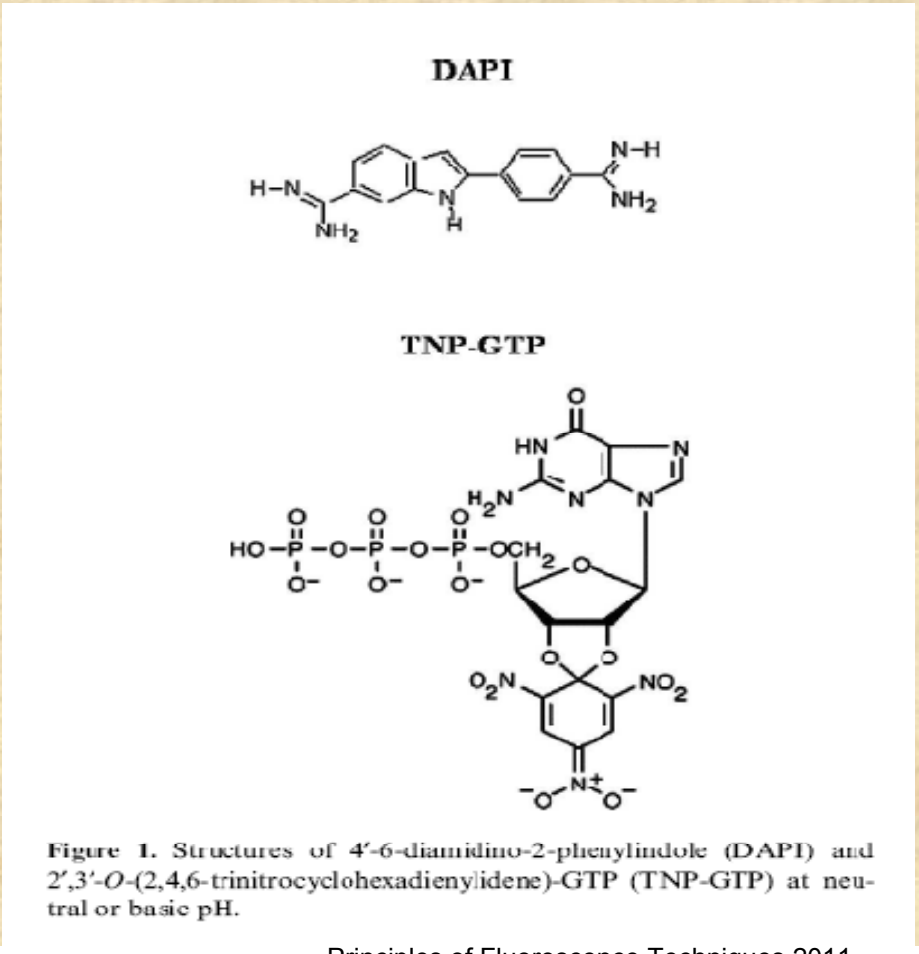

Figure 1. Structures of 4′-6-diamidino-2-phenylindole (DAPI) and 2′,3′-*O*-(2,4,6-trinitrocyclohexadienylidene)-GTP (TNP-GTP) at neutral or basic pH.

Assuming a κ^2 value of 2/3, one would calculate the DAPI-TNP-GTP distance to be ~43 Angstoms

But DAPI is bound non-covalently - hence has no local motion so its polarization is high (~0.42)

And, TNP-GTP is also non-covalently bound and has a short lifetime and hence a high polarization (~0.48)

These observed polarization values are close to the limiting polarization values for these probes: 93% and 100% respectively, for DAPI and TNP-GTP

Using the Dale-Eisenger-Blumberg plot one can then estimate that κ^2 can be anywhere between 0.02 and 3.7!

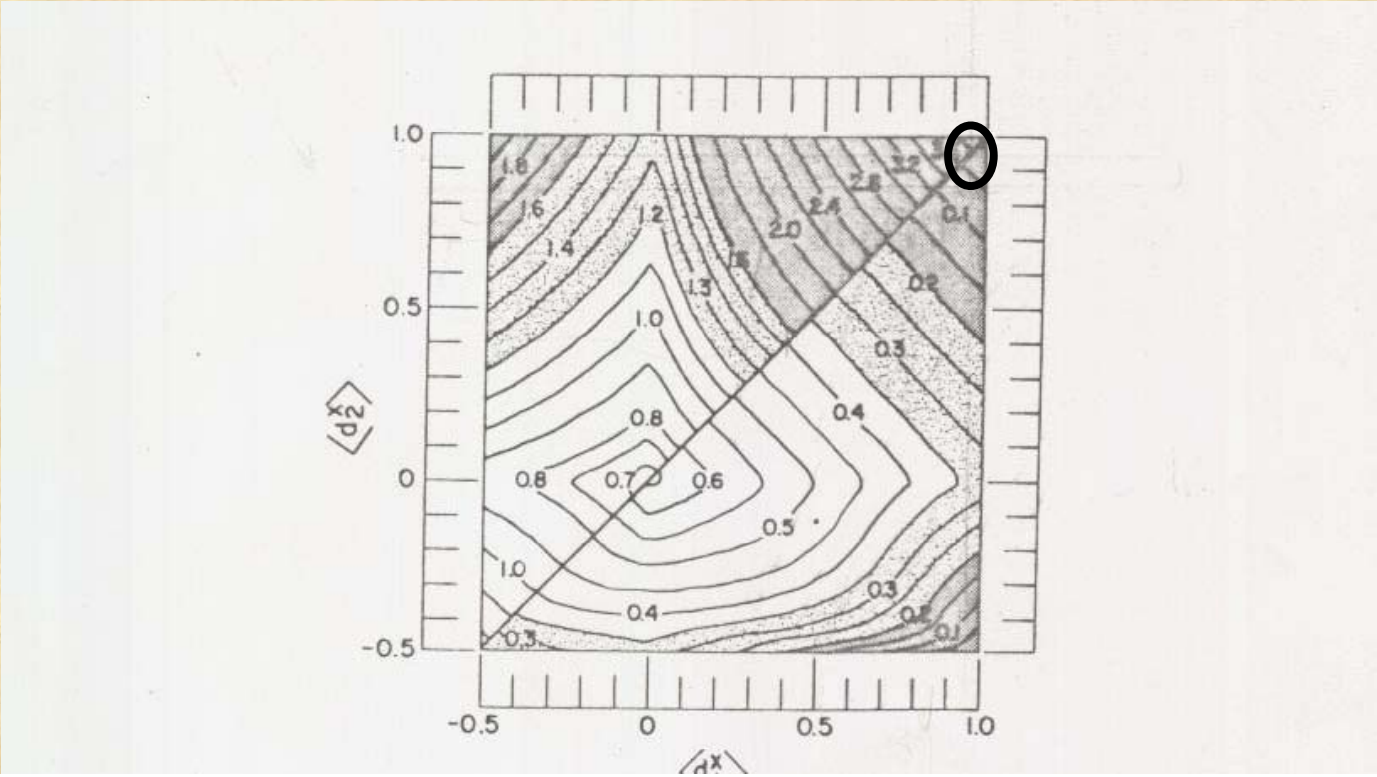

In fact the authors concluded, based on other information, that the distance between DAPI and TNP-GTP bound to tubulin was likely to ~ 30 Angstroms.

BIOPOLYMERS VOL. 13, 1607–1620 (1974)

Energy Transfer in tRNA^{Phe} (Yeast). The Solution Structure of Transfer RNA

W. E. BLUMBERG, R. E. DALE,* J. EISINGER, and
D. M. ZUCKERMAN, *Bell Laboratories, Inc.,*
Murray Hill, New Jersey 07974

TABLE II
Maximum and Minimum Values of the Orientation Factor and Ratio of Derived Separation R to that Obtained Using the Dynamic Random Average (Isotropic) Value $R_{2/3}$

Model[a]		Figure[a]	$Y-A$	$\langle\kappa^2\rangle$	$R/R_{2/3}$
4(1)	*cc*	10	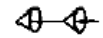	3.13 ± 0.08	1.29 ± 0.01
	cC	11	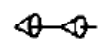	3.13 ± 0.08	1.29 ± 0.01
	Cc	11	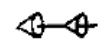	3.13 ± 0.08	1.29 ± 0.01
	CC	12	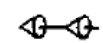	3.13 ± 0.08	1.29 ± 0.01
4(2)	*cc*	13	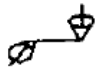	0.115 ± 0.012	0.75 ± 0.01
	cC	14	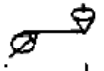	0.115 ± 0.012	0.75 ± 0.01
	Cc	14	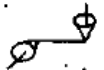	0.115 ± 0.012	0.75 ± 0.01
	CC	15	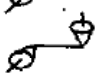	0.115 ± 0.012	0.75 ± 0.01

CCA Terminus—Anticodon Separation

Assuming an average value of 2/3 for κ^2, Beardsley and Cantor[2] estimated the separation between the *Y* base adjacent to the anticodon and acriflavine bound at the CCA terminus of $tRNA^{Phe}$ (yeast) to be about 46 Å. The analysis presented here indicates a possible range of 34–61 Å at the most.

Taking into account the uncertainty in the location of the acriflavine chromophore with respect to the CCA stem (as indicated above it may well be intercalated back into a nearby double-helical region, not necessarily in the CCA limb), the upper limit is reasonably consistent with the 77 Å separation between the extended CCA terminus and the anticodon triplet recently determined by X-ray crystallography.[2]

Quantitative distance determinations using FRET – i.e., as a true “spectroscopic ruler” - remain **difficult at best**

But FRET can be very powerful when used to detect changes in a system, such as alterations in distance and or orientation between donor and acceptor attached to biomolecules, i.e., due to ligand binding or protein-protein interactions

The renaissance of fluorescence resonance energy transfer

Paul R. Selvin

Recent advances in fluorescence resonance energy transfer have led to qualitative and quantitative improvements in the technique, including increased spatial resolution, distance range, and sensitivity. These advances, due largely to new fluorescent dyes, but also to new optical methods and instrumentation, have opened up new biological applications.

nature structural biology • volume 7 number 9 • september 2000

The development of Fluorescent Proteins has led to a significant increase in FRET studies

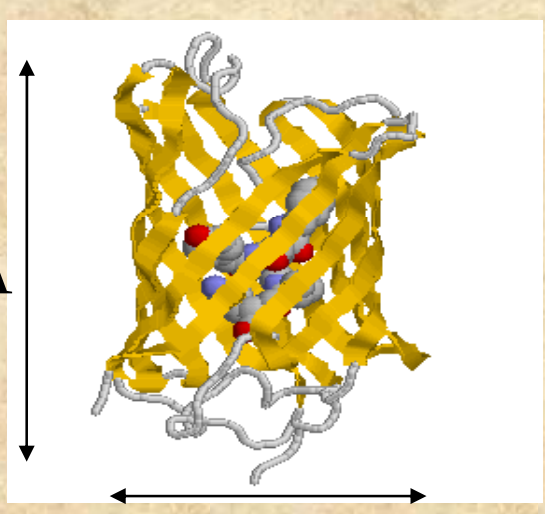

The GFP is fused to the protein of interest and expressed in the organism under study.

Fluorescent proteins with the appropriate absorption and emission properties are chosen as donors and acceptors. Such systems can be used in vitro as well as in vivo

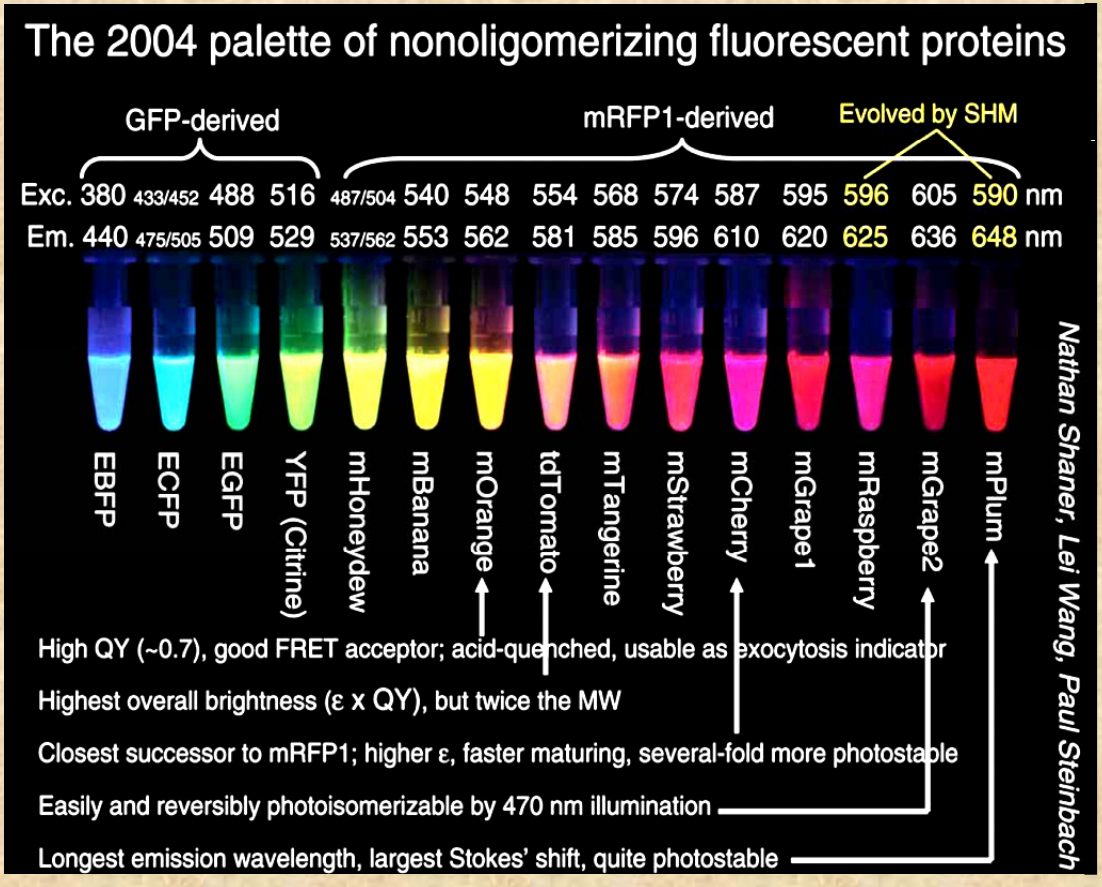

Homo-transfer of electronic excitation energy

So far, we considered the donor and acceptor molecules to be different.However, if the probe excitation spectrum overlaps its emission spectrum, FRET can occur between identical molecules.

« Il suffit qu'un transfert d'activation puisse se produire entre deux molécules voisines d'orientation différentes, c'est a dire portant des oscillateurs non parallèles, pour qu'il en résulte en moyenne une diminution de l'anisotropie de distribution des oscillateurs excites et par suite de la polarisation de la lumière émise. »

(F. Perrin *Ann de Phys.* 1929)

It suffices that a transfer of activation can occur between two neighboring molecules with different orientations, that is with non-parallel oscillators, in order to have, on average, a decrease in the anisotropy of the distribution of excited oscillators, and therefore a decrease of the polarization of the emitted light.

« …L'existence de transferts d'activation est expérimentalement prouvée pour de telles molécules par la décroissance de la polarisation de la lumière de fluorescence quand la concentration croit… »
(F. Perrin *Ann de Phys*. 1932)

…The existence of transfer of activation is proven experimentally for such molecules by the decrease in polarization of the fluorescent light when the concentration is increased…

Electronic energy transfer between identical fluorophores was originally observed by Gaviola and Pringsheim in 1924.

Über den Einfluß der Konzentration auf die Polarisation der Fluoreszenz von Farbstofflösungen.

Von **E. Gaviola** und **Peter Pringsheim** in Berlin.

Mit zwei Abbildungen. (Eingegangen am 24. März 1924.)

Tabelle 2. Uranin in ganz wasserfreiem Glycerin.

C	p	C	p	C	p	C	p
$\frac{1}{4}$	0	$\frac{1}{32}$	6,5	$\frac{1}{256}$	15	$\frac{1}{2048}$	39,2
$\frac{1}{8}$	?	$\frac{1}{64}$	8,1	$\frac{1}{512}$	19,5	$\frac{1}{4100}$	43,5
$\frac{1}{16}$	3,2	$\frac{1}{128}$	11,1	$\frac{1}{1024}$	30,7	etwa $\frac{1}{20000}$	45

(note: uranin is the sodium salt of fluorescein)

Homo-transfer of electronic excitation energy

"…Excitation transfer between alike molecules can occur in repeated steps. So the excitation may *migrate* from the absorbing molecule over a considerable number of other ones before deactivation occurs by fluorescence or other process. Though this kind of transfer cannot be recognized from fluorescence spectra, it may be observed by the decrease of fluorescence polarization…" (Förster, 1959)

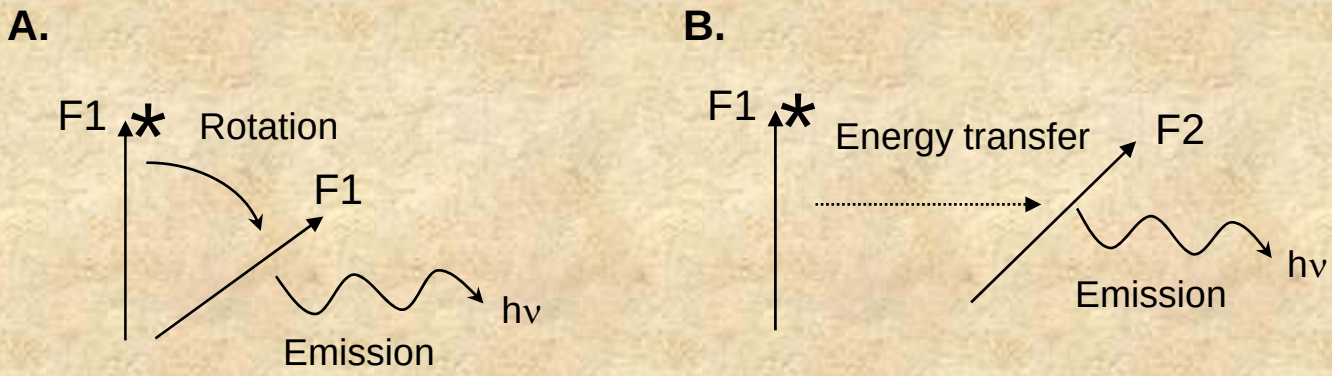

A. Depolarization resulting from rotational diffusion of the fluorophore. The excited fluorophore (F1*) rotates then emits light. **B.** The excited fluorophore (F1*) transfer energy to another fluorophore F2 which in turn emits light.

Weber's Red-Edge Effect

In 1960 Weber was the first to report that homotransfer among indole molecules disappeared upon excitation at the red-edge of the absorption band - this phenomenon is now known as the "Weber red-edge effect".

In 1970 Weber and Shinitzky published a more detailed examination of this phenomenon. They reported that in the many aromatic residues examined, transfer is much decreased or undetectable on excitation at the red edge of the absorption spectrum .

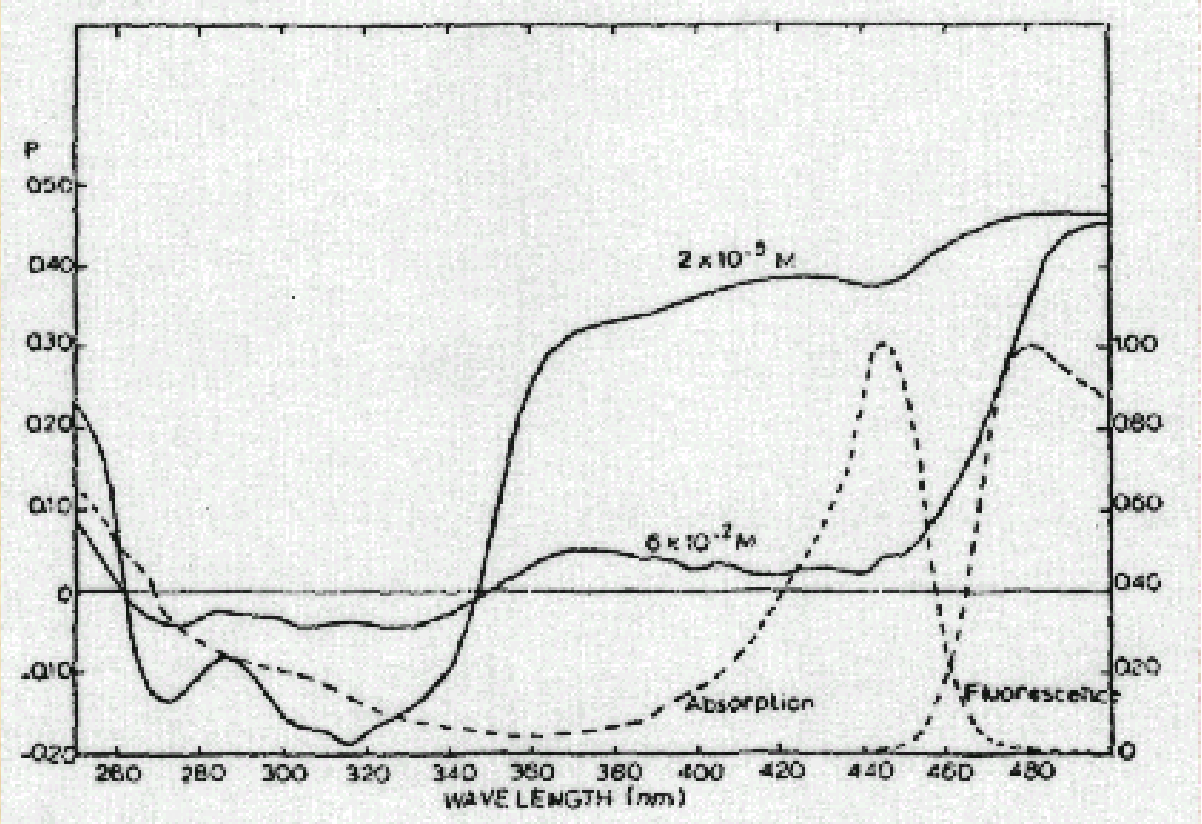

Distance determination using homotransfer

The efficiency of transfer can be calculated from a knowledge of the polarization in the absence and presence of energy transfer.

The steady state expression for the efficiency of energy transfer (*E*) as a function of the anisotropy is given by

$$E = 2(r_d - \langle r \rangle)/(r_d - r_a)$$

Where r_d and r_a are the anisotropy decay of the donor and acceptor only, respectively and $\langle r \rangle$ is the observed anisotropy in presence of both donor and acceptor. If κ^2 =2/3 then r_a = 0 and

$$E = 2(r_d - \langle r \rangle)/r_d$$

An example of homo-FRET used to study protein interactions is the work by Hamman et al (Biochemistry *35*:16680) on a prokaryotic ribosomal protein

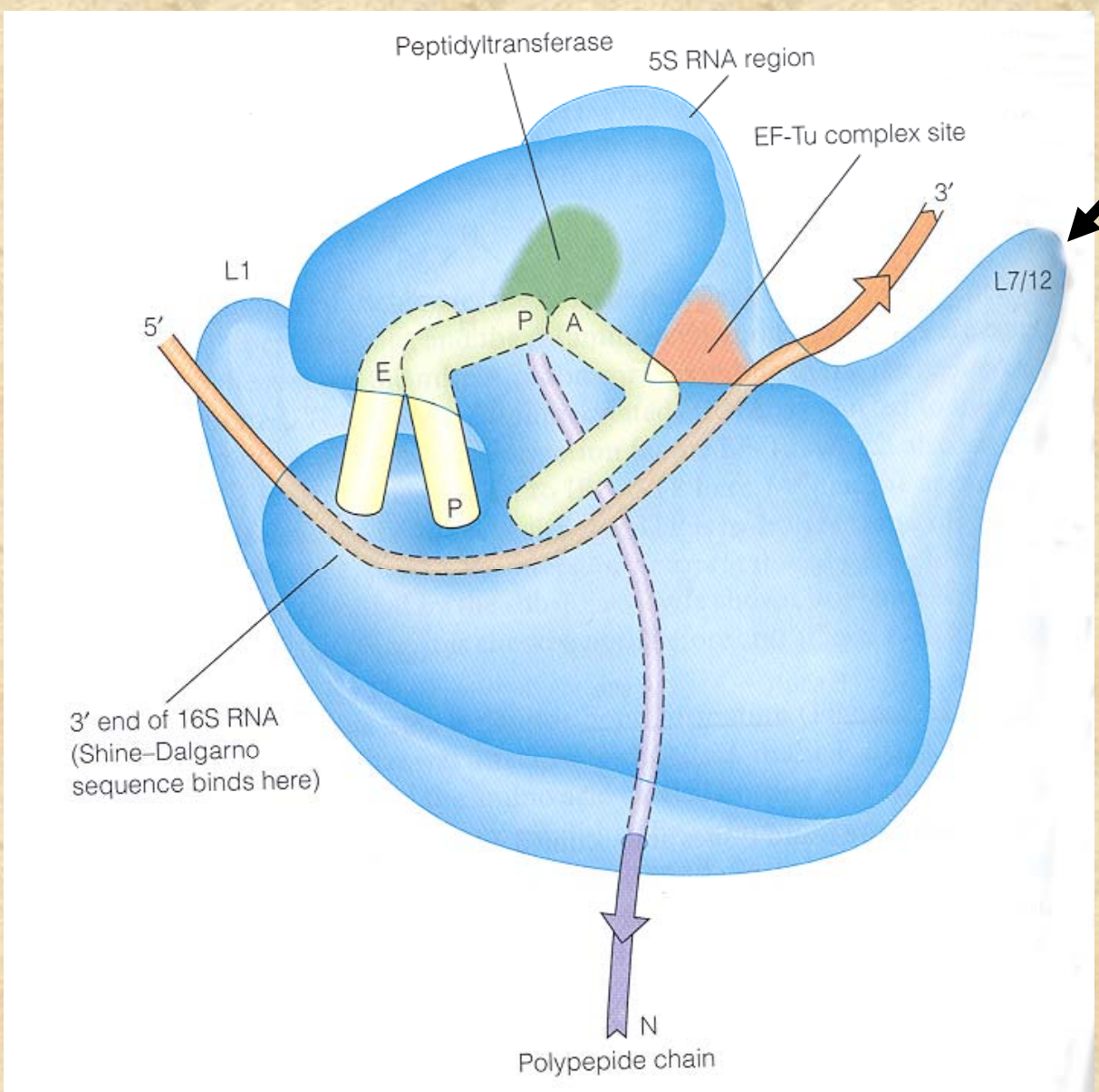

L7/L12 is present as two dimers in the ribosome. An X-ray structure of monomeric C-terminal domains led to the speculation that the C-terminal domains of L7/L12 interacted through hydrophobic surfaces as shown below

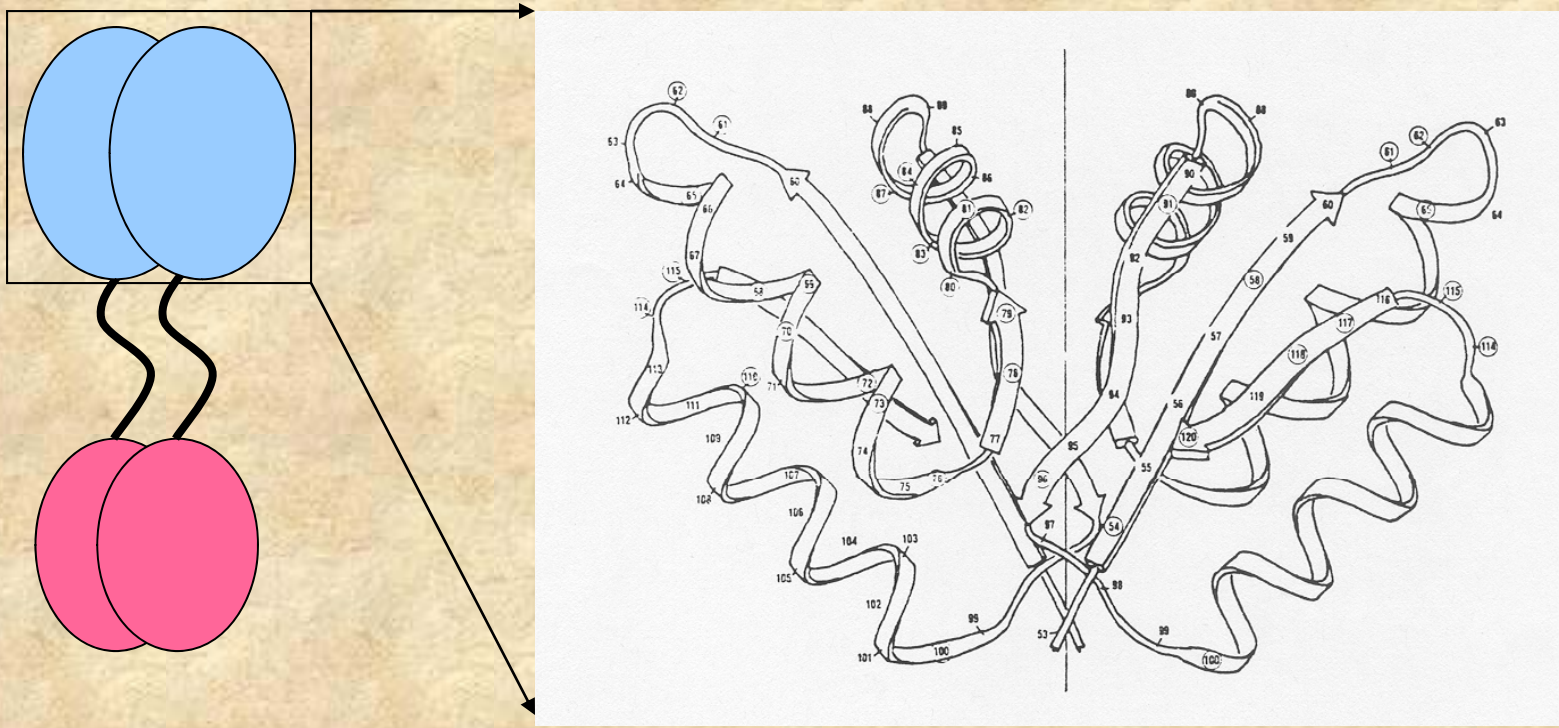

To study this protein fluorescence probes were introduced at specific locations along the L7/L12 peptide backbone.

To introduce these probes at specific locations site-directed mutagenesis was used to place cysteine residues in different locations

Sulfhydryl-reactive fluorescence probes were then covalently attached to these cysteine residues

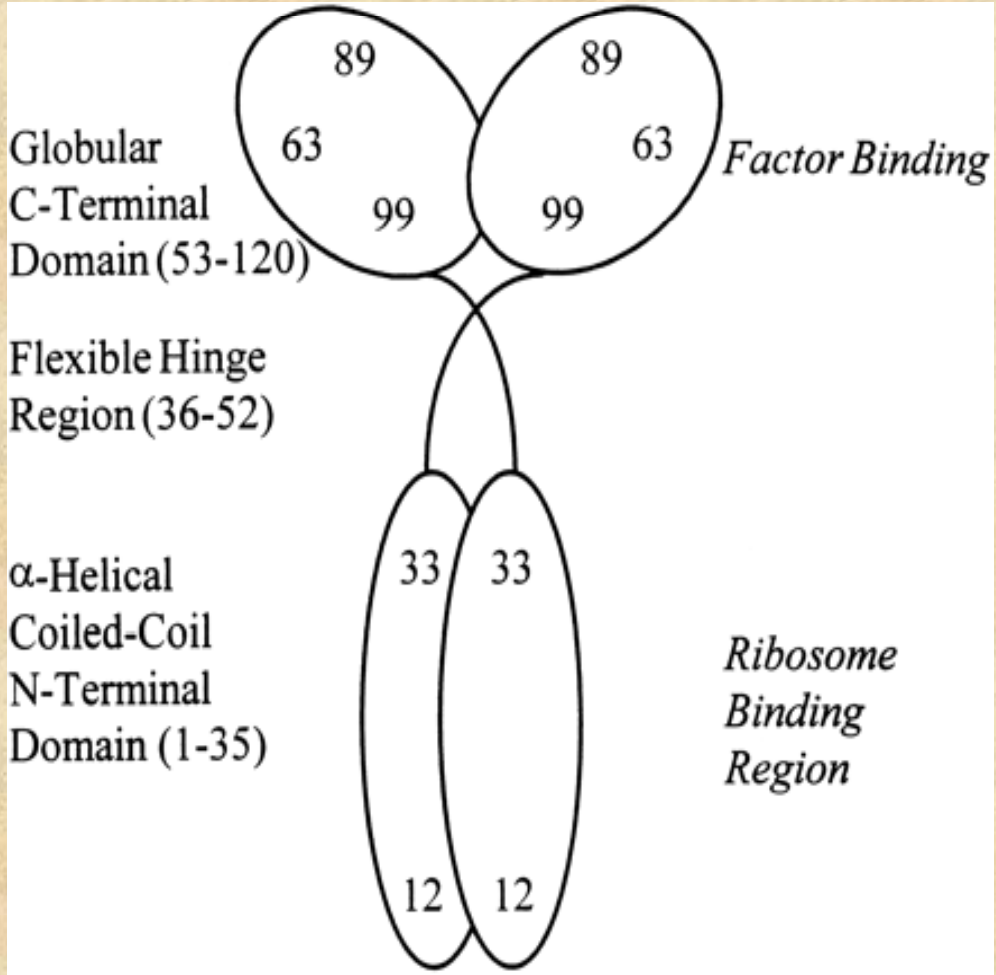

Subunit exchange experiments allowed the preparation of singly labeled dimers

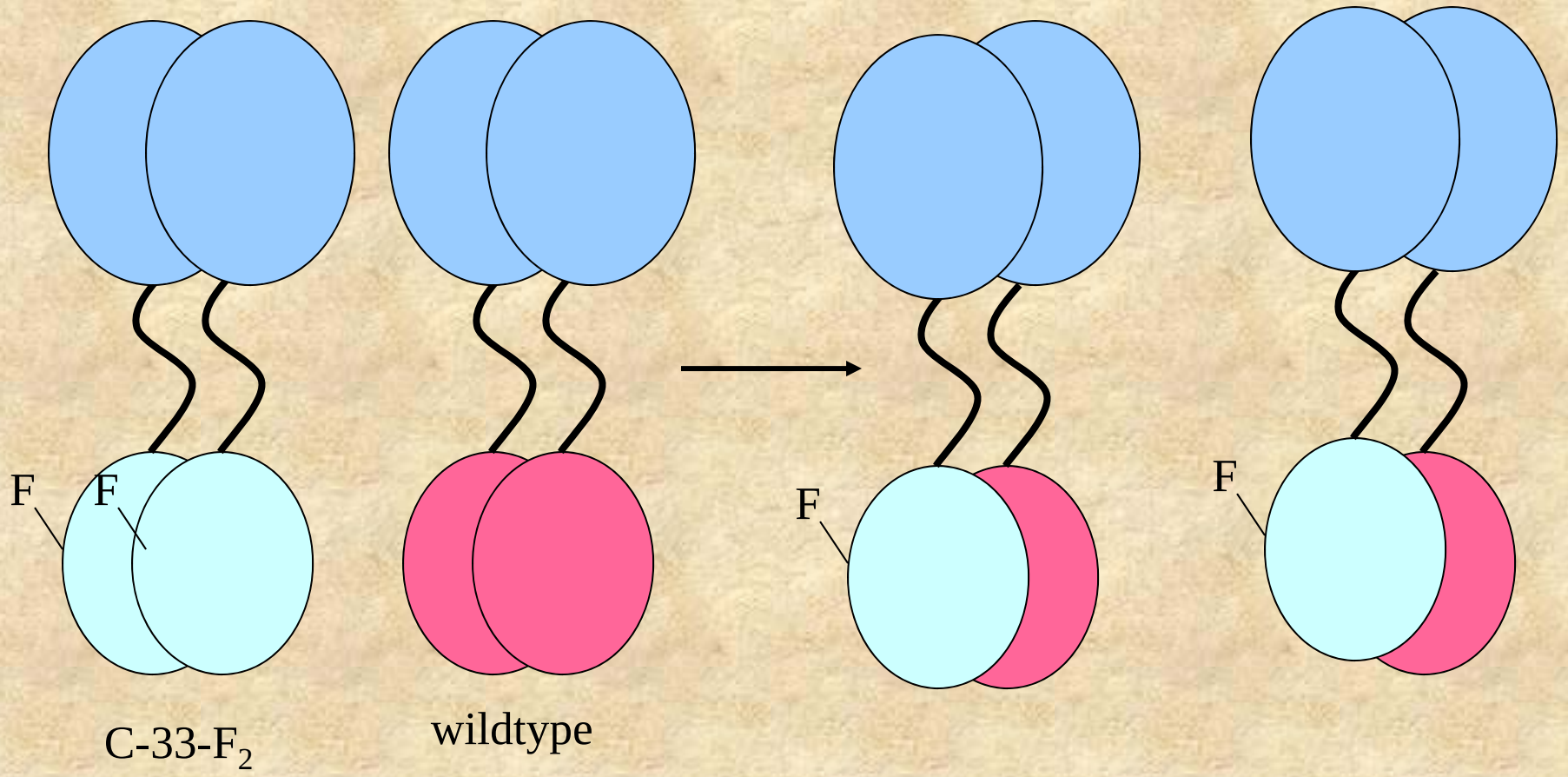

The presence of homoFRET was evident in the excitation polarization spectrum as shown by the Weber Red-Edge Effect.

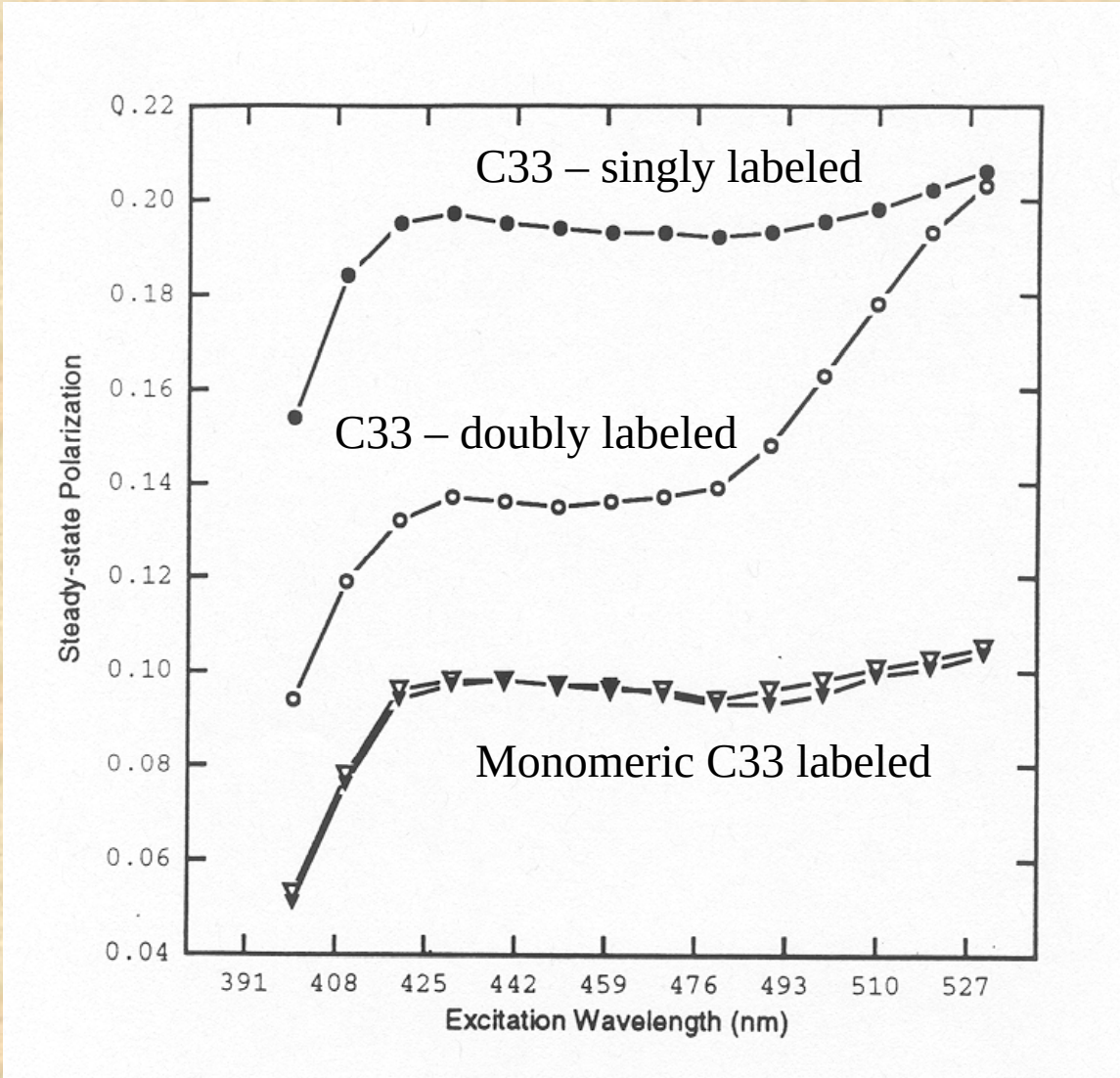

The polarization values, before and after subunit exchange, indicate which residues undergo homoFRET. The polarization data below are for fluorescein labeled constructs before (violet) and after (magenta) subunit exchange

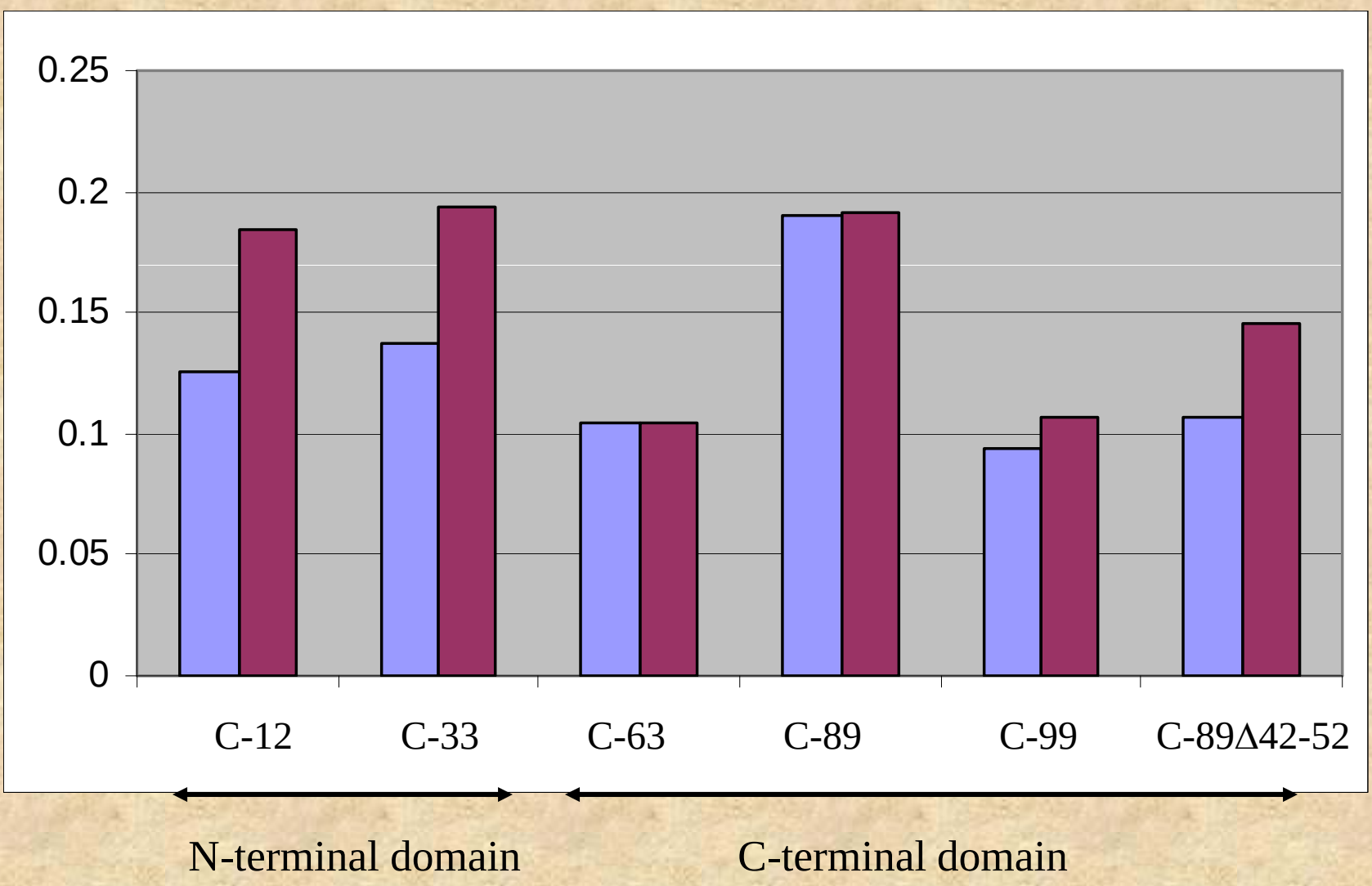

These changes in polarization due to homoFRET allow us to assign maximum proximity values for the C-terminal domains.

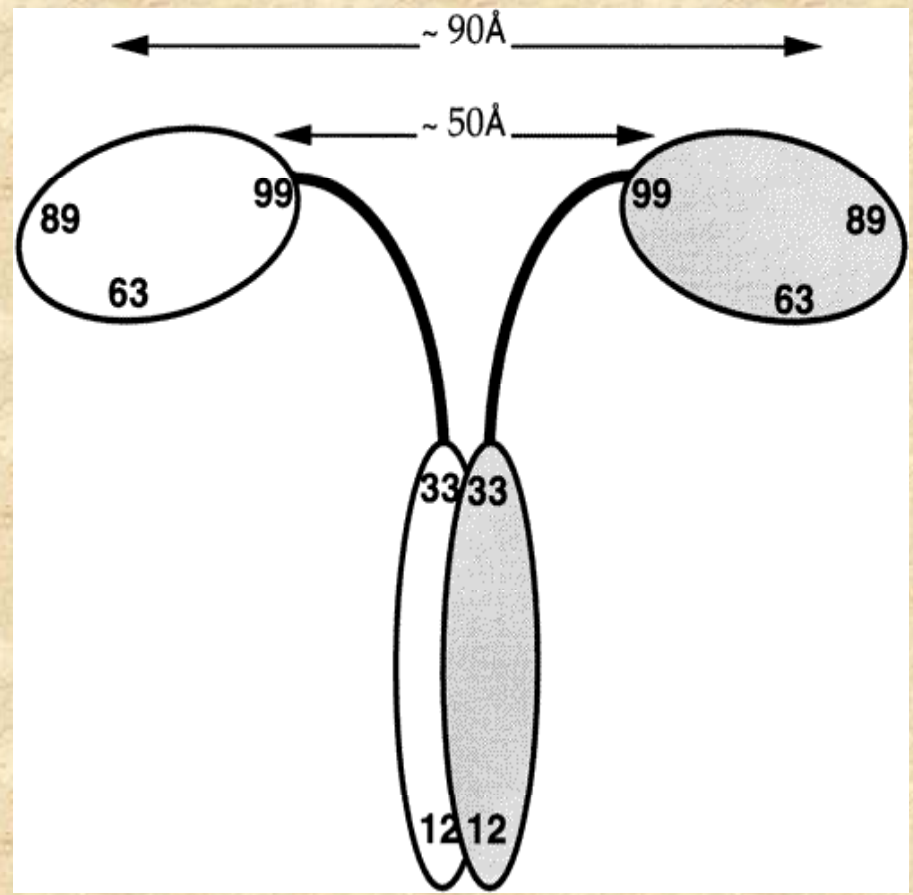

The conclusion is that the C-terminal domains are well-separated – contrary to the original model from the X-ray studies and the usual depictions in the literature

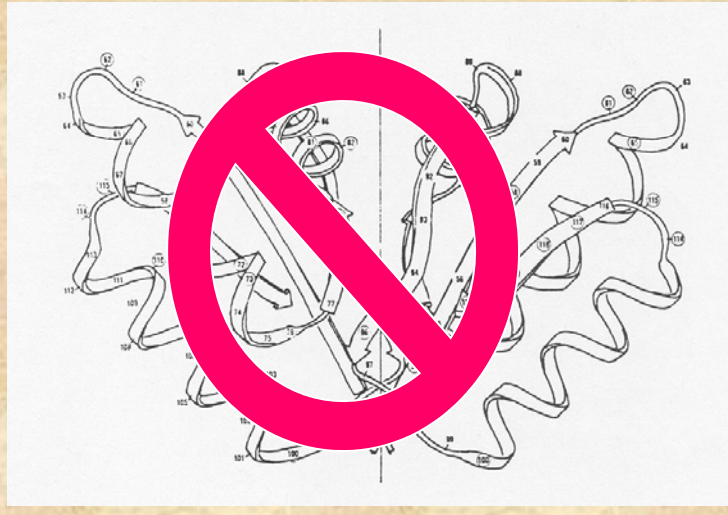

Homo-FRET Microscopy in Living Cells to Measure Monomer-Dimer Transition of GFP-Tagged Proteins

I. Gautier,* M. Tramier,* C. Durieux,* J. Coppey,* F. B. Pansu,† J-C. Nicolas,‡ K. Kemritz,§ and M. Coppey-Moisan*

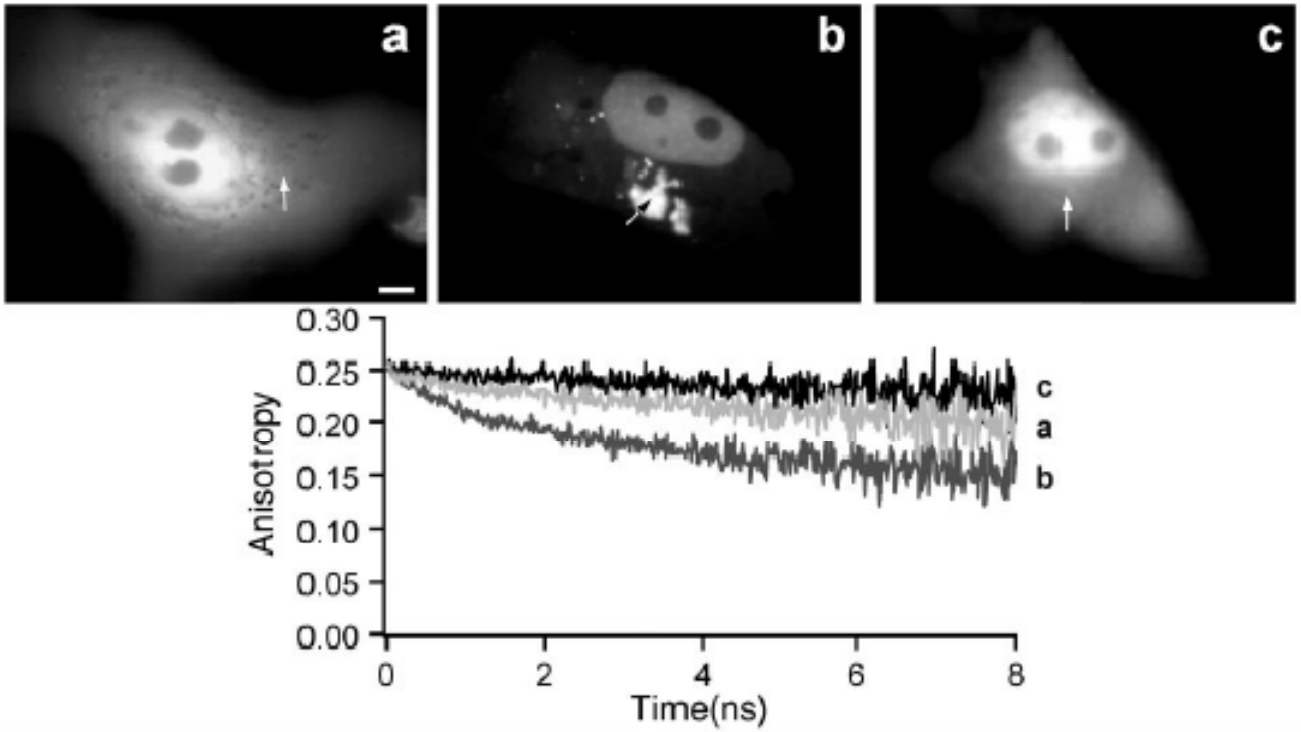

FIGURE 1 Subcellular fluorescence anisotropy decays of $TK_{27}GFP$ and $TK_{366}GFP$ proteins. (*Top*) Steady-state fluorescence images of Vero cells expressing $TK_{27}GFP$ (*a*) and $TK_{366}GFP$ (*b* and *c*). (*a* and *c*) Cells presenting only a diffuse cytoplasmic and nuclear fluorescence pattern; (*b*) Cells containing fluorescent aggregates. (*Bottom*) Time-resolved fluorescence depolarization from a cytoplasmic area of diffuse fluorescence (*a* and *c*) and from an area inside an aggregate (*b*). The subcellular location of the illuminated volume (~1 μm^3) from which the anisotropy decay was performed is indicated by an arrow. For cells containing aggregates, anisotropy decays from nuclear or cytoplasmic area of diffuse fluorescence were similar to that obtained from aggregates (*b*). Bar in *a*, 5 μm.

Biophys J, June 2001, p. 3000-3008, Vol. 80, No. 6

Other examples of homo-FRET *in vivo* can be found in: Tramier et al., 2003 "Homo-FRET versus hetero-FRET to probe homodimers in living cells" Methods Enzymol. 360:580-97.

To summarize this lecture is not intended to prepare you to start FRET measurements immediately but rather to make you aware of the salient principles and pitfalls

Several books on this topic are available as well as MANY articles in the primary literature

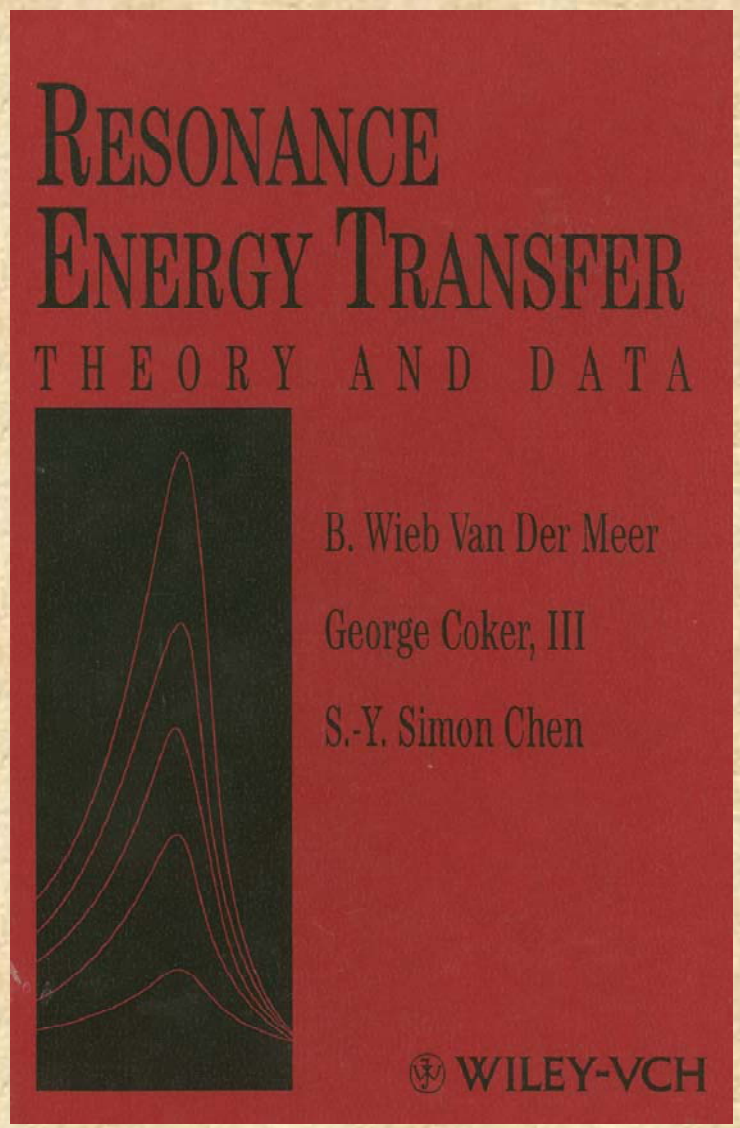

Fluorescence Probes

In vitro *(or In Silico)*

Will be briefly covered now

In vivo (or more accurately in cells)

Will be discussed later in this course by Richard Day

Many of these slides were prepared by
Susana Sanchez
and
Ewald Terpetschnig

Classification:

- Intrinsic Fluorophores
- Extrinsic Fluorophores

Intrinsic Fluorophores

Naturally Occurring Fluorophores

Proteins: Naturally Occurring Fluorophores

Aromatic amino acids

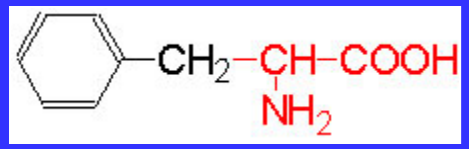

Phenylalanine (Phe – F)
Ex/Em 260 nm/282 nm

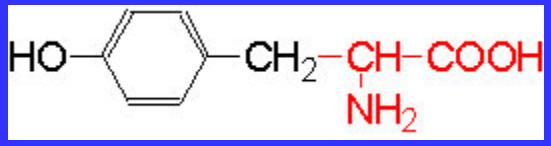

Tyrosine (Tyr – Y)
Ex/Em 280 nm/303 nm

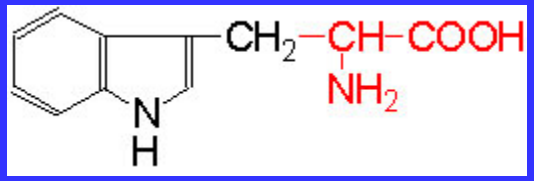

Tryptophan (Trp-W)
Ex/Em 280, 295nm/ 305-350 nm

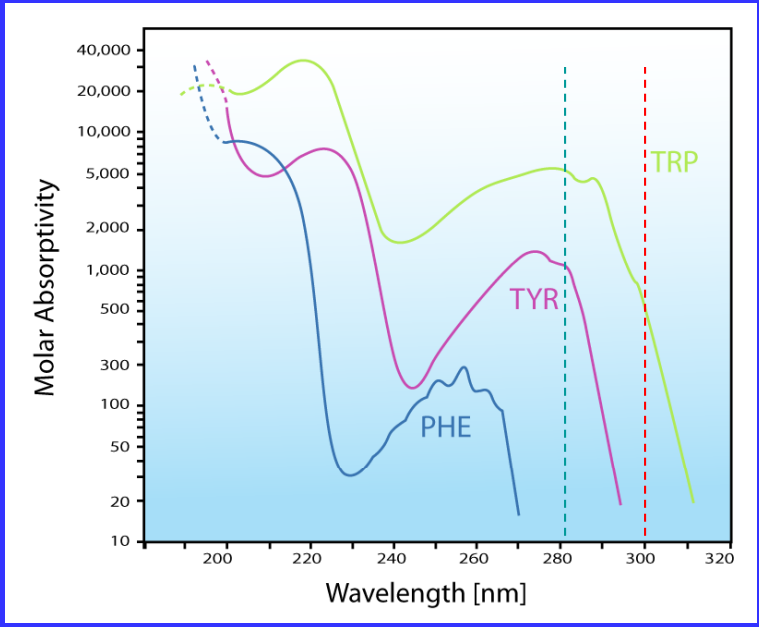

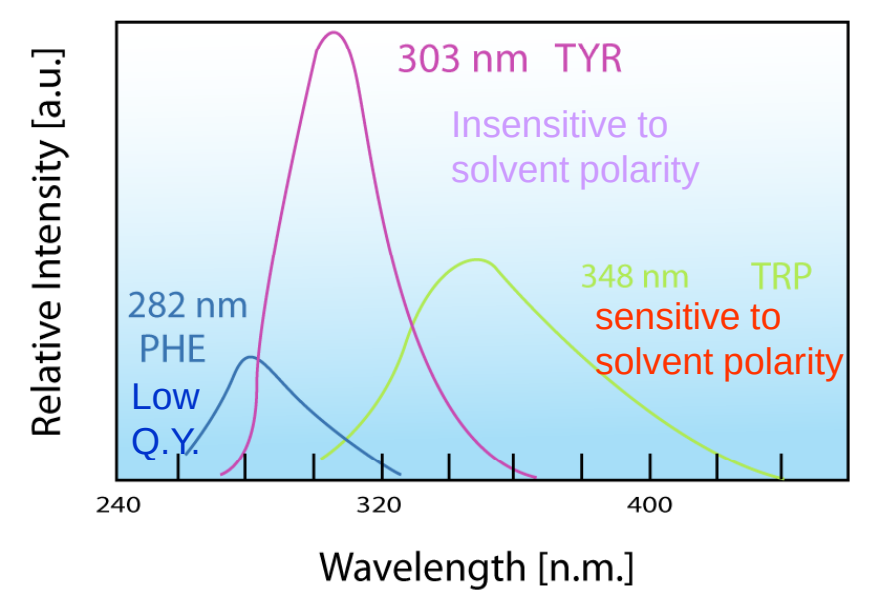

Tryptophan derivatives

Tryptophan derivatives may be genetically incorporated in a protein

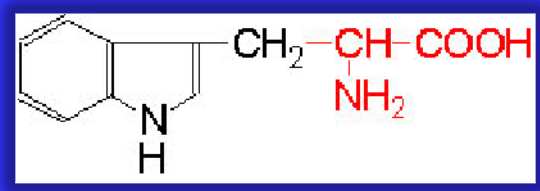

Tryptophan
ex/em 280, 295nm/ 305-350 nm

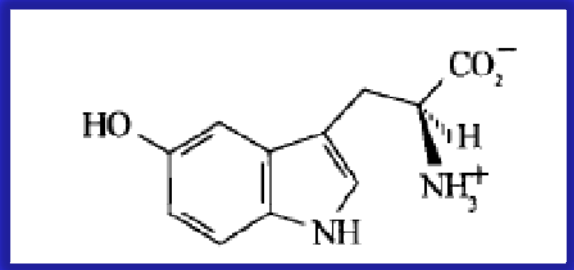

5-Hydroxy-tryptophan
ex/em 310nm/339 nm

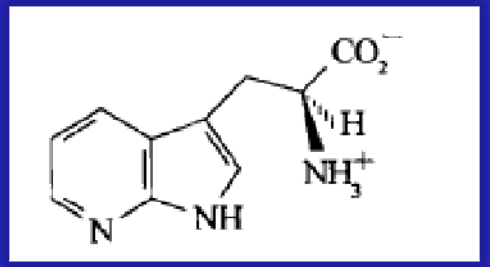

7-azatryptophan
ex/em 320nm/403nm

Φ =0.14	Φ= 0.097	Φ = 0.017
•solvent-sensitive emission	•solvent-insensitive emission	•Large emission shift in water

Φ =Number of photons emitted/number of photons absorbed

Protein Science *(1997), 6, 689-697.*

Absorbance spectrum is red-shifted with respect to that of tryptophan.

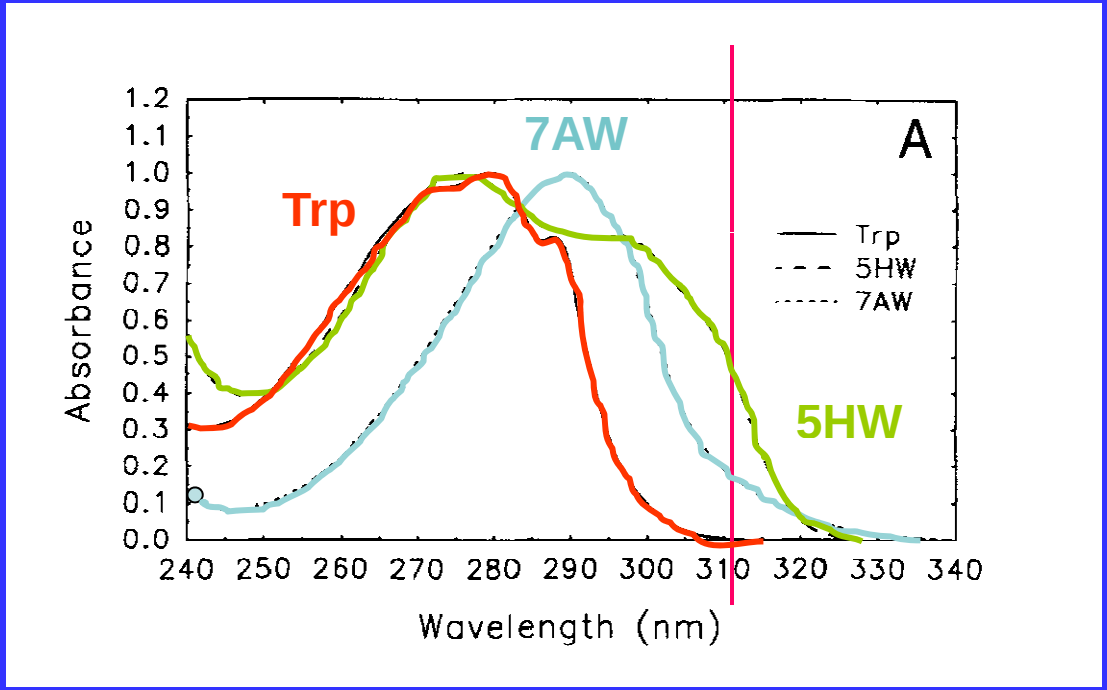

It is possible to selectively excite them, in the presence of tryptophan of other proteins

Protein Science (1997), 6, 689-697.

Enzymes Cofactors

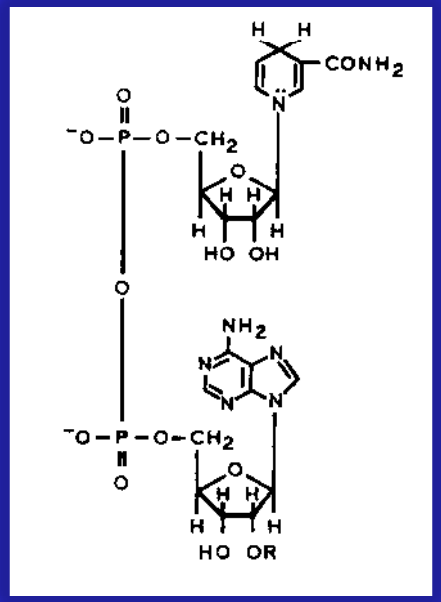

NADH
(oxido-reductases)
Ex/Em 340/460 nm

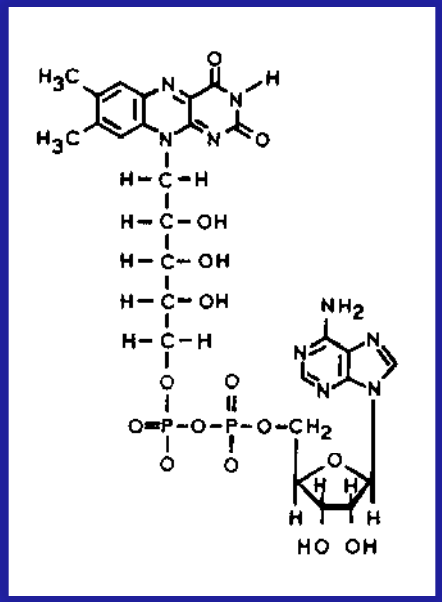

FAD
(metabolic enzymes
(ex/em 450nm/540 nm)

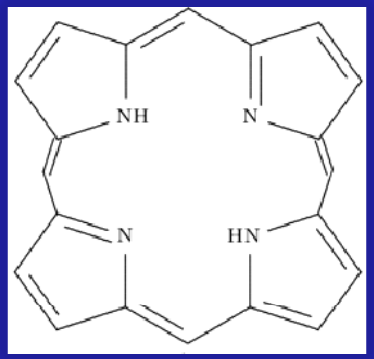

Porphyrins
(ex/em 550 nm/620 nm),

Extrinsic Fluorophores

Synthetic dyes or modified biochemicals that are added to a specimen to produce fluorescence with specific spectral properties

Fluorescent Probes:

- Non covalent interactions

  A fluorescent probe is a fluorophore designed to localize within a specific region of a biological specimen or to respond to a specific analyte.

- Covalent interactions

Extrinsic probes

(not present in the natural molecule/macromolecule)

Non-covalent Attachment

Barely fluorescent in pure water but their fluorescence can be strongly enhanced if the environment becomes hydrophobic (hydrophobic patches on proteins)

1,8-ANS

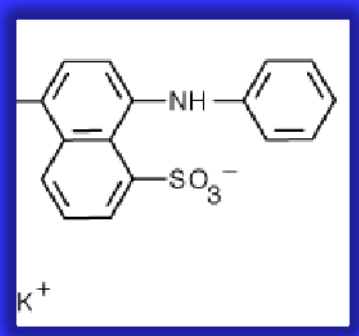

bis-ANS

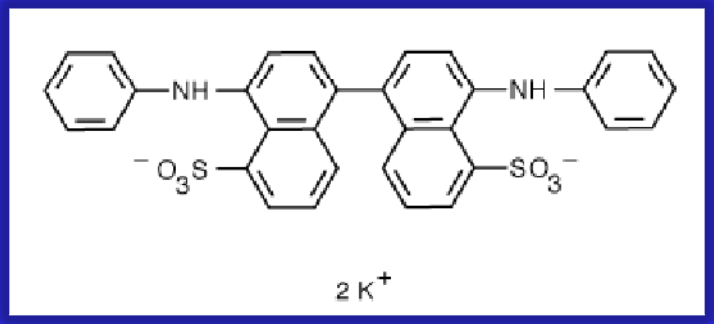

2,6 TNS

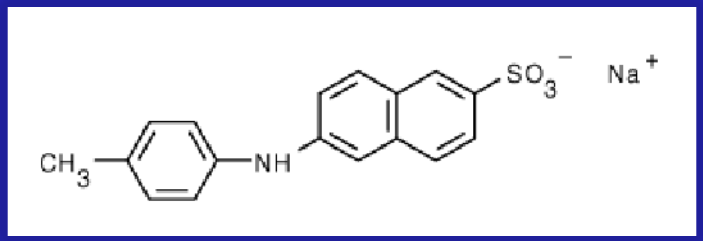

Fluorescent Probes

Non-covalent

1,8-ANS

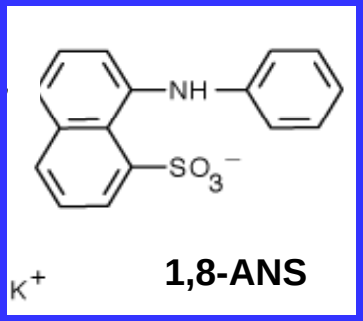

1,8-ANS

Developed by G. Weber in the early 1950's

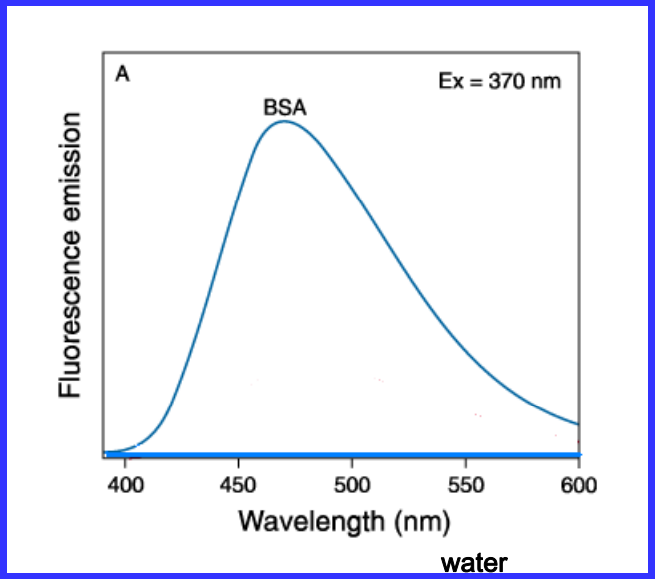

Barely fluorescent in water - fluorescence is strongly enhanced in hydrophobic environments

It is interesting to note that even today, more than 50 years after that first report, ANS is still being used in protein studies, quite often as an indicator of the "molten globular" state.

Fluorescent groups

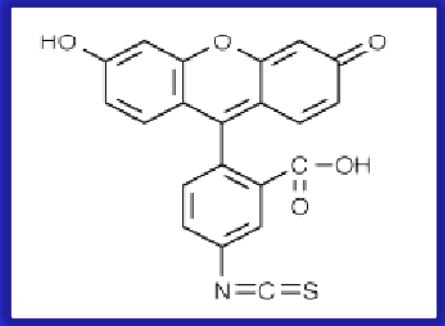

FITC
(488/512) t ≈ 4.05

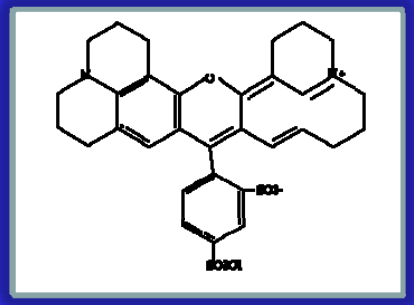

Texas Red
(595-615), t ≈ 3.5 ns

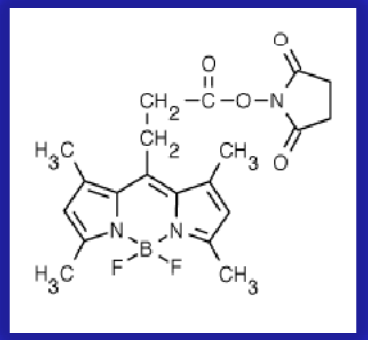

BODIPY
(493/503), t = 6 ns

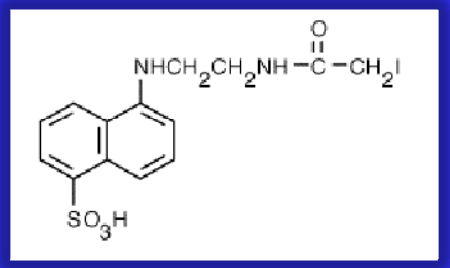

IAEDANS
(360/480) *t* ≈ 15 ns

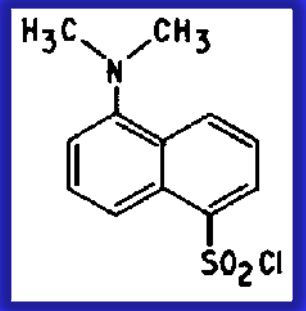

1,5 Dansyl chloride
(335/518) t ≈ 10-17 ns

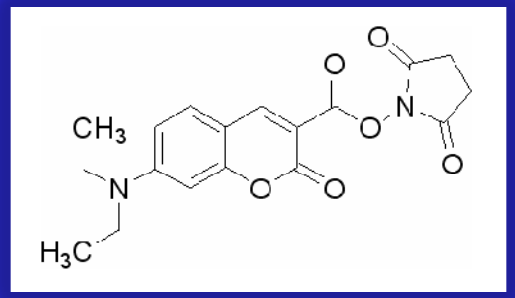

Coumarin-3-carboxylic acid -NHS
(445/482), *t* ≈ 2 -3 ns

The Alexa-Fluor series

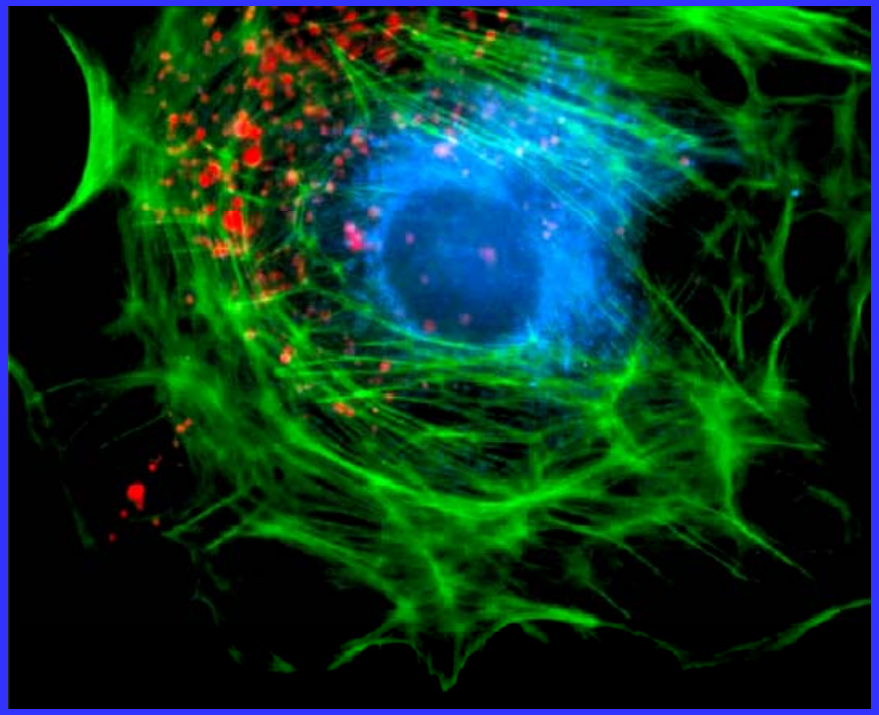

1999
"there is a need
for probes with high fluorescence quantum yield and high photostability to allow detection of low-abundance biological structures with great sensitivity and selectivity"

The Journal of Histochemistry & CytochemistryVolume 47(9): 1179–1188, 1999.Molecular Probes, Inc., Eugene, Oregon

Designed to be more photostable than their commonly used spectral analogues

Coumarin-AMCA → **Alexa 350** 346/442

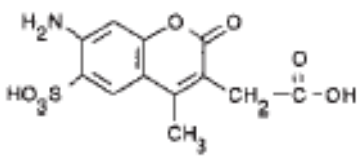

Lucifer Yellow → **Alexa 430** 434/539

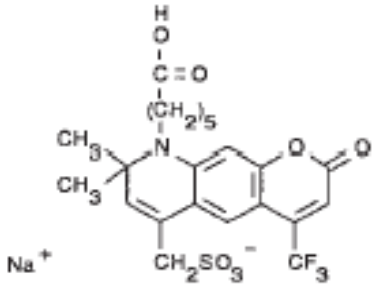

fluorescein → **Alexa 488** 495/519

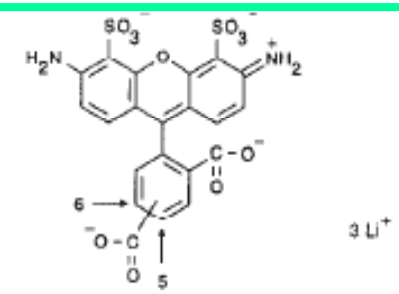

rhodamine 6G → **Alexa 532** 531/554

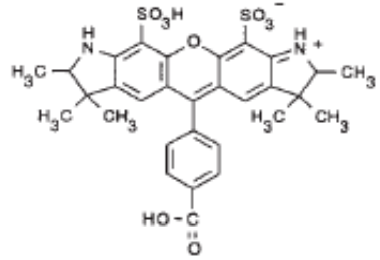

lissamine rhodamine B → **Alexa 568** 578/603

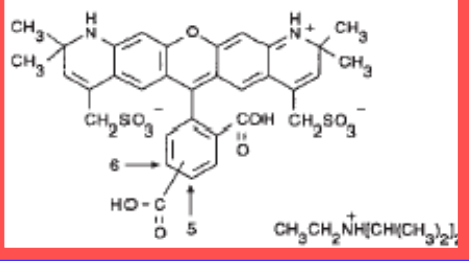

Texas Red → **Alexa 594** 590/617

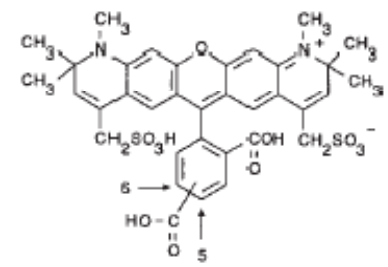

All Alexa dyes and their conjugates are more fluorescent and more photostable than their commonly used spectral analogues.

In addition, Alexa dyes are insensitive to pH in the 4–10 range.

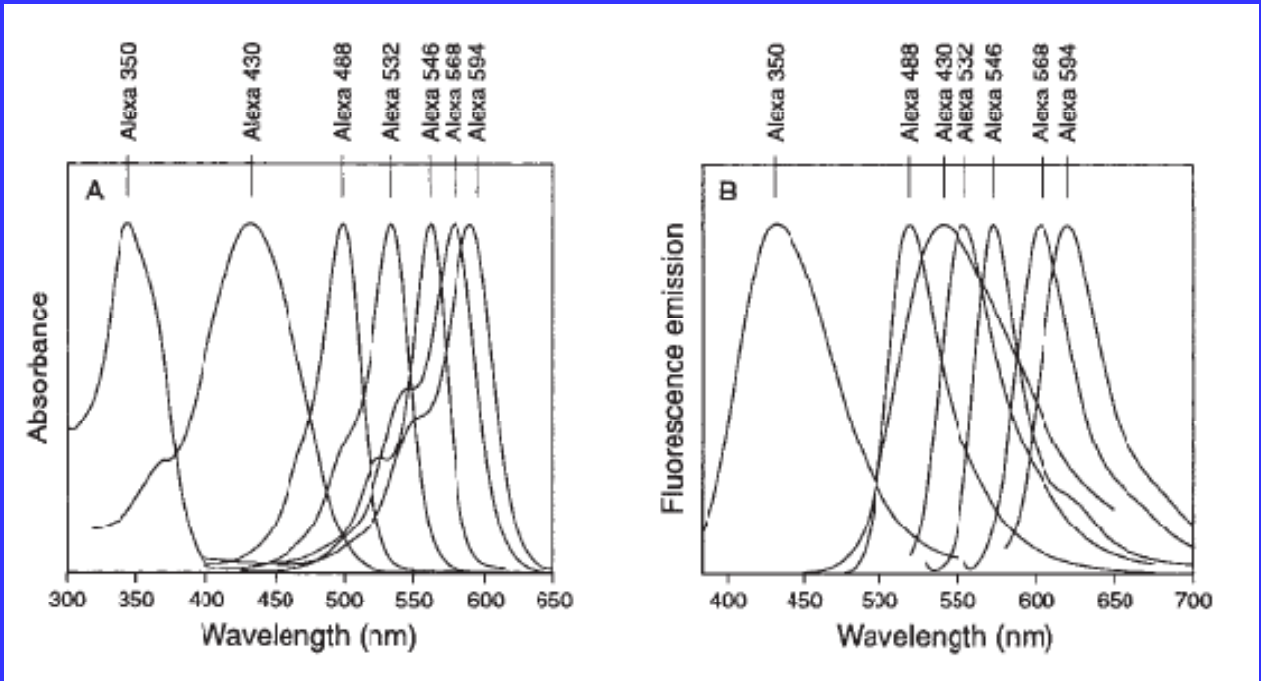

The Journal of Histochemistry & CytochemistryVolume 47(9): 1179–1188, 1999.
Molecular Probes, Inc., Eugene, Oregon

Photostability
Alexa Fluor 488 v/s fluoresceine

Photo bleaching profile

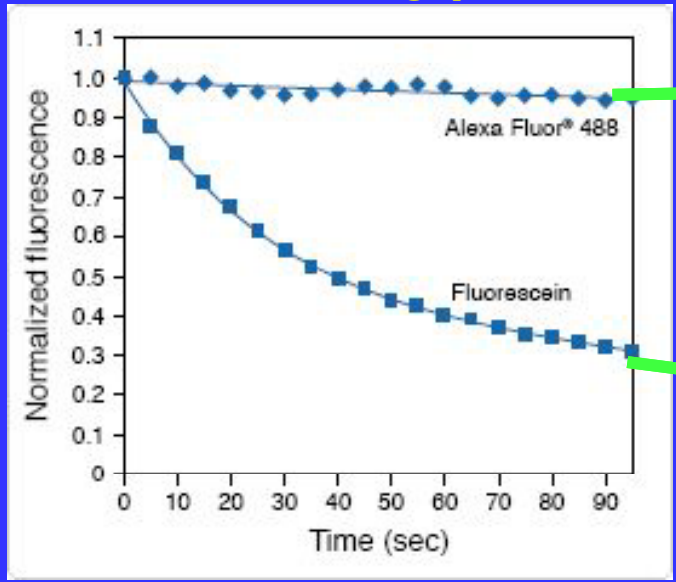

Alexa 488

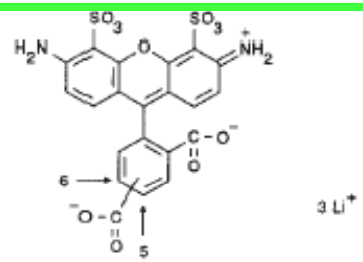

FLUORESCEINE

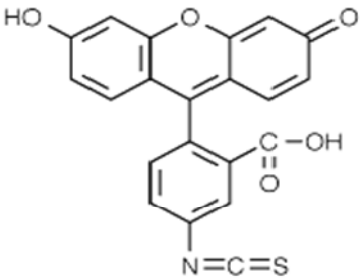

- Cells stained with Alexa Fluor488 or fluorescein conjugates of goat anti–mouse IgG antibody

- Samples were continuously illuminated and images were collected every 5 seconds with a cooled CCD camera.

http://www.invitrogen.com/

The Alexa series expanded

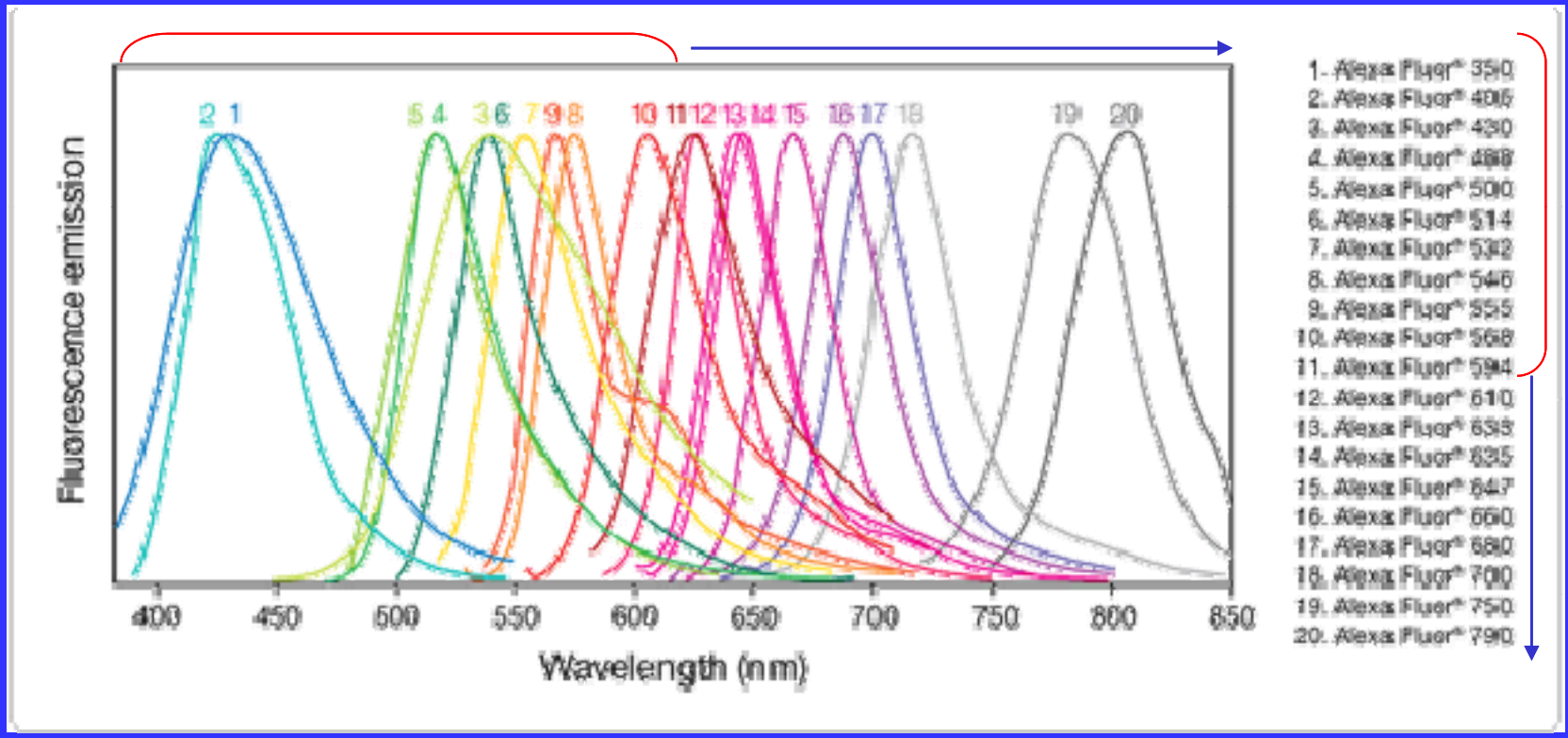

Alexa Fluor dyes are available as amine-reactive succinimidyl esters

Fluorescence quantum yields (QY) and lifetimes (τ) for Alexa Fluor dyes–

Alexa Fluor Dye *	QY †	τ (ns) ‡
Alexa Fluor 488	0.92	4.1 §
Alexa Fluor 532	0.61	2.5
Alexa Fluor 546	0.79	4.1
Alexa Fluor 555	0.10	0.3
Alexa Fluor 568	0.69	3.6 §
Alexa Fluor 594	0.66	3.9 §
Alexa Fluor 647	0.33	1.0
Alexa Fluor 660	0.37	1.2 **
Alexa Fluor 680	0.36	1.2
Alexa Fluor 700	0.25	1.0
Alexa Fluor 750	0.12	0.7

http://www.invitrogen.com

Protein Labeling

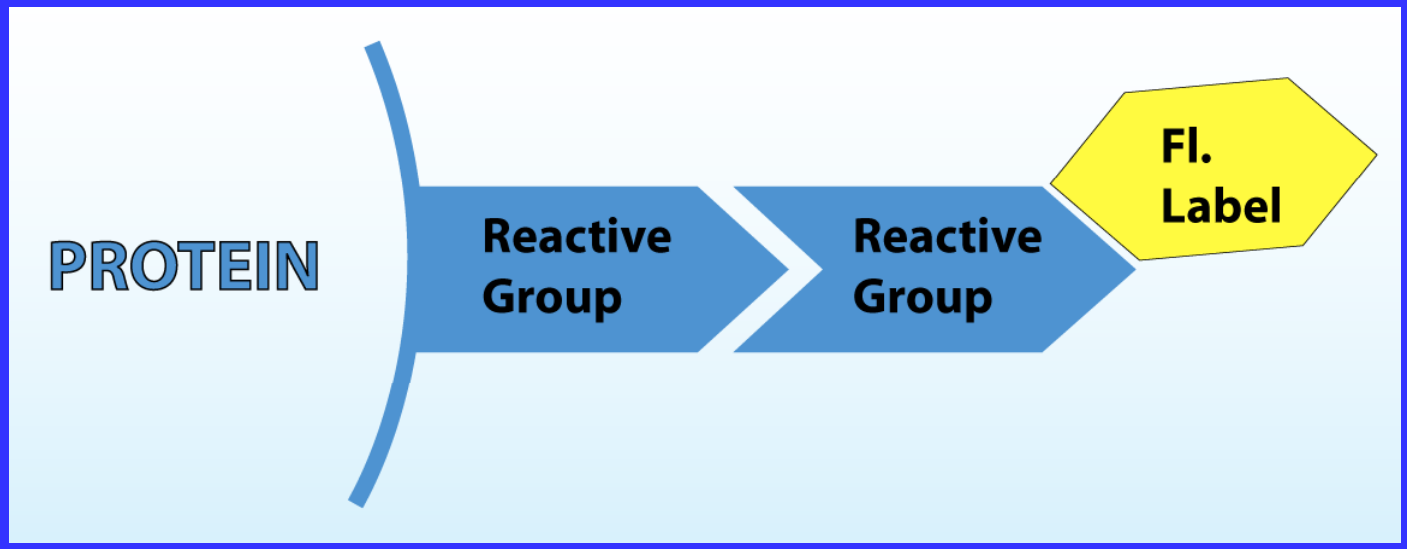

Reactive groups on proteins

NH_2 Lysine N-terminus

SH Cysteine

Depends on the reactive group on the protein

Light source

Spectral properties

Autofluorescence

Photostability

Labeling should not alter the biological activity of biomolecules

Protein Labeling

Amino-Modification:

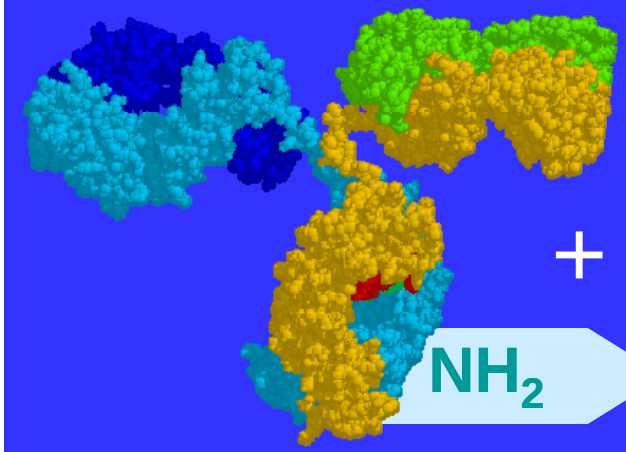

Protein-NH_2

Lysine
N-terminus

isothiocyanate:
Fl-N=C=S

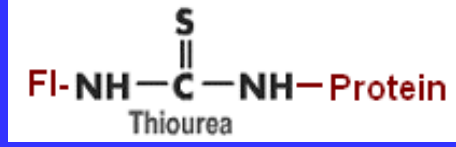

succinimidyl ester:

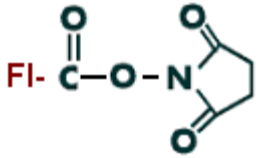

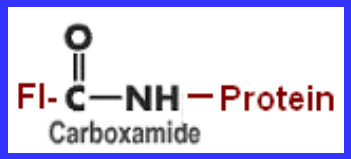

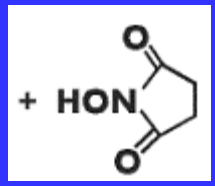

sulfonyl chloride:
Fl-SO_2Cl

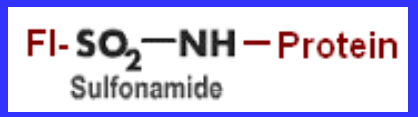

+ HCl

aldehyde:

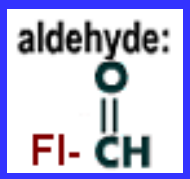

reduction

Protein Labeling

Thiol-Modification:

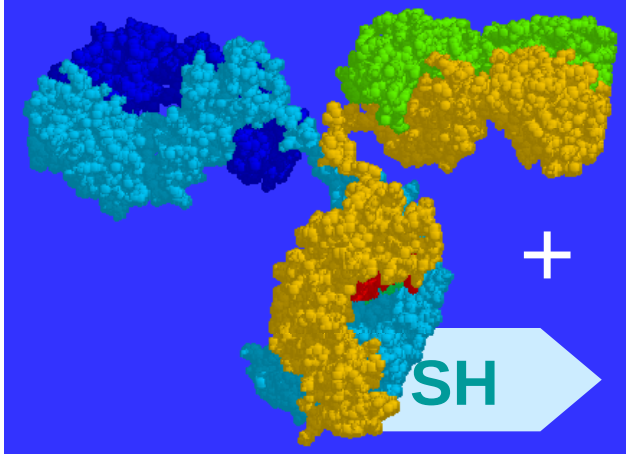

Protein-SH

Cysteine

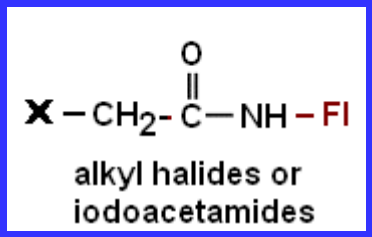

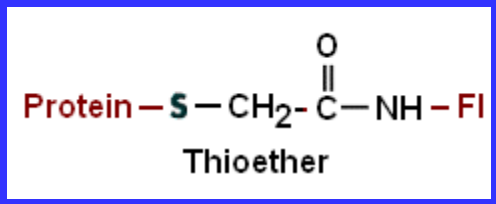

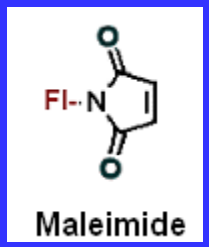

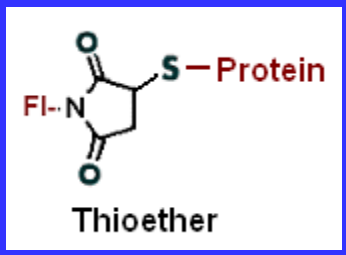

Labeling Procedure

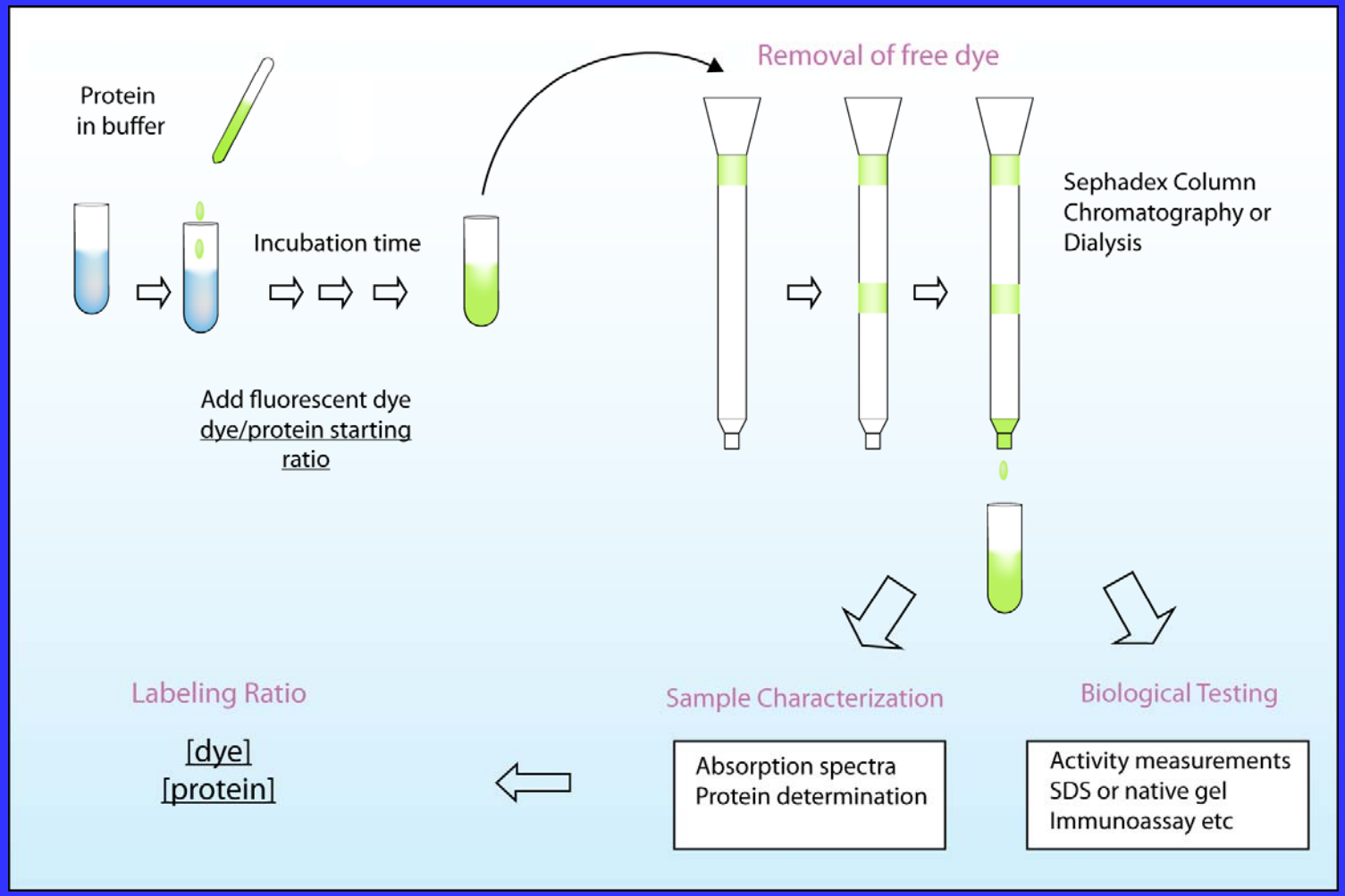

Characterization after the labeling

Protein-Fluorescein

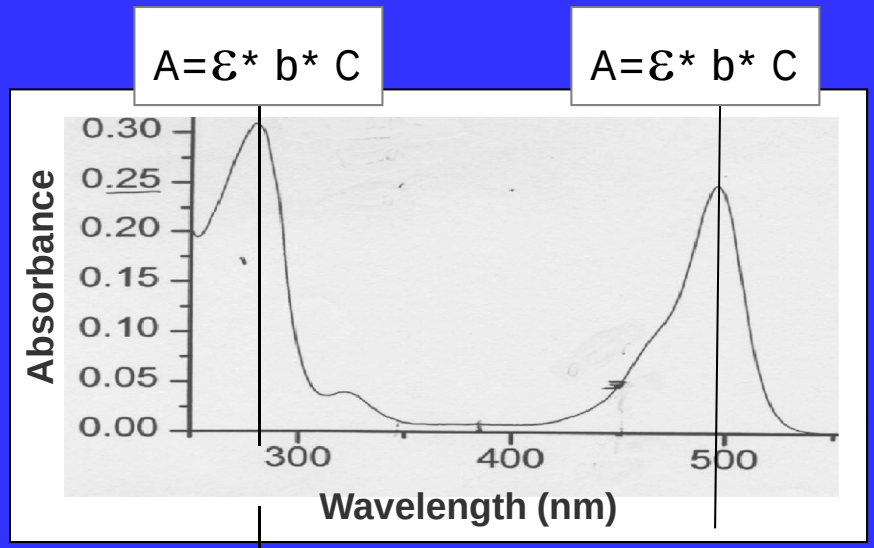

Fluorescein

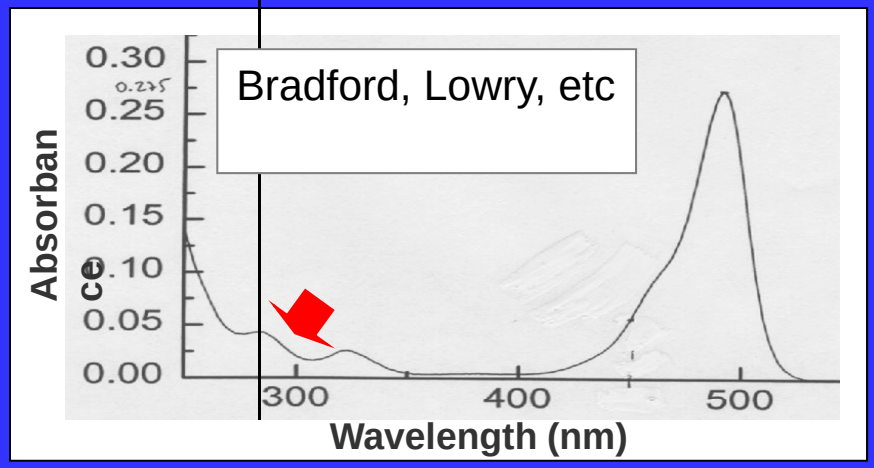

Labeling should not change the biological activity of the protein.

Labeling membranes

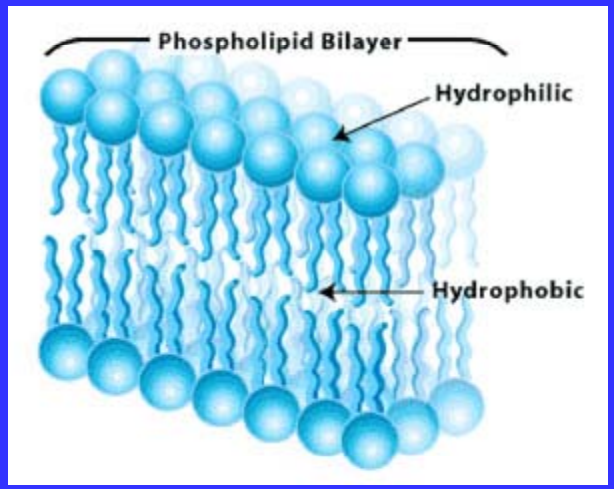

- Analogs of fatty acids and phospholipids

- Di-alkyl-carbocyanine and Di-alkyl-aminostyryl probes.

- Other nonpolar and amphiphilic probes.
DPH, Laurdan, Prodan, Bis ANS

Membrane Probes

Microviscosity and Order in the Hydrocarbon Region of Micelles and Membranes Determined with Fluorescent Probes. I. Synthetic Micelles*

M. Shinitzky,† A.-C. Dianoux,‡ C. Gitler,§ and G. Weber||

ABSTRACT: The viscosity in micelle interiors, termed here as microviscosity, was derived from an adequate comparison of the degree of fluorescence depolarization of perylene or 2-methylanthracene when dissolved in the tested micelles and in American white oil U. S. P. 35. The latter was used as a reference system of known viscosities. In the series studied, lauryltrimethylammonium bromide, myristyltrimethylammonium bromide, cetyltrimethylammonium bromide (CTABr), and stearyldimethylbenzylammonium bromide, the determined microviscosities at 27° are all in the range of 17–50 cP. The change in microviscosity with temperature in this series was found to follow a simple exponential form with an activation energy in the range of 6.1–9.6 kcal mole^{-1}. Added salts affected only slightly the microviscosity values. Mixed micelles of perylene-labeled CTABr with cetyl alcohol or cholesterol and with sodium 1-hexadecanesulfonate, were used to test the effect of charge isolation and charge neutralization on the fluidity of the micelle interior. The microviscosity of these mixed micelles was found to increase rapidly with concentration of the admixed component, and at a molar ratio close to 1:1 microviscosities of several poises were obtained. The changes in apparent rotational diffusion with wavelength of excitation indicate that the depolarizing rotations are strongly anisotropic. In-plane rotations in perylene are ten times faster than out-of-plane rotations, independently of the medium (micelles, propylene glycol at −14°, propylene glycol–glycerol at 4°). This indicates that the resistance to the motion in the micelles must be close to isotropic. A summary of the findings presented leads to the conclusion that micelle interiors are similar in nature to aliphatic hydrocarbon solvents.

In general, the fluorescence emitted from molecules which are dispersed in a viscous medium is partially polarized. This is customarily expressed in terms of molecular anisotropy, r, or degree of polarization, p, which are measured at right angle to a polarized excitation beam and are defined as

$$r = \frac{I_{||} - I_{\perp}}{I_{||} + 2I_{\perp}} \qquad p = \frac{I_{||} - I_{\perp}}{I_{||} + I_{\perp}} \tag{1}$$

When $I_{||}$ and $I_{\perp}$ are the fluorescence intensities observed through a polarizer oriented parallel and perpendicular to the plane of polarization of the excitation beam. For a rotating fluorescent sphere the observed r or p values obey the well known Perrin (1926) equation in which r_0 and p_0 are the values

$$\frac{r_0}{r} = \frac{\frac{1}{p} - \frac{1}{3}}{\frac{1}{p_0} - \frac{1}{3}} = 1 + \frac{6R_s}{\lambda} \tag{2}$$

of r and p when the emitting molecules maintain their orientation excitation and emission (*e.g.*, in a very viscous solvent), R_s is the rate of rotation of the sphere and λ is the rate of fluorescence emission. The term r_0/r is defined here as the degree of depolarization.

* From the Biochemistry Department, School of Chemical Sciences, University of Illinois, Urbana, Illinois 61801. *Received December 9, 1970*. This work has been supported by a grant (U. S. Public Service GM-11223) from the National Institutes of Health.

† U.S.P.H. Postdoctoral Associate. Present Address: Weizmann Institute, *Rehovoth*, Israel.

‡ Fellow of the Centre National de la Recherche Scientifique (France).

§ Visiting Professor, Department of Biochemistry, Instituto Politecnico Nacional, Mexico.

|| To whom correspondence should be addressed.

DPH - diphenylhexatriene

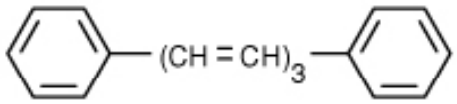

THE JOURNAL OF BIOLOGICAL CHEMISTRY
Vol. 249, No. 8, Issue of April 25, pp. 2652-2657, 1974
Printed in U.S.A.

Dynamics of the Hydrocarbon Layer in Liposomes of Lecithin and Sphingomyelin Containing Dicetylphosphate*

(Received for publication, September 12, 1973)

MEIR SHINITZKY AND YECHEZKEL BARENHOLZ

From the Department of Biophysics, The Weizmann Institute of Science, Rehovot, Israel, and the Department of Biochemistry, The Hebrew University-Hadassah Medical School, Jerusalem, Israel

SUMMARY

Physical properties of the hydrocarbon region in lipid bilayers were studied in a series of liposomes of lecithin and sphingomyelin containing different concentrations of dicetylphosphate. The technique used was described previously and is based on fluorescence polarization analysis of a specific probe embedded in the analyzed region. The two probes employed in this study were perylene and 1,6-diphenyl-1,3,5-hexatriene, which simulate a rotating disc and a rotating rod, respectively. The determined dynamic properties of the hydrocarbon region in the lecithin liposomes differ markedly from those of the sphingomyelin liposomes. The hydrocarbon region of the lecithin liposomes is of an invariant phase between 0° and 60° characterized by a microviscosity at 25°, $\bar{\eta}$ (25°), of 0.8 ± 0.1 poise and a fusion activation energy, ΔE, of 8 ± 2 Cal per mole. In contradistinction to lecithin, the hydrocarbon region of the sphingomyelin liposomes displays a distinct phase transition at 32° ± 2°. The phase at temperatures above the transition point, presumably a liquid crystalline phase, is characterized by ΔE = 16 ± 4 Cal per mole, whereas the phase below it, presumably a gel state, possesses a ΔE value lower than 3 Cal per mole. In addition to that, the hydrocarbon layer in sphingomyelin liposomes is much more viscous than in lecithin liposomes as shown by $\bar{\eta}$ (25°) = 6 ± 1 poise. All of the above characteristics are only slightly and irregularly affected by the presence of dicetylphosphate, despite the strong effects it exerts on the surface charge potential of the liposomes. This indicates that the forces which dictate the dynamic properties of the hydrocarbon region in lipid bilayers predominantly originate from hydrophobic interactions.

different and specific value for each mammalian species. In some membranes this ratio changes drastically with age (1, 2).

The molecular structure of sphingomyelin and lecithin can be separated into two distinct regions: the hydrophilic region, which contains the phosphorylcholine moiety in both lipids, and the hydrophobic region, which contains the hydrocarbon chains. In addition to the phosphorylcholine group, the polar region of lecithin contains two ester bonds, whereas that of sphingomyelin contains an amide bond, an hydroxyl group, and a *trans* double bond. These groups result in difference in the net dipole moment and in the ability to form hydrogen bonds (3, 4). In the hydrophobic region the average length of the hydrocarbon chains in lecithin is shorter and the degree of unsaturation is greater than in sphingomyelin (1). The special nature of these regions in sphingomyelin and lecithin is therefore expected to exert specific effects on structure and dynamics of lipid layers.

In this study, structure and dynamic properties of sonicated liposomes, made of sphingomyelin or lecithin containing dicetylphosphate, were investigated. The method employed was described previously (5, 6) and is based on determination of fluorescence polarization of a hydrocarbon probe and translating it into microviscosity, $\bar{\eta}$, which is obtained in absolute macroscopic units (*e.g.* poise). From the temperature profile of $\bar{\eta}$ phase transitions were detected and the fusion activation energies, ΔE, of each phase were determined (5, 6).

EXPERIMENTAL PROCEDURES

Phospholipids—Lecithin was prepared from egg yolks (7) and purified chromatographically on alumina and silica columns (8). For chemical analysis lecithin was first hydrolyzed by mild alkali (0.4 N KOH in 90% methanol for 2 hours at 37°) and the fatty acids were extracted and methylated with diazomethane. The methyl esters were then analyzed with a Packard gas-liquid chromatograph on 15% ethylene glycol succinate column. The obtained

Fatty acids analogs and phospholipids

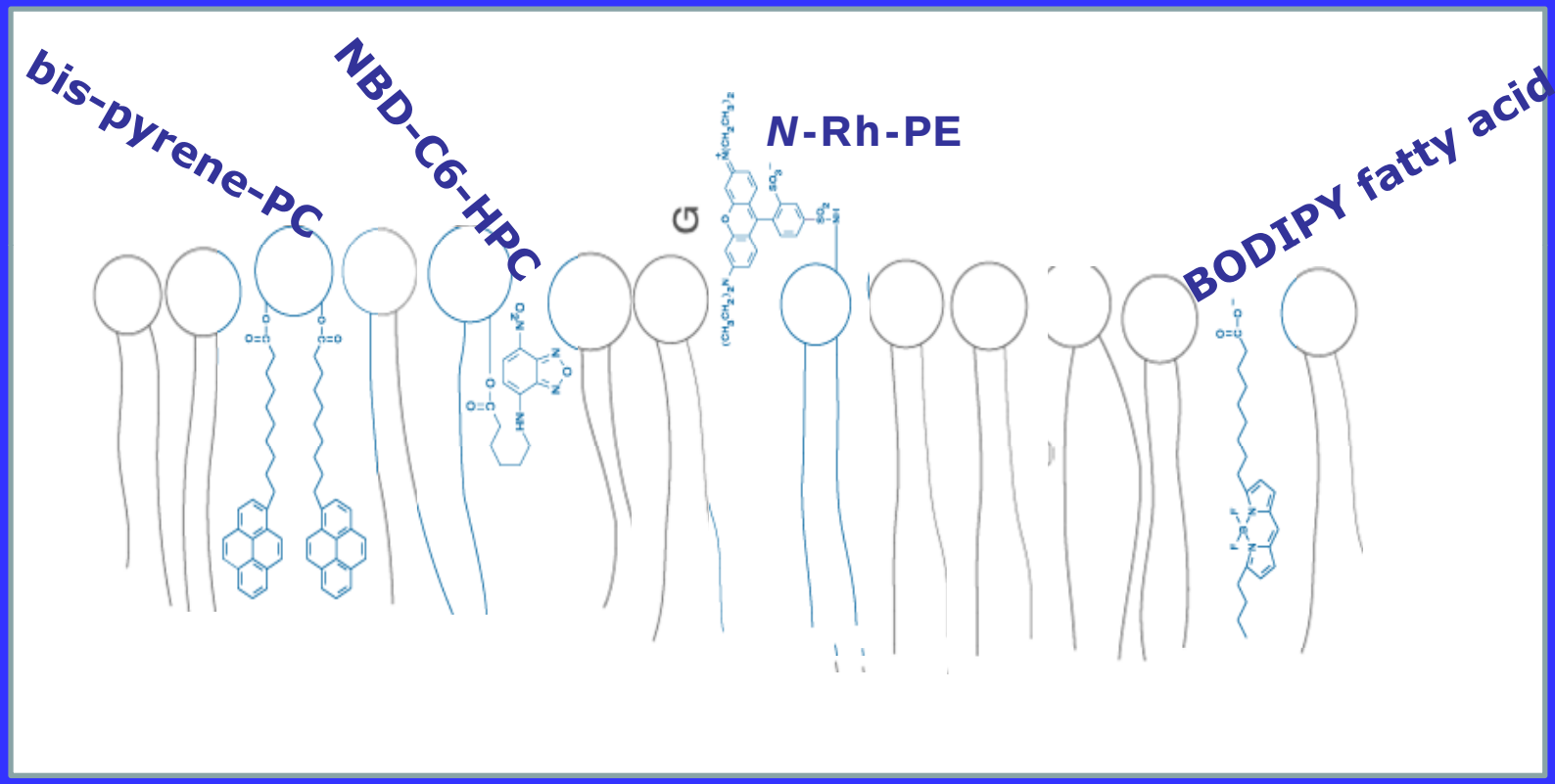

Di-alkyl-carbocyanine probes.

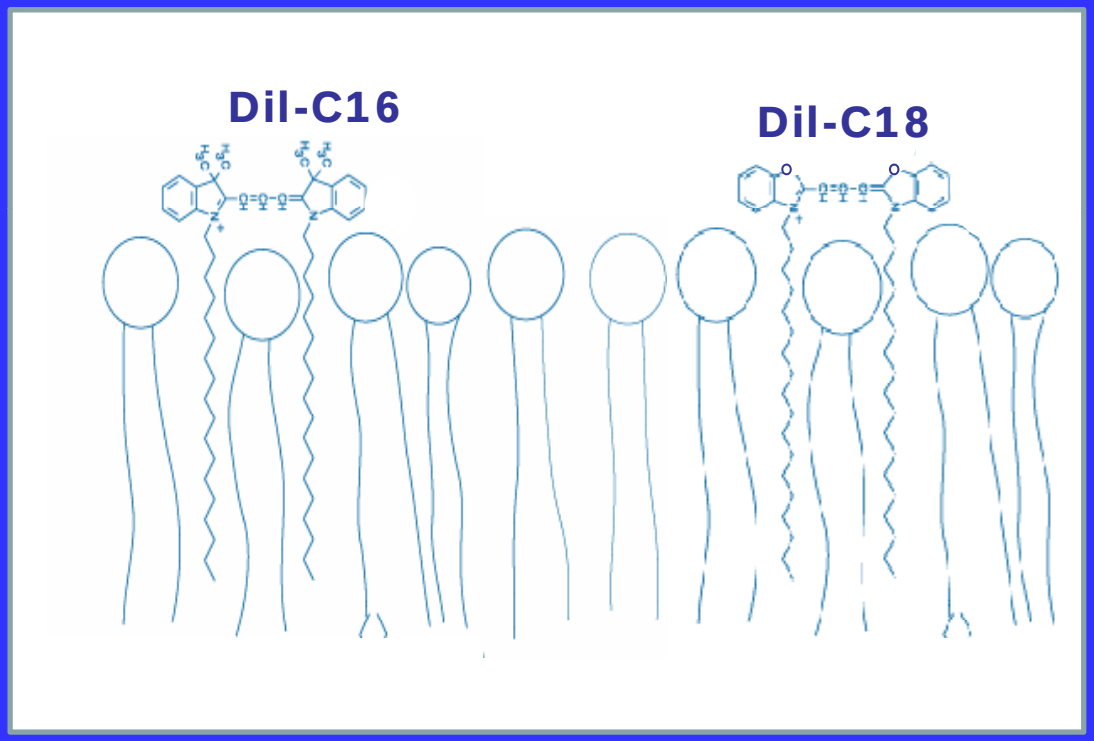

SM / DOPC / Chol (1:1:1)

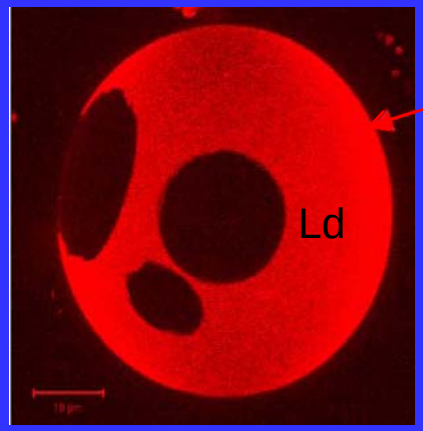

Chem.and Phys. of Lipids 141 (2006) 158–168

Nonpolar probes

example: *Laurdan.*

(environment-sensitive spectral shifts)

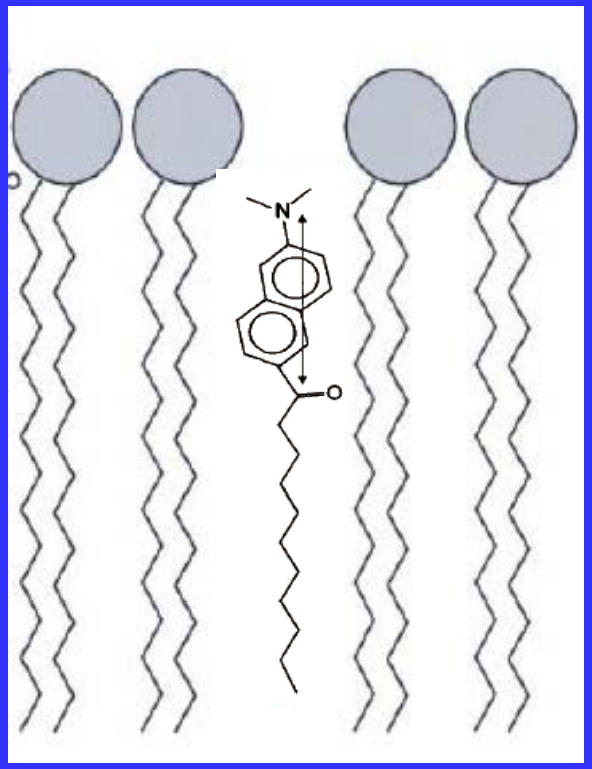

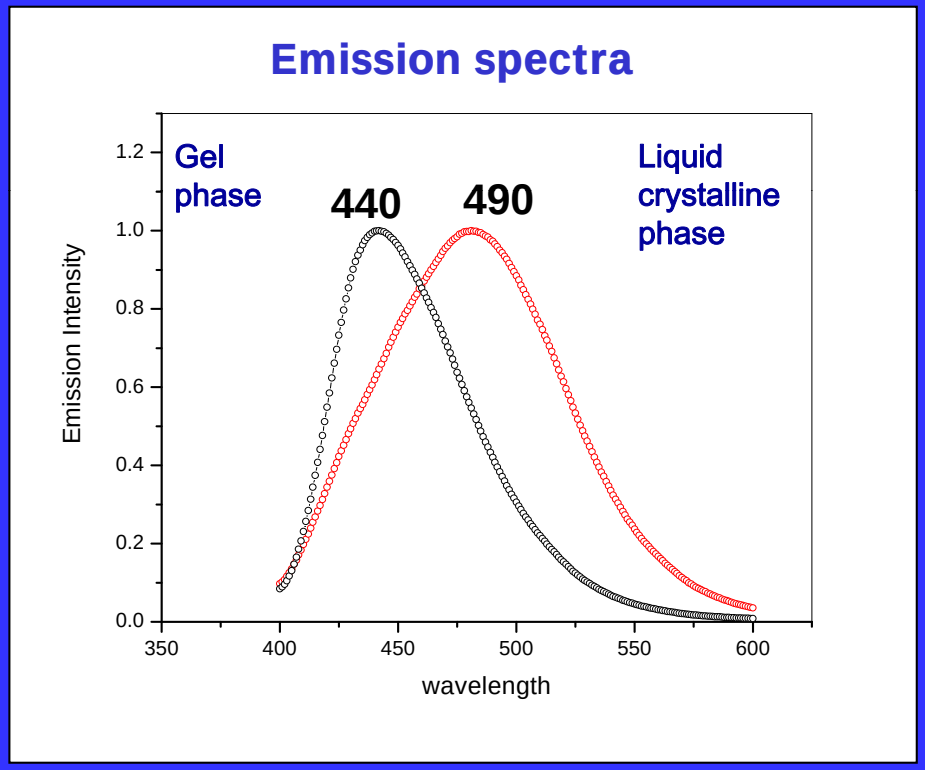

Weber, G. and Farris, F. J.Biochemistry, 18, 3075-3078 (1979) .

Laurdan Generalized Polarization (GP)

Emission spectra

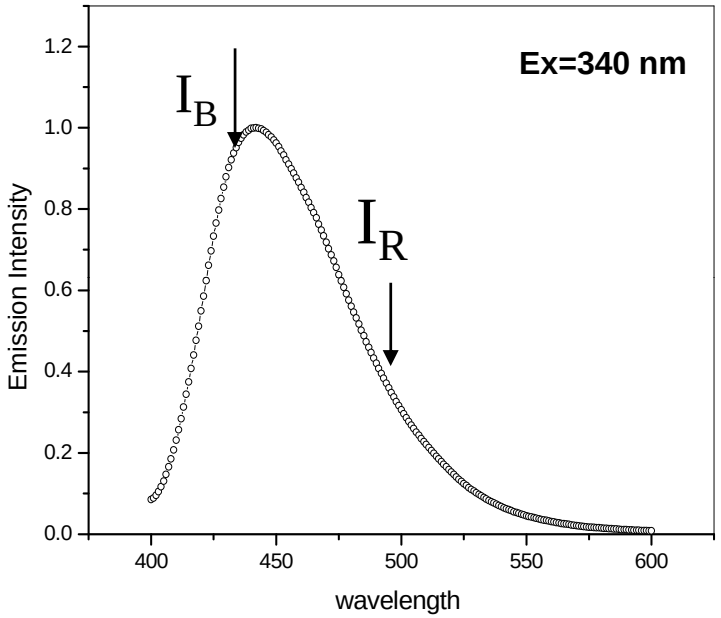

$$GP_{ex} = \frac{I_B - I_R}{I_B + I_R}$$

-0.2
loose lipid packing → **0.6**
tight lipid packing

Parasassi et al. Biophysical J., 60, 179-189 (1991).

GP in the cuvette

MLVs, SUVs, LUVs

Lipid Phase Transition

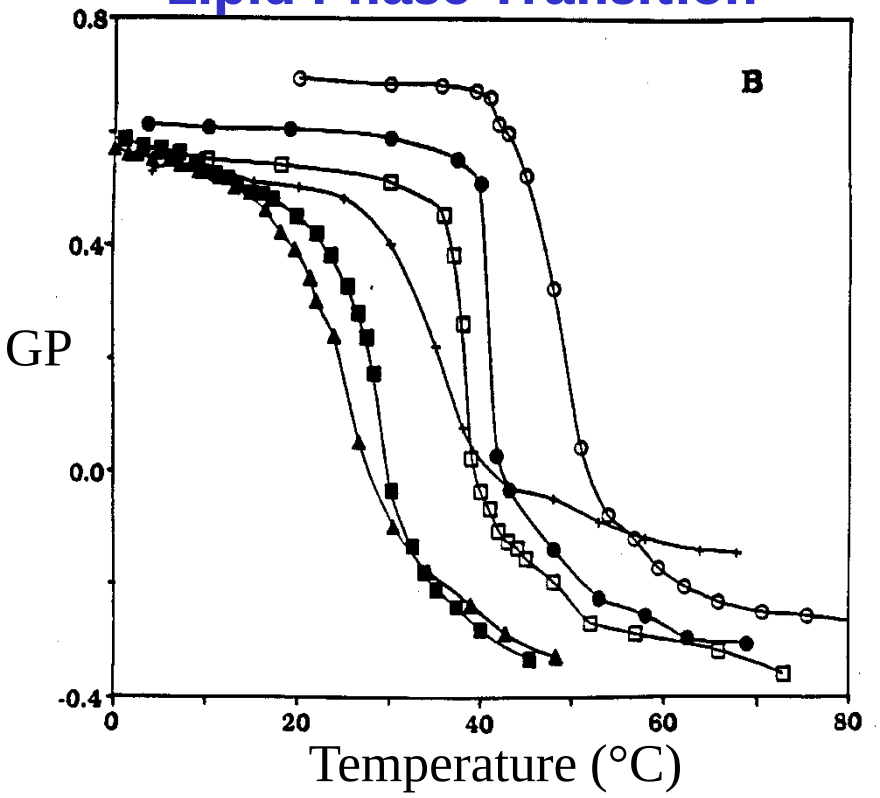

DPPC ●
DPPS:DPPC (2:1) ○
DPPG:DPPC (2:1) +
DMPA:DMPC (2:1) □
DPPG:DLPC (1:1) ■
DPPC:DLPC (1:1) ▲

Parassassi et al. Biophys. J. 60, 179 (1991)

GP in the microscope
(2-photon excitation)

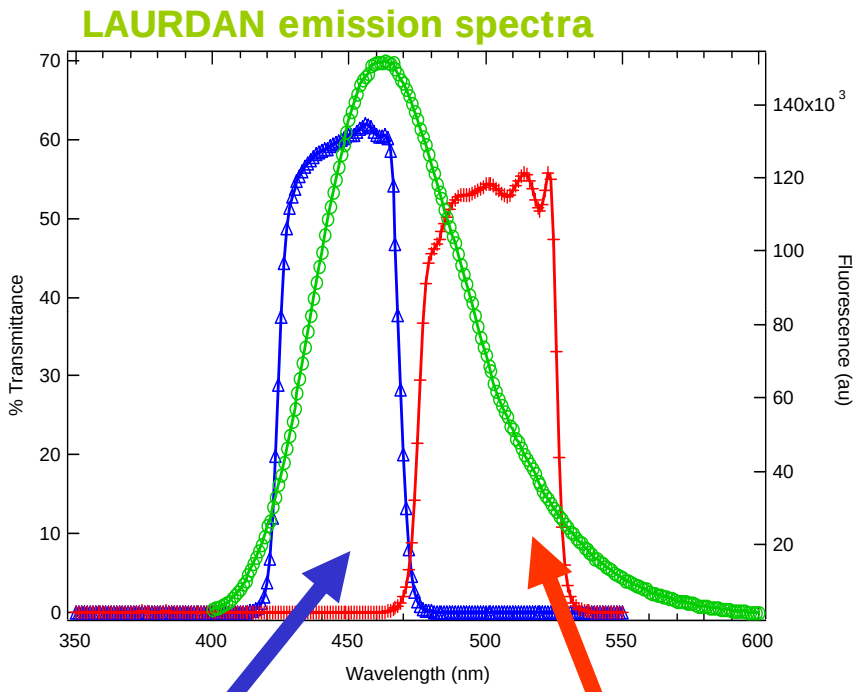

SimFCS software

Ch1: Blue filter

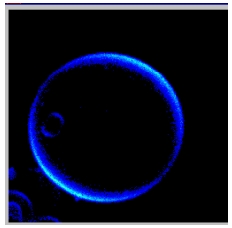

Ch2: Red filter

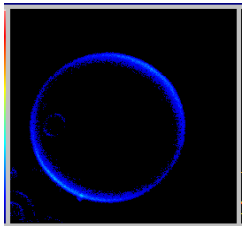

GP image

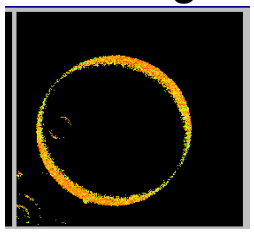

GP histogram

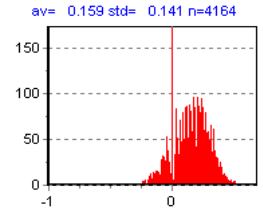

Fluorescent Ion-Probes

Fluorescence probes have been developed for a wide range of ions:

Cations:

H^+, Ca^{2+}, Li^+, Na^+, K^+, Mg^{2+}, Zn^{2+}, Pb^{2+} *and others*

Anions:

Cl^-, PO_4^{2-}, Citrate, ATP, *and others*

Probes For Calcium determination

UV

FURA
(Fura-2, Fura-4F, Fura-5F, Fura-6F, Fura-FF)
INDO
(Indo-1, Indo 5F)

Ratiometric

VISIBLE

FLUO
(Fluo-3, Fluo-4, Fluo5F, Fluo-5N, Fluo-4N)
RHOD (Rhod-2, Rhod-FF, Rhod-5N)
CALCIUM GREEN (CG-1, CG-5N,CG-2)
OREGON GREEN 488-BAPTA

Non Ratiometric

Ratiometric: 2 excitation / 1emission

FURA-2

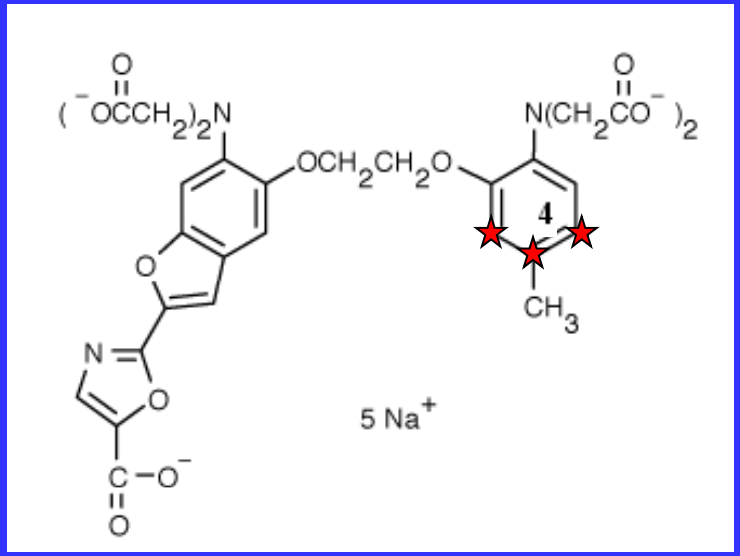

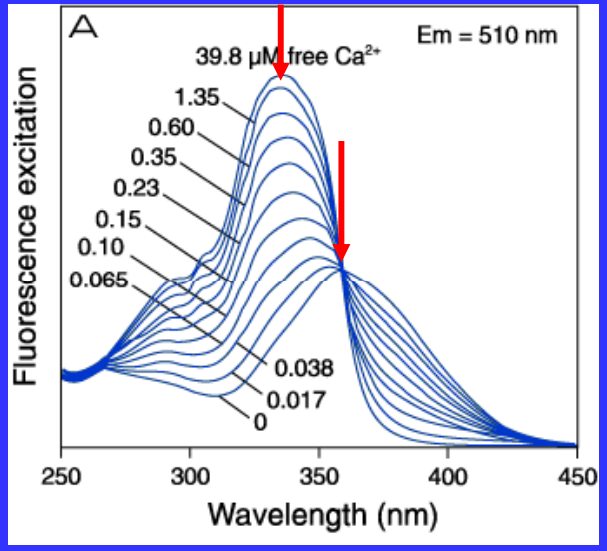

Indicator	$K_d(Ca^{2+})$
Fura-2	0.14 μM
Fura-5F	0.40 μM
Fura-4F	0.77 μM
Fura-6F	5.30 μM
Fura-FF (5,6)	35 μM

Most used in microscopic imaging

Good excitation shift with Ca^{2+}

Rationed between 340 / 350 and 380 / 385 nm

Ratiometric: 1excitation / 2emission

Indo-1

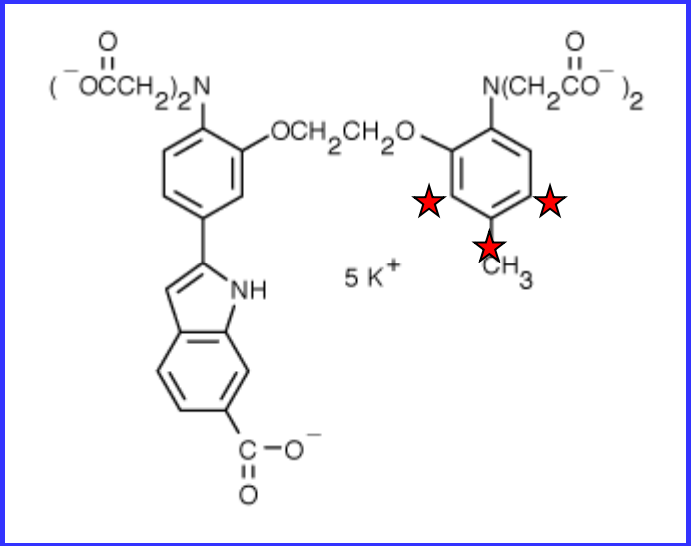

Indicator	K_d (Ca^{2+}) (μM)
indo-1	0.23
indo-5F	0.47

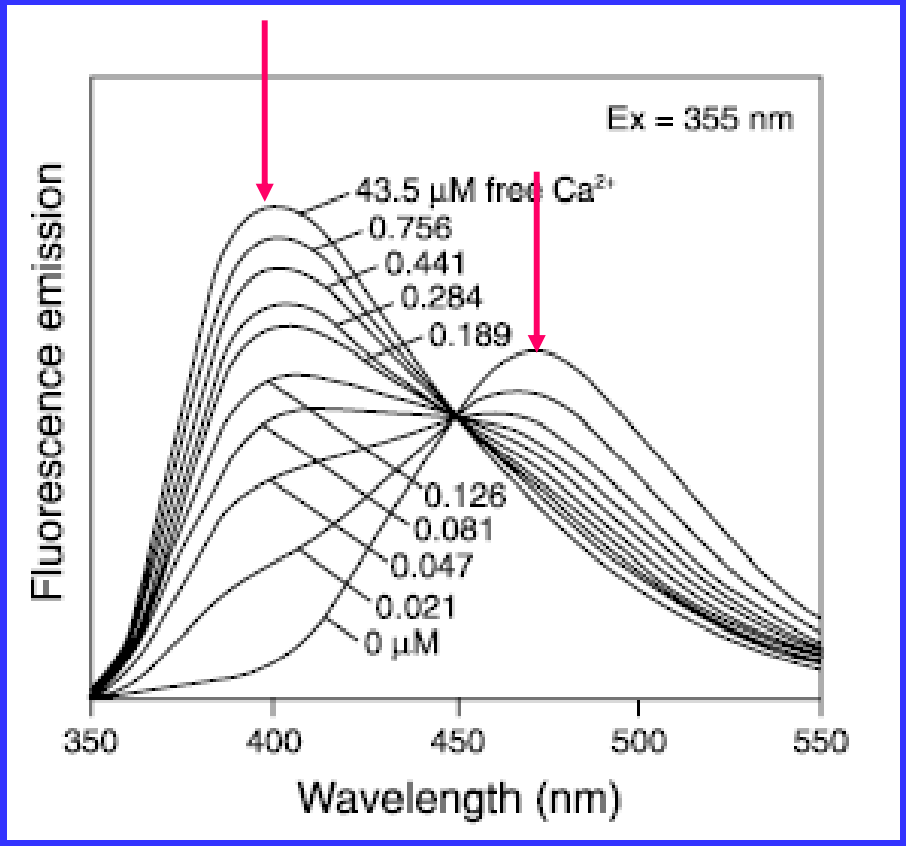

CalciumGreen-5N

Non-Ratiometric

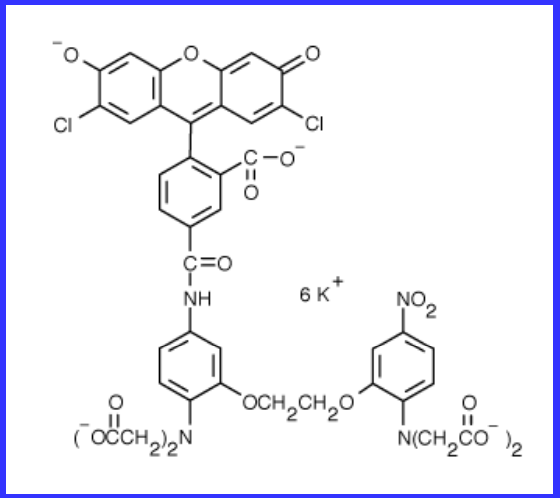

Fluorescence Intensity

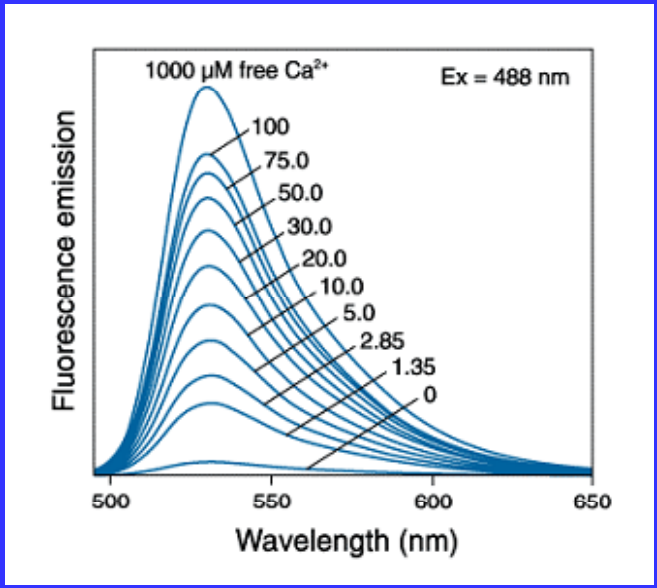

Fluorescence Lifetime

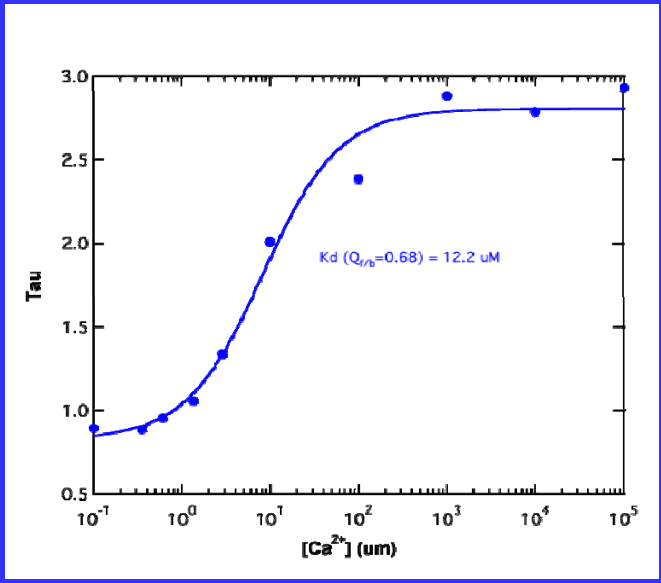

pH-Probes

Probe	pH Range	Measurement Mode
SNARF indicators	6.0-8.0	Em. ratio 580/640 nm
HPTS (pyranine)	7.0-8.0	Exc. ratio 450/405 nm
BCECF	6.5-7.5	Exc. ratio 490/440 nm
Fluoresceins and Carboxyfluoresceins	6.0-7.2	Exc. ratio 490/450 nm
Oregon Green dyes	4.2-5.7	Exc. ratio 510/450 nm
LysoSensor Yellow/Blue DND-160	3.5-6.0	Em. ratio 450/510 nm

Molecular Probes' pH indicator families, in order of decreasing pK_a

BCECF

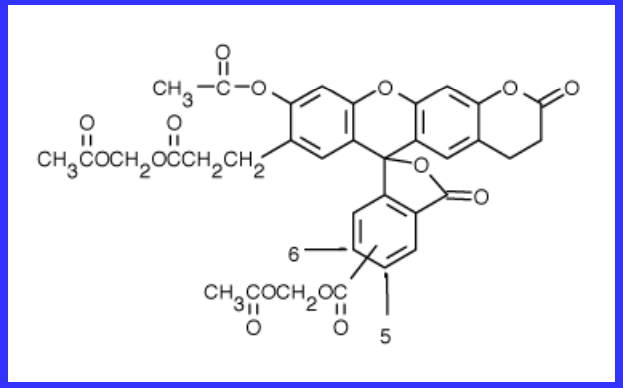

R. Tsien 1982

Most widely used fluorescent indicator for intercellular pH

Membrane-permeant AM: pKa ~ 6.98 is ideal for intracellular pH measurements

Excitation-ratiometric probe with Ip at 439 nm, which is used a the reference point

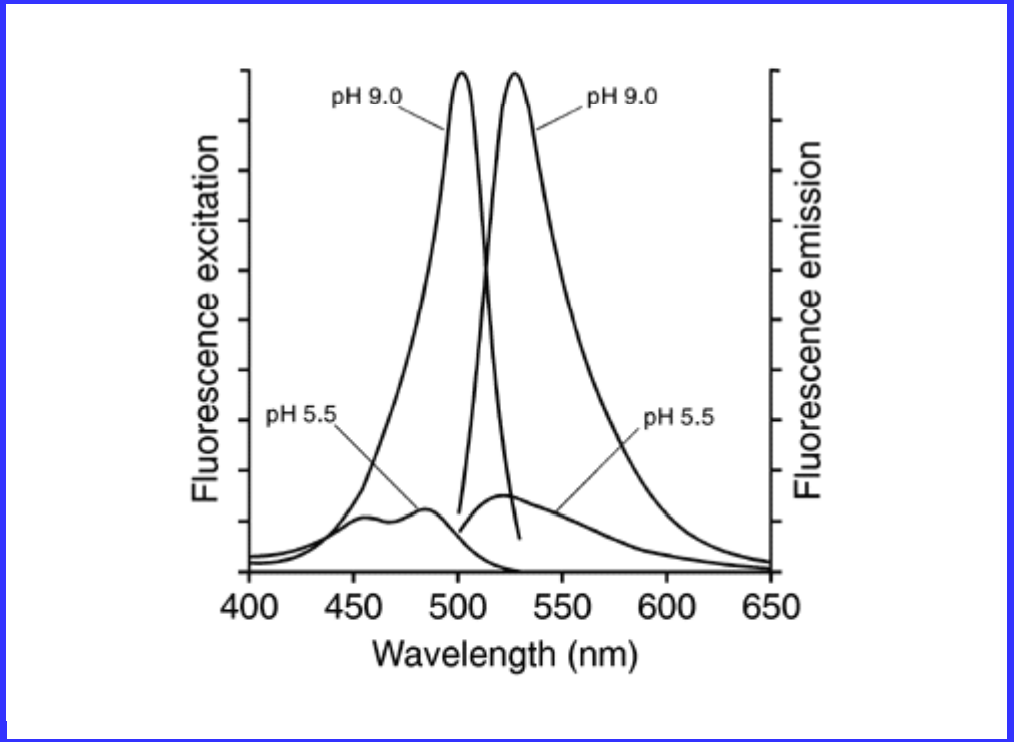

Quantum Dots

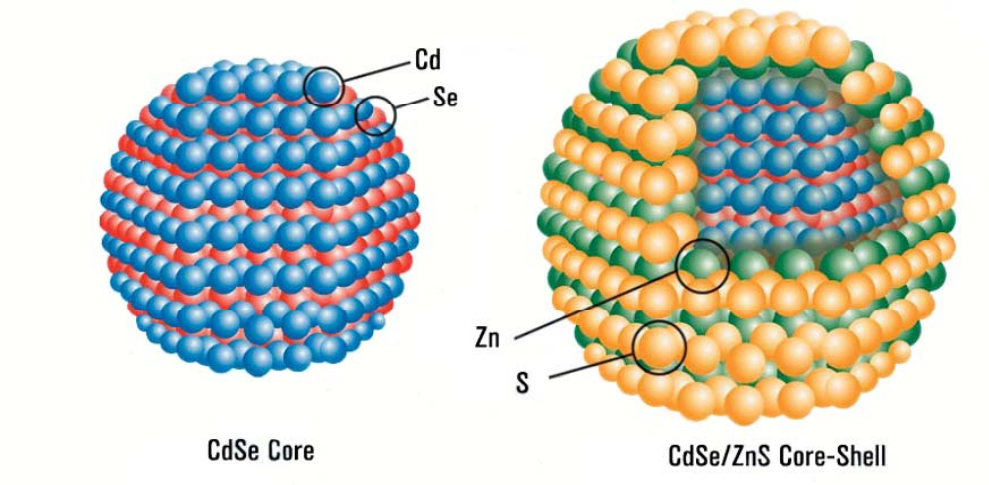

Quantum Dots

Nanometer-Scale Atom Clusters

CORE

Cadmium selenide (**CdSe**), or Cadmium telluride (**CdTe**)
few hundred – few thousand atoms

The semiconductor material is chosen based upon the emission wavelength, however it is the **size** of the particles that **tunes the emission wavelength**.

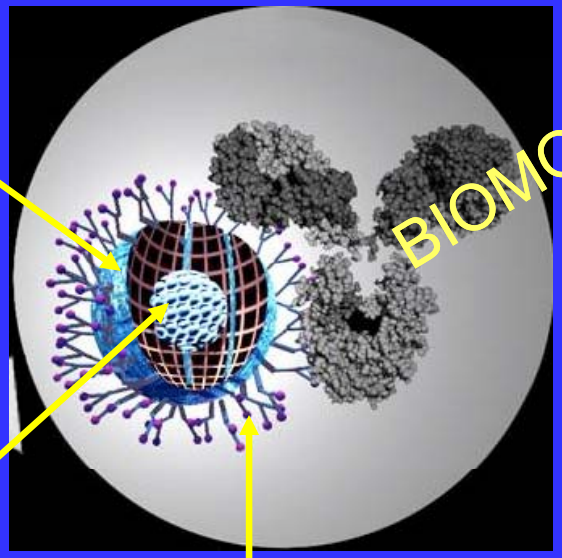

SHELL

In the core emission is typically weak and always unstable.
The shell material (**ZnS**) has been selected to be almost entirely unreactive and completely insulating for the core.

COATING

A layer of organic ligands covalently attached to the surface of the shell. This coating provides a **surface for conjugation** to biological (antibodies, streptavidin, lectins, nucleic acids) and nonbiological species and makes them "water-soluble"
.

Quantum Dots

Nanometer-Scale Atom Clusters

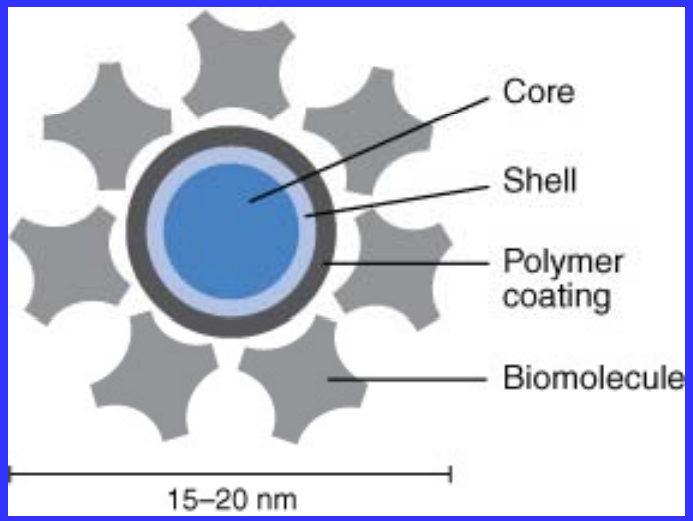

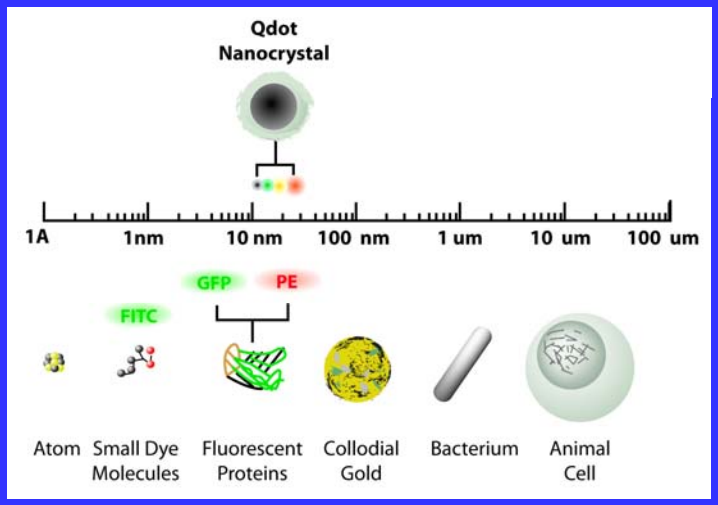

Quantum Dot Material System	Emission Range	Quantum Dot Diameter Range	Quantum Dot Type	Standard Solvents	Example Applications
CdSe	465nm - 640nm	1.9nm - 6.7nm	Core	Toluene	Research, Solar Cells, LEDs
CdSe/ZnS	490nm - 620nm	2.9nm - 6.1nm	Core-Shell	Toluene	VisibleFluorescence Applications, Electroluminescence, LEDs
CdTe/CdS	620nm - 680nm	3.7nm - 4.8nm	Core-Shell	Toluene	Deep Red Fluorescence Apps.

Qdot Optical Spectra

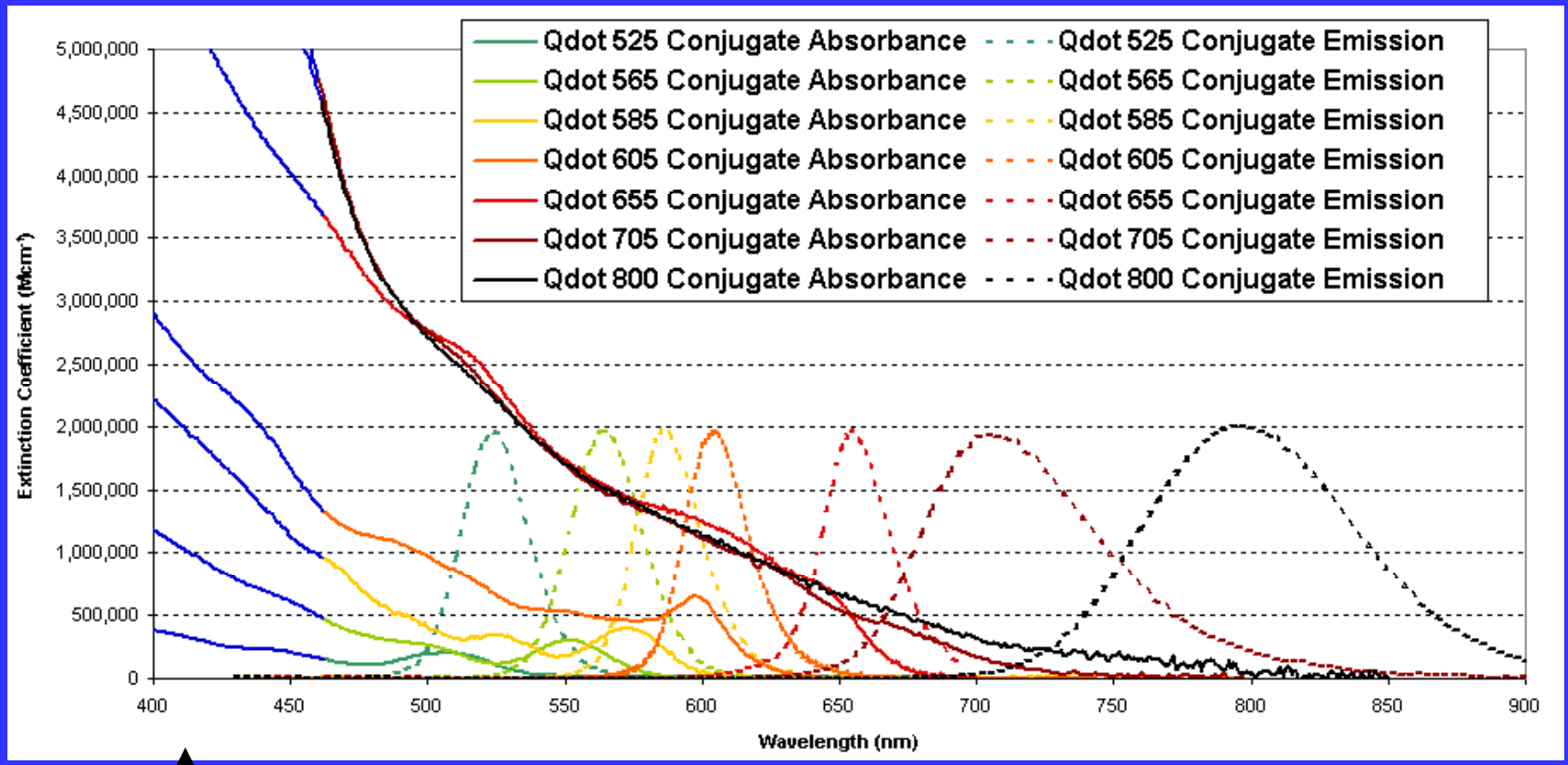

Violet excitation

Absorbance × Quantum Yield = Brightness

photons in **fraction converted** **photons out**

Broad range of emissions

High absorbance means increased brightness

Single-color excitation, multicolor emission for easy multiplexing

Courtesy of Invitrogen

Qdot Summary

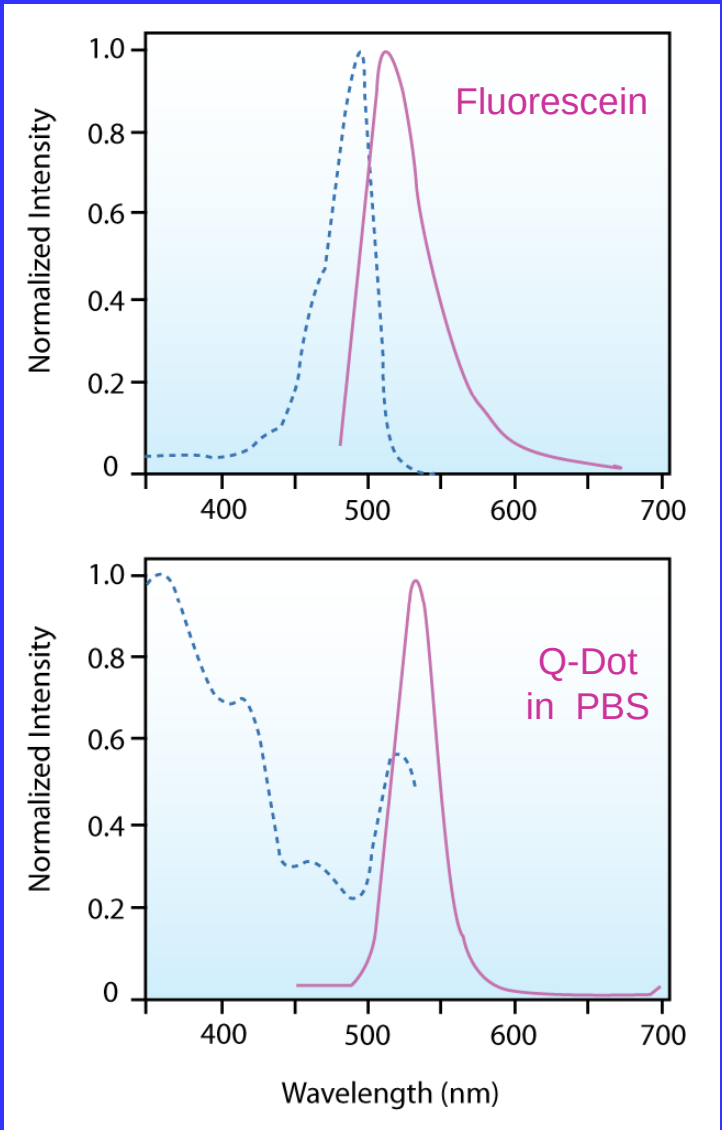

Advantages:

Broad absorption spectra, making it possible to excite all colors of QDs simultaneously with a single light source - **Multiplexing**

Narrow and symmetrical emission spectra

Emission tunable with size and material composition

Exhibit excellent **photo-stability**

Disadvantages:

Large size and **high mass** limit their use in applications requiring high diffusional mobility

QDot	λ_{max} (abs) [nm]	λ_{max} (em) [nm]	ε ($M^{-1}cm^{-1}$)	Q.Y.
655	350	655	9,000,000	~0.5
705	350	705	13,000,000	~0.5
800	350	800	13,000,000	~0.5

That's all!!!